TRC2106

Applying UAS LiDAR for Developing Small Project Terrain Models

Dr. Clinton M. Wood
Dr. Jackson David Cothren
Ashraf Siddiqui
Malcolm Williamson

University of Arkansas - Fayetteville
College of Engineering, Department of Civil Engineering
Fulbright College of Arts & Sciences, Department of Geosciences

Final Report

December 2023

TRC2106

Applying UAS LiDAR for Developing Small Project Terrain Models

Dr. Clinton M. Wood
Dr. Jackson David Cothren
Ashraf Siddiqui
Malcolm Williamson

University of Arkansas - Fayetteville
College of Engineering, Department of Civil Engineering
Fulbright College of Arts & Sciences, Department of Geosciences

Final Report

December 2023

Arkansas Department of Transportation

Notice of Nondiscrimination

The Arkansas Department of Transportation (ARDOT) complies with all civil rights provisions of federal statutes and related authorities that prohibit discrimination in programs and activities receiving federal financial assistance. Therefore, the Department does not discriminate on the basis of race, sex, color, age, national origin, religion (not applicable as a protected group under the Federal Motor Carrier Safety Administration Title VI Program), disability, Limited English Proficiency (LEP), or low-income status in the admission, access to and treatment in the Department's programs and activities, as well as the Department's hiring or employment practices. Complaints of alleged discrimination and inquiries regarding the Department's nondiscrimination policies may be directed to Civil Rights Officer Joanna P. McFadden (ADA/504/ Title VI Coordinator), P. 0. Box 2261, Little Rock, AR 72203, (501) 569-2298, (Voice/TTY 711), or the following email address: joanna.mcfadden@ardot.gov.

Free language assistance for Limited English Proficient individuals is available upon request.

This notice is available from the ADA/504/Tittle VI Coordinator in large print, on audiotape and Braille

Disclaimer:

The contents of this report reflect the views of the authors, who are responsible for the facts and the accuracy of the data presented herein. The contents do not necessarily reflect the official views or policies of ARDOT and they assume no liability for the contents or use thereof. This report does not constitute a standard, specification, or regulation. Comments contained in this report related to specific testing equipment and materials should not be considered an endorsement of any commercial product or service; no such endorsement is intended or implied.

TECHNICAL REPORT DOCUMENTATION

1. Report No. TRC2106	2. Government Accession No.	3. Recipient's Catalog No.
4. Title and Subtitle Applying UAS LiDAR for Developing Small Project Terrain Models		**5. Report Date** December 2023
		6. Performing Organization Code
7. Author(s) Clinton M. Wood and Malcolm Williamson		**8. Performing Organization Report No.**
9. Performing Organization Name and Address Department of Civil Engineering University of Arkansas 4190 Bell Engineering Center Fayetteville, Arkansas 72701		**10. Work Unit No. (TRAIS)**
		11. Contract or Grant No. Project TRC2106
12. Sponsoring Agency Name and Address Arkansas Department of Transportation PO Box 2261 Little Rock, Arkansas 72203-2261		**13. Type of Report and Period Covered** FINAL
		14. Sponsoring Agency Code
15. Supplementary Notes Project performed in cooperation with the Federal Highway Administration		

16. Abstract

The work described in this report assessed the accuracy of using unmanned aerial systems (UAS) LiDAR on small bridge replacement projects, compared the accuracy of UAS LiDAR and conventional surveying techniques (global navigation satellite system real time kinematics and total station), and discussed the cost savings of different surveying methods. The study considered five small bridge projects where UAS LiDAR was flown, and conventional surveying checkpoints were measured in the LiDAR survey area. The results indicate that for hard surfaces, UAS LiDAR is generally accurate to within -1.0 inch to +1.0 inch, with variations observed across the different sites. Soft surfaces, particularly grass, exhibited LiDAR overestimation ranging from 0.0 to +2.0 inches and up to +3.0 inches at the Humnoke site. Tall grass and tree checkpoints demonstrated larger errors, with variations among the sites. Overall, the root mean squared errors for the different surface types ranged from 0.5 to 7.0 inches, with asphalt having the lowest error and trees having the highest. The study concludes that UAS LiDAR provides good accuracy for hard surfaces, with expected larger errors for soft surfaces, and offers cost benefits over alternative surveying methods. Comparative cost analyses revealed that UAS LiDAR is approximately $1,195.41 less expensive per project than helicopter LiDAR and $10,539.18 less expensive per bridge project compared to conventional surveys, resulting in a 20 and 25 percent cost reduction, respectively. Despite having slightly less accuracy for soft surfaces, the cost effectiveness of UAS LiDAR makes it a favorable choice for small-area bridge projects.

17. Key Words Survey, Accuracy, LiDAR, UAS	**18. Distribution Statement** This document is available to the US public through the National Technical Information Service, Springfield, Virginia 22161		
19. Security Classification (of this report) Unclassified	**20. Security Classification (of this page)** Unclassified	**21. No of Pages** 105	**22. Price**

METRIC CONVERSIONS

SI* (MODERN METRIC) CONVERSION FACTORS

APPROXIMATE CONVERSIONS TO SI UNITS

Symbol	When You Know	Multiply By	To Find	Symbol
LENGTH				
in	inches	25.4	millimeters	mm
ft	feet	0.305	meters	m
yd	yards	0.914	meters	m
mi	miles	1.61	kilometers	km
AREA				
in^2	square inches	645.2	square millimeters	mm^2
ft^2	square feet	0.093	square meters	m^2
yd^2	square yard	0.836	square meters	m^2
ac	acres	0.405	hectares	ha
mi^2	square miles	2.59	square kilometers	km^2
VOLUME				
fl oz	fluid ounces	29.57	milliliters	mL
gal	gallons	3.785	liters	L
ft^3	cubic feet	0.028	cubic meters	m^3
yd^3	cubic yards	0.765	cubic meters	m^3
NOTE: volumes greater than 1000 L shall be shown in m^3				
MASS				
oz	ounces	28.35	grams	g
lb	pounds	0.454	kilograms	kg
T	short tons (2000 lb)	0.907	megagrams (or "metric ton")	Mg (or "t")
TEMPERATURE (exact degrees)				
°F	Fahrenheit	5 (F-32)/9 or (F-32)/1.8	Celsius	°C
ILLUMINATION				
fc	foot-candles	10.76	lux	lx
fl	foot-Lamberts	3.426	candela/m^2	cd/m^2
FORCE and PRESSURE or STRESS				
lbf	poundforce	4.45	newtons	N
lbf/in^2	poundforce per square inch	6.89	kilopascals	kPa

APPROXIMATE CONVERSIONS FROM SI UNITS

Symbol	When You Know	Multiply By	To Find	Symbol
LENGTH				
mm	millimeters	0.039	inches	in
m	meters	3.28	feet	ft
m	meters	1.09	yards	yd
km	kilometers	0.621	miles	mi
AREA				
mm^2	square millimeters	0.0016	square inches	in^2
m^2	square meters	10.764	square feet	ft^2
m^2	square meters	1.195	square yards	yd^2
ha	hectares	2.47	acres	ac
km^2	square kilometers	0.386	square miles	mi^2
VOLUME				
mL	milliliters	0.034	fluid ounces	fl oz
L	liters	0.264	gallons	gal
m^3	cubic meters	35.314	cubic feet	ft^3
m^3	cubic meters	1.307	cubic yards	yd^3
MASS				
g	grams	0.035	ounces	oz
kg	kilograms	2.202	pounds	lb
Mg (or "t")	megagrams (or "metric ton")	1.103	short tons (2000 lb)	T
TEMPERATURE (exact degrees)				
°C	Celsius	1.8C+32	Fahrenheit	°F
ILLUMINATION				
lx	lux	0.0929	foot-candles	fc
cd/m^2	candela/m^2	0.2919	foot-Lamberts	fl
FORCE and PRESSURE or STRESS				
N	newtons	0.225	poundforce	lbf
kPa	kilopascals	0.145	poundforce per square inch	lbf/in^2

CONTENTS

LIST OF FIGURES

LIST OF TABLES

LIST OF ABBREVIATIONS, ACRONYMS, AND SYMBOLS

AASHTO	Association of State Highway and Transportation Officials
AGS	Arkansas Geological Survey
ARDOT	Arkansas Department of Transportation
B/C	Benefit cost ratio
DEM	Digital elevation map
DOT	Department of Transportation
DTM	Digital Terrain Model
DJI	Da-Jiang Innovations
FAA	Federal Aviation Administration
FHWA	Federal Highway Administration
GCP	Ground Control Point
GIS	Geographic information system
GNSS	Global navigation satellite system
GPS	Global Positioning System
LiDAR	Light Detection and Ranging
NBI	National Bridge Inventory
NED	National Elevation Dataset
NGS	National Geodetic Survey
ODOT	Oregon Department of Transportation
PPK	Post Processed Kinematic
RTK	Real Time Kinematics
TAMP	Transportation Asset Management Plan
TPP	Transportation Planning and Policy
sUAS	Small Unmanned Aerial System
USDOT	US Department of Transportation
USGS	US Geological Survey

EXECUTIVE SUMMARY

The TRC2106 research project, funded by the Arkansas Department of Transportation (ARDOT) and conducted by the University of Arkansas at Fayetteville, focused on assessing the accuracy and benefits of using unmanned aerial systems (UAS) LiDAR to collect survey data for small-area projects, particularly bridge replacement projects. The project aimed to compare UAS LiDAR data with conventional surveying methods.

For the project, five bridge sites were selected for UAS LiDAR and conventional survey data collection, which include Lincoln Bridge 1 (East), Lincoln Bridge 2 (West), Humnoke, Frenchman's Bayou, and Mountain Home. Data for each site were collected during the 2021–2022 winter. A DJI M600 Pro and Phoenix LiDAR Systems AL3-16 LiDAR unit were used for the UAS LiDAR measurements. The conventional survey equipment used included a global navigation satellite system (GNSS) real time kinematics (RTK) system and a robotic total station. LiDAR missions were planned using a combination of Google Earth®, Phoenix LiDAR Systems' Flightplanner, and Litchi Mission Hub. Flights were conducted at an altitude of 45 meters above ground level (AGL), with 50 percent side lap, ensuring comprehensive coverage. Weather and environmental conditions were carefully considered for optimal data collection. The LiDAR data were processed using Phoenix LiDAR System's LiDARMill online software service. The processing involved GNSS data correction, trajectory optimization, and LiDAR data alignment and classification. Additionally, LAStools were employed to enhance ground classification, reduce noise, and generate accurate digital elevation models.

The accuracy of UAS LiDAR was assessed by comparing the UARK and ARDOT LiDAR datasets and ground truth data collected using GNSS and total station checkpoints for hard and soft surfaces. Errors between the UAS LiDAR and checkpoints were compared using aerial photos, bar graphs, and box and whisker plots, and direct raster comparisons were made whenever multiple LiDAR datasets were available. For hard surfaces, such as asphalt, UAS LiDAR's accuracy was generally within -1.0 inch to +1.0 inch, with slight variations among the sites. Notably, higher variations were observed in Humnoke and Mountain Home, while lower variations were observed at Frenchman's Bayou. For soft surfaces, UAS LiDAR tended to overestimate grass elevations by 0.0 inches to +2.0 inches, with Humnoke exhibiting a larger overprediction, likely due to its taller grass. Tall grass checkpoints showed higher overpredictions, with Frenchman's Bayou having lower errors than the other sites. Tree checkpoints displayed the highest variability, with errors ranging from +2.0 inches to +6.0 inches.

Comparing the root mean squared (RMS) error for each site, it was observed that for hard surfaces (asphalt), RMS errors of 0.5 inches to 1.5 inches were common, with Humnoke having a higher error and Frenchman's Bayou displaying the lowest error. Gravel checkpoints had slightly higher RMS errors ranging from 1.0 inches to 2.0 inches. For soft surfaces (grass), an RMS error of 1.0 inches to 3.0 inches was observed, depending on the grass height. Tall grass had higher RMS errors of 2.0 inches to 5.0 inches, and tree checkpoints had the highest RMS errors ranging from 2.0 inches to 7.0 inches.

Overall, errors of up to approximately 1.0 inch can be expected for hard surfaces, with potential for both over- and under-predictions. An overprediction error of 1.0 inch to 3.5 inches can be expected for grass surfaces, depending on grass height. Larger overprediction errors of 2.0 inches to 5.0 inches can be expected for tall grass areas, while errors ranging between 2.0 inches and 7.0 inches can be expected for tree areas.

The cost savings analysis performed in this study determined that UAS LiDAR demonstrated an average cost reduction of $1,195.41 per project compared to helicopter LiDAR, resulting in a 20 percent reduction in the cost of collecting data for small-area bridge projects. In addition, UAS LiDAR exhibited an average cost reduction of $10,539.18 per bridge project compared to conventional survey methods, resulting in a 25 percent reduction in the cost of surveys for small-area bridge projects.

Overall, UAS LiDAR proves to be a valuable tool for obtaining elevation data, with good accuracy for hard surfaces and expected variations for soft surfaces. Despite the limitations, the cost savings analysis underscored the economic benefits of UAS LiDAR, highlighting its clear advantage over both helicopter LiDAR and conventional surveying methods for small-area bridge projects.

CHAPTER 1. PROJECT OVERVIEW

PROBLEM STATEMENT

Providing digital terrain models and survey data for small-area projects such as bridge replacements requires obtaining ground elevations in vegetated areas, which is time consuming when using conventional total station surveying techniques. Other typical surveying methods, such as airborne photogrammetry, have challenges obtaining ground elevations in the typically wooded areas surrounding the project sites. One of the strengths of light detection and ranging (LiDAR) is its ability to penetrate vegetated areas by obtaining multiple returns to the sensor for a given horizontal position. Unmanned aerial systems (UAS) with a LiDAR sensor can reduce the time and effort required to develop these terrain models without sacrificing the accuracy of the data. UAS LiDAR has advanced significantly in the last 5 years, providing easier-to-use systems with more standardized workflows for developing elevation models from raw LiDAR data.

The TRC2106 research project was funded by the Arkansas Department of Transportation (ArDOT) and conducted by the University of Arkansas at Fayetteville. This project involved collecting several survey datasets for small bridge replacement projects which used UAS LiDAR and conventional surveying (GNSS and total station). These datasets were used to compare the accuracy of UAS LiDAR and conventional survey methods.

OBJECTIVES OF THE STUDY

The overarching objective of this research effort was to assess the accuracy and benefits of using UAS LiDAR to collect high-quality survey data for small-area projects such as bridge replacements. This study adhered to Federal Regulations 14 CFR Part 107, the Federal Aviation Administration's regulations for small UASs. The study's sub-objectives are detailed below. The ArDOT survey division identified five bridge projects to use as test sites and delivered previously measured UAS LiDAR or helicopter LiDAR data for three of those sites.

UAS LiDAR data were acquired at each of the five sites using a UAS owned by the University of Arkansas. This system is described in detail in the Equipment section of this report. In addition to the UAS LiDAR, conventional survey methods (total station/GNSS) were also used to collect data at each site to establish checkpoints (CP) which were compared with the processed LiDAR data at each site. Various ground (trees, bush, open ground, etc.) and traffic (heavy and light) conditions were covered by the CPs at each site. The collected LiDAR data were compared with conventional GNSS or total station surveys for different surface conditions (hard and soft). The UAS LiDAR data were also compared with other UAS or helicopter LiDAR data at select sites. The testing and comparison were aimed at establishing the accuracy and cost effectiveness of each data collection tool.

REPORT OVERVIEW

This report comprises seven chapters. Chapter 1 includes some general information and an introduction to the project. Chapter 2 encompasses a review of the relevant literature, which includes UAS and LiDAR

methods along with their uses in department of transportation (DOT) projects. Chapter 3 discusses the equipment used for the project, the sites included in the study, and the methodology used to collect and process the study data. Chapter 4 compares the LiDAR-derived elevations and GNSS/total station CPs for each site included in the study. Chapter 5 discusses the results of all the sites combined together. Chapter 6 is a cost-savings analysis of using UAS LiDAR for small-area bridge projects, and Chapter 7 presents the overall conclusion, recommendations, and future work.

CHAPTER 2. LITERATURE REVIEW

INTRODUCTION

This literature review focuses on light detection and ranging (LiDAR) and unmanned aerial systems (UAS), as well as the department of transportation's (DOT) use of the technology.

LIGHT DETECTION AND RANGING (LIDAR)

Applying lasers in distance measurement has a rich history dating back to the early 1960s, when Hughes introduced their first "lidar" (laser radar) technology. Although the acronym has since evolved to the current "light detection and ranging", the fundamental concept of emitting a pulse of laser light and measuring the time it takes for it to reflect back from an object has remained unchanged. Over the years, lidar technology has continued to evolve, and its applications have expanded significantly.

The early adoption of commercial airborne LiDAR systems for topographic mapping marked a major milestone in the mid-1990s. These systems resulted from advancements in laser technology as well as the concurrent progress in global positioning systems (GPS) and inertial measurement units (IMUs), which enabled the precise positioning and orientation of their sensors. Together, these technologies laid the foundation for efficient elevation data collection.

Airborne LiDAR is traditionally collected from both fixed-wing planes and helicopters. During a typical collection for topographic mapping, two to eight pulses of laser light are directed at each square meter of terrain. Each pulse can interact with and reflect off multiple surfaces, such as tree branches, low vegetation, and the ground, resulting in multiple "returns" that represent the positions of these surfaces. Modern systems can capture up to four returns per light pulse, while some advanced systems record the full waveform of the reflected light, allowing for post-processing decisions on surface identification. In the case of lower-flying planes and helicopters, data collection can be even denser, with up to 32 or more pulses directed at each square meter. These high densities are particularly valuable in fields like forestry, agriculture, and urban planning, where fine-scale detail is crucial.

Although airborne LiDAR systems provide high-quality data, they come at a significant cost. The hardware alone can cost up to a million dollars, not including the expenses for the aircraft, pilot, and operator. Furthermore, regardless of the size of the data collection area, there is always a substantial minimum deployment cost required to get the plane and equipment airborne and to the survey site. Moreover, survey-grade ground control points are usually required to ensure accurate georeferencing. Weather limitations, the need to collect data during leaf-off conditions, and the time required for processing large datasets can extend the turnaround time for receiving processed airborne LiDAR data to several months.

Fortunately, recent years have witnessed a welcome addition to the LiDAR landscape. Small and relatively affordable LiDAR sensors originally designed for mobile laser scanning and autonomous vehicle navigation have been adapted for use with multi-rotor UAS. These short-range sensors are well-suited for low-altitude flights, and their slow flight speeds result in a high density of LiDAR measurements. As manufacturers continue to enhance these systems, they have carved out a unique niche in the world of

LiDAR, offering data collection from aerial perspectives not achievable from the ground. These systems can provide point densities that rival terrestrial LiDAR for areas ranging from a few acres to hundreds of acres.

This development represents a significant leap in accessibility and affordability for LiDAR data collection, opening up new possibilities for a wide range of applications, from environmental monitoring to infrastructure assessment and urban planning. As these LiDAR technologies continue to mature, they promise to revolutionize the way we capture and utilize high-resolution geospatial data.
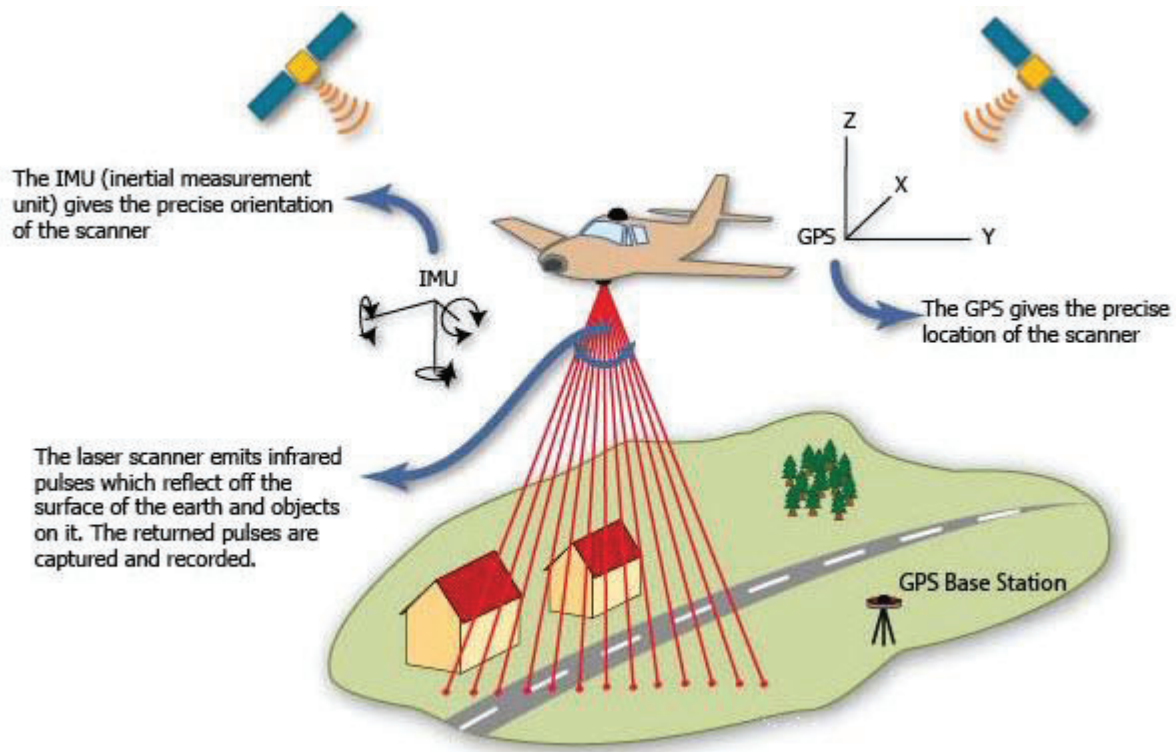
Figure 1. Light Detection and Ranging System Components (elprocus.com)

UNMANNED AERIAL SYSTEMS (UAS)

The advent of small radio-controlled (R/C) airplanes and helicopters marked the beginning of remote-controlled aviation more than half a century ago. However, the landscape of UAS has undergone a remarkable transformation in the past decade, giving rise to many relatively affordable and versatile drones. This transformation can be attributed to three key technological advancements: the development of highly energy-dense lithium-ion and lithium-polymer batteries, the emergence of high-efficiency electric motors utilizing rare-earth magnets, and the availability of compact, powerful, yet cost-effective microcomputers. These technological breakthroughs have paved the way for the rapid development of

both multi-rotor and fixed-wing unmanned aircraft, creating numerous opportunities and challenges in the commercial, research, and government sectors in the United States.

As these new unmanned aircraft rapidly multiplied, potential users found themselves grappling with a complex regulatory environment. It was not until August 2016 that a significant milestone was achieved with the introduction of federal regulations known as 14 CFR Part 107, commonly referred to as Part 107. These regulations, under the authority of the Federal Aviation Administration (FAA), establish a specific class of UASs with a take-off weight of less than 55 pounds, termed small UAS (sUAS). Part 107 outlines detailed requirements relating to registering, operating, and maintaining sUAS. Notably, operators of sUAS are mandated to obtain certification as remote pilots from the FAA.

Part 107 comprises several critical provisions that dictate where and when sUAS may be flown. These regulations include flying sUAS at altitudes below 400 ft above ground level or 400 ft above a structure, ensuring that flights remain within visual line-of-sight, avoiding controlled or restricted airspace, refraining from flying over people or moving vehicles, and avoiding nighttime operations. While these restrictions may appear excessive at first glance, they have ultimately proven to be an asset in ensuring the safe and responsible commercial use of these unmanned aircraft.

Part 107 provides flexibility by allowing individuals to apply for waivers from the FAA. These waivers can provide exemptions from specific rules; however, obtaining them typically involves a rigorous application and approval process. Nonetheless, the introduction of the online Low Altitude Authorization and Notification Capability has streamlined the process of obtaining airspace waivers, allowing for real-time approval in certain cases.

For sUAS utilized in tasks such as mapping and aerial surveys, the aircraft typically follow programmed flight paths, relying on onboard GPS, electronic compasses, and IMUs to maintain the correct course and speed. The accuracy of GPS data can vary depending on the quality of the onboard receivers and whether they incorporate correction data from ground-based receivers. Onboard sensors, including cameras and more advanced payloads like LiDAR, often require precise location information and sometimes pose information (orientation of the sensor) to accurately process data. Some sensors rely on the location and pose information provided by the sUAS, while others may use separate and potentially more accurate GPS, compasses, or IMUs.

The flight time of sUAS is influenced by various factors, including the design of the system, the weight of the current payload, battery capacity, and prevailing weather conditions. It is intuitive that increased payloads lead to decreased flight time. However, less obvious factors such as temperature come into play, as cold batteries cannot provide as high a current as warm batteries, impacting overall flight duration. Wind speed is another factor, particularly for multi-rotor aircraft, as wind speeds higher than the speed of flight require additional power, regardless of the direction of flight. Consequently, flight planning is just as critical for sUAS as it is for large manned aircraft, ensuring safety, efficiency, and mission success.

Figure 2. DJI Matrice 600 Pro (M600 Pro) Hexacopter (left, aeroexpo) and Phoenix LiDAR Systems AL3-16 (right, maverickdrone.com)

DEPARTMENTS OF TRANSPORTATION'S USE OF UAS LIDAR

Ever since the inception of UAS, DOT have been interested in using the tool to increase their productivity and produce better results for various applications, including surveying, bridge inspection, traffic monitoring, public outreach, construction observation, and many more. However, over the past five years, DOT's interest and research into these system has ramped up significantly. There are currently over 20 DOT-related research projects focusing on UAS, especially on the many areas of UAS use, including bridge inspection, traffic studies, and potential crash issues on roadways. Additionally, many overview type projects which provide potential uses for UAS have been completed (Brooks et al. 2014). However, very few projects have focused primarily on UAS for direct surveying applications and even fewer have focused on using UAS LiDAR systems (Jozkow et al. 2017, Jozkow et al. 2016, Amon et al. 2015). This project will be one of the first transportation-related projects to evaluate both the accuracy and cost benefit of using LiDAR systems to develop digital terrain models for transportation projects.

CHAPTER 3. METHODOLOGY AND STUDY AREAS

This chapter provides information on the equipment used for the project, the field testing configurations and data collection methodology used, and the individual sites studied.

PROJECT EQUIPMENT

UAS AND LIDAR EQUIPMENT

A DJI M600 Pro with TB48S batteries, which has a bare weight (with batteries) of 22 lb (see Figure 3), was flown over the five project sites. Phoenix LiDAR Systems' AL3-16 payload weighed 8 lb and was mounted rigidly on the airframe centerline, directly below the body, with a global navigation satellite system (GNSS) antenna mounted on center, directly above the body. Total take-off weight was 30 lb, approximately 4 lb under the maximum recommended take-off weight. There were no modifications to the UAS other than the sensor system. The AL3-16 utilizes a Velodyne Puck 16 sensor, along with a KVH 1725 FOG-based inertial measurement unit and Novatel GNSS receiver utilized in PPK/PPP mode, providing a specified accuracy of 25/35 mm and a root mean squared error in the 50 mm range. The system has a maximum recommended altitude during measurement of 40–45 m. A CHC X900 GNSS receiver was used as a local PPK base station (see Figure 4). A small UAS (DJI Mavic Air or Phantom) was utilized for test flights to ensure safe operation of the M600 over the planned flight path. A 55-ft manlift was utilized at all sites to allow the remote pilot to observe the UAS more easily during flight (see Figure 5).

CONVENTIONAL SURVEY EQUIPMENT

For this project, conventional surveying for checkpoints was completed using both a GNSS RTK system and a robotic total station. Leica Viva GS15 receivers and CS15 controllers were used to collect survey-grade data for the project (see Figure 6). The GS15s are multi-capacity, GNSS-capable units that can simultaneously track the US NAVSTAR, Russian GLONASS, and European GALILEO satellites. These units are also capable of acquiring the next generation L5 frequency. The CS15s are comprehensive data loggers used to configure the GS15 receivers. This system was used to collect most of the checkpoints used for the project. However, for areas with extensive tree cover, a Trimble 5600 DR200+ Robotic total station, which possesses long-range surveying capabilities, was used to survey the checkpoints for the project (See Figure 7). This instrument is capable of 2-inch angular precision, and using an active prism, the electronic distance measure can measure distances of up to 5,500 m, with an accuracy of 2 mm +/- 2 ppm.

Figure 3. UAS and LiDAR Being Setup for Flight at the Site

Figure 4. CHC 900 GNSS Base Station for LiDAR and Wifi Antenna

Figure 5. Manlift (55 ft) for Lifting the UAS Operator to Maintain His/Her Visual Line-of-Sight During Flight

Figure 6. The Leica Viva GS-15 (left) and Leica Viva GS-15 GNSS Systems

Figure 7. The Trimble 5600 DR200+ Robotic Total Station (left) and the Trimble Setup on Site (right)

GENERAL DATA COLLECTION METHODOLOGY

Before heading to the project sites, mission plans were created for the flights. Flight plans were designed to cover at least 400 foot each side of the current roadway. A combination of Google Earth, Phoenix LiDAR Systems' Flightplanner, and Litchi Mission Hub were used to create the flight plans. Using terrain-following based on USGS 1m 3DEP elevation data, flight paths were created at an altitude of 45 m above ground level (AGL), with 50 percent side laps between adjacent flight lines. A cross-tie flight line was included at the end of each flight path, 90° to the other flight lines, to better tie together the flight line data during processing. Road crossings were kept to a minimum in the flight plans.

Data collection days were selected based on weather (no precipitation, good visibility, and acceptable wind speeds) and environmental (leaf-off, no snow on ground, and dry vegetation) conditions. To maintain the visual line-of-sight of the UAS during data collection, a Genie TZ50/30 towable manlift (50-ft vertical work height) was used as a piloting platform. Visual observers, equipped with two-way radios, were used as traffic spotters. The LiDAR system GNSS base station, located on a pin that would be included in the GNSS/RTK survey checkpoints as part of the project data, was turned on before all flights on each mission and shutdown after all flights were completed.

Each LiDAR flight began with a 5-min static alignment of the inertial measurement unit (IMU) while the UAS was on the ground. Next, the UAS was launched to the altitude of the first waypoint, then flown at 10 m/s in a straight line for 10 seconds, the first step in the dynamic alignment of the IMU. Afterward, the UAS was manually flown a full 360° in each direction (figure-eight) to complete the dynamic alignment. Finally, the UAS was flown to line up with the first waypoint, and the flight plan was uploaded. At this point, the LiDAR sensor was enabled, and the LiDAR operator confirmed that LiDAR data were being collected. The UAS flew the entire flight plan, then stopped at the last waypoint. LiDAR collection was then disabled. To complete the mission, the dynamic and static alignment steps were repeated, this time in the reverse order. The UAS was then landed manually. After 5 min of static alignment on the ground, the UAS was shut down in preparation for the next flight.

At the recommended altitude of 45 m AGL, the point density on the ground averaged about 240 points per square meter (22 points per square foot). Data were recovered from the onboard LiDAR computer and the GNSS base station after the flights were completed.

For each site, conventional surveying was completed at the same time as the UAS flights except for the Mountain Home site, where the UAS was damaged during takeoff, leading to the UAS LiDAR data being collected approximately 5 weeks after the conventional survey data was collected. For the GNSS/RTK, a base station was set up to record static over an ARDOT survey monument that was part of the control survey for the project. This way, both the UAS LiDAR and conventional surveying were tied into the horizontal and vertical datums of the ARDOT control survey. The GPS rover was used to collect checkpoints. An average of 100 checkpoints were collected at each site. The checkpoints were taken along the roadway of each site and divided into two types—hard and soft surface points. Hard surface points include points on asphalt roads, concrete roads, pavements, and parking areas, while soft surface points include grass points and bare ground. Grass points were further classified as tall and short grass. A few

points were also taken under trees, which fall into the soft surface group. Soft surface points were taken on either side of the hard surfaced roads. Figure 8 shows examples of each surface type used for the project. The total station was also set up over an ARDOT control point and back sighted against another control point. Checkpoints were taken on both hard and soft surfaces, with a focus on soft surface points under tree cover.

GENERAL DATA PROCESSING METHODOLOGY

Initial LiDAR data processing was performed using Phoenix LiDAR System's LiDARMill online software service. GNSS data from the base station were uploaded first and submitted to both the National Geodetic Service's OPUS online correction service and Trimble's RTX correction service; whichever solution had the least error was the one used. The IMU trajectory data and rover GNSS data were uploaded next; these were processed against the corrected base station data to calculate and optimized trajectory for the drone and LiDAR system. Finally, the raw LiDAR data were uploaded to LiDAR mill, where they were corrected, aligned, and fused to adjacent flight lines. LiDARMill then used an artificial intelligence classification algorithm to classify the LiDAR points into ground, buildings, vegetation, noise, etc. The LiDAR was projected to the specified State Plane coordinate system, either AR North or AR South.

Horizontal: NAD83(2011)/Arkansas North (ftUS) (EPSG:6411) (US survey foot), Vertical: NAVD88 height (EPSG:5703) (US survey foot), Geoid us_noaa_g2018u0.tif (EPSG:6319) (EPOCH 2010)

Or

Horizontal: NAD83(2011)/Arkansas South (ftUS) (EPSG:6413) (US survey foot), Vertical: NAVD88 height (EPSG:5703) (US survey foot), Geoid us_noaa_g2018u0.tif (EPSG:6319)

All the project sites fall in the Arkansas North State Plane (Zone 301) except the bridge site at Humnoke of Arkansas, which falls in the Arkansas South State Plane (Zone 302).

Downloadable products included processing reports, a classified point cloud (.LAZ format), a gridded digital terrain model (DTM) (.LAZ format), contours (.shp), and rasterized DTM and canopy height models. Although a good starting point, the ground class of points in the classified point cloud was found to be rather sparse, with many ground points being unclassified. Additionally, the entire point cloud needed to be translated to correct for differences in the position of the OPUS/RTX-corrected base station and its surveyed location, which was tied into the ARDOT control survey for each project. To achieve this, LAStools (https://lastools.org) were used to reclassify the point cloud and derive a more dense ground classification. See Appendix A for a detailed LAStools Workflow section. This workflow was aimed at reducing the "noise" in the LiDAR data to more accurately determine the ground surface. To this end, median values were calculated for the "fuzzy" layer of points that should be that single surface, after first removing vegetation and buildings. Once this new classification was computed, it was translated in the X, Y, and Z axes by the differences in the position of the OPUS/RTX-corrected base station and its surveyed location. Afterwards, LAStools were used to create a raster DEM file at a resolution of 0.25 ft (pixel size). The general workflow is provided below as an example.

Point cloud was downloaded from LiDARMill and reclassified through the following steps:

1. The unclassified dataset was set to Classification 1. The raw LAS file was tiled, maintaining less than 15 million points in each tile and including a 60-ft buffer.
2. The data were checked, and exact duplicate points were removed.
3. The isolated points as noise, especially those below the ground.
4. The function "lasthin" was used to classify a subset of points with Classification code 8 on which the ground classification was run. Each point that was closest to the 5th percentile in elevation was classified per 0.75 ft x 0.75 ft grid cell, provided there were at least 20 non-noise points in a cell. The process was repeated by increasing the cell size to 1.50 ft x 1.50 ft and 3.00 ft x 3.00 ft.
5. The points temporarily classified into Classification code 8 in the previous step were classified using the function "lasground". The resulting ground points were a lower envelope of the "fluffy" sampled surfaces produced by the Velodyne LiDAR. The "lasheight" classification was used to thicken the ground by moving all points between 0.03 ft below and 0.18 ft above the TIN of these "low-ground" points to a temporary Classification code 6, which represents a "thick ground". The overly aggressive noise classification was also undone above the ground by setting all higher points back to Classification code 1 (i.e., unclassified).
6. From the "thick ground", a "median ground" was computed using the function "lasthin" in a fashion similar to that in Step 4.
7. The function "lasnoise" was run again with more conservative settings to remove the noise points that were sprinkled around the scene.
8. The function "lasclassify" was then used to classify the scene. The unused classifications were moved to Classification code 1 (unclassified).
9. The buffers from the tile were then removed.
10. The tiles were merged into a single .LAZ format point cloud.
11. The entire point cloud was translated to align with the surveyed measurement of LiDAR base station pin.
12. A 0.25-ft resolution bare earth DEM was finally created in NAD83 State Plane Arkansas North (U.S. survey feet) from the only points in ground classification.

The GNSS/RTK data were processed to get the exact coordinates as well as the ellipsoidal and orthometric heights for each point. For each project, the survey was tied into the ArDOT control survey by placing the GNSS base station over a known ArDOT control point. The GNSS rover was post processed to correct the coordinates with the base station coordinates.
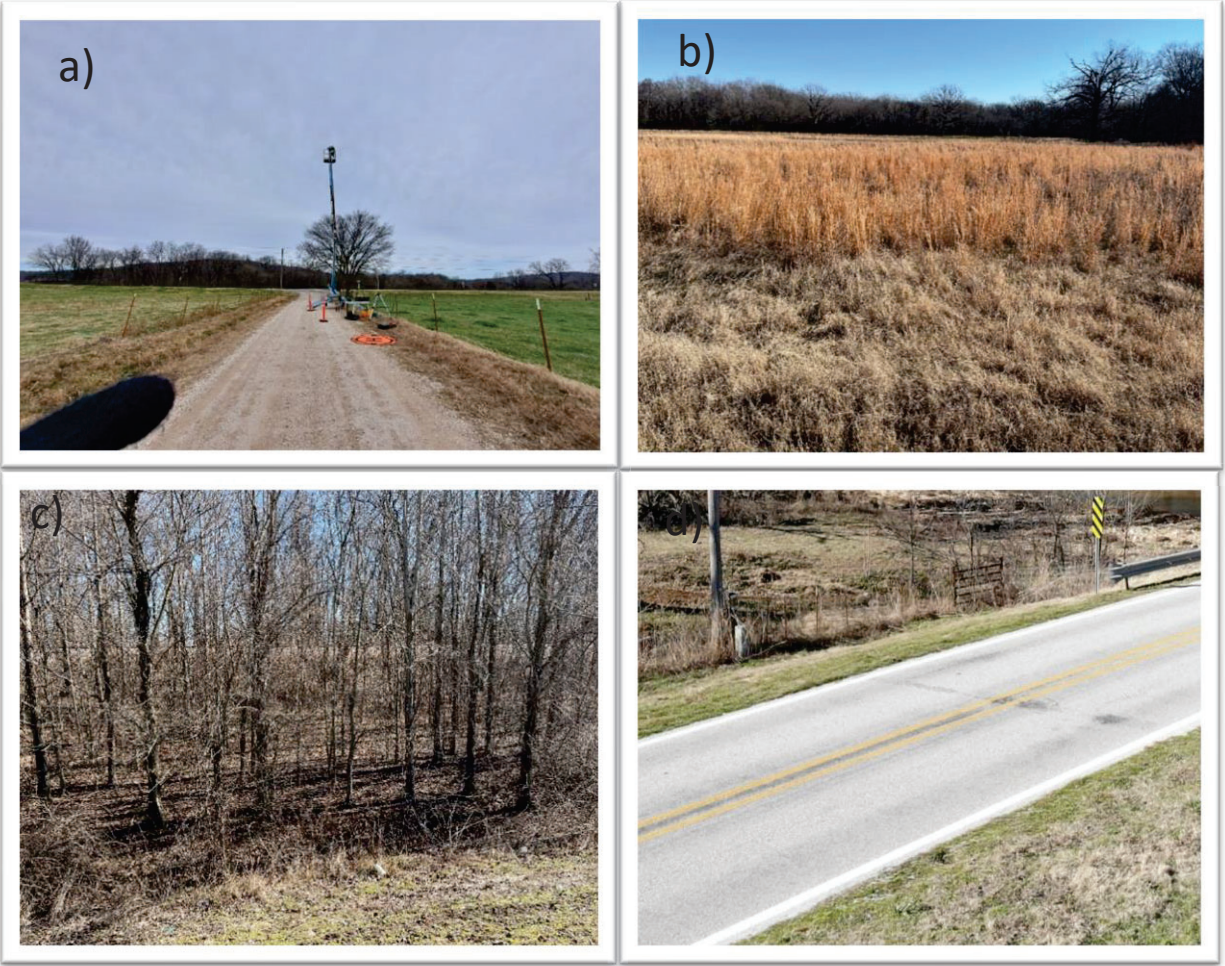
Figure 8. Different Surface Types at the Bridge Project Sites. A) Gravel Road, b) Grass and Tall Grass, c) Trees, and d) Asphalt Road

PROJECT SITE INFORMATION

For this project, five bridge sites were selected from which UAS LiDAR and conventional survey data were collected using the methodology discussed above. The locations of the test sites are presented in Figure 9. The location of each test site, along with the ARDOT job number, latitude, longitude, and date when LiDAR and conventional surveying were completed, is tabulated in Table 1. A description of each site is provided in the next section.

Figure 9. Locations of the Test Sites in Arkansas. (Clockwise From Top Left) Lincoln Bridge 1 (East) and 2 (West), Humnoke, Frenchman's Bayou, and Mountain Home

Table 1. Sites for the TRC2106 Project

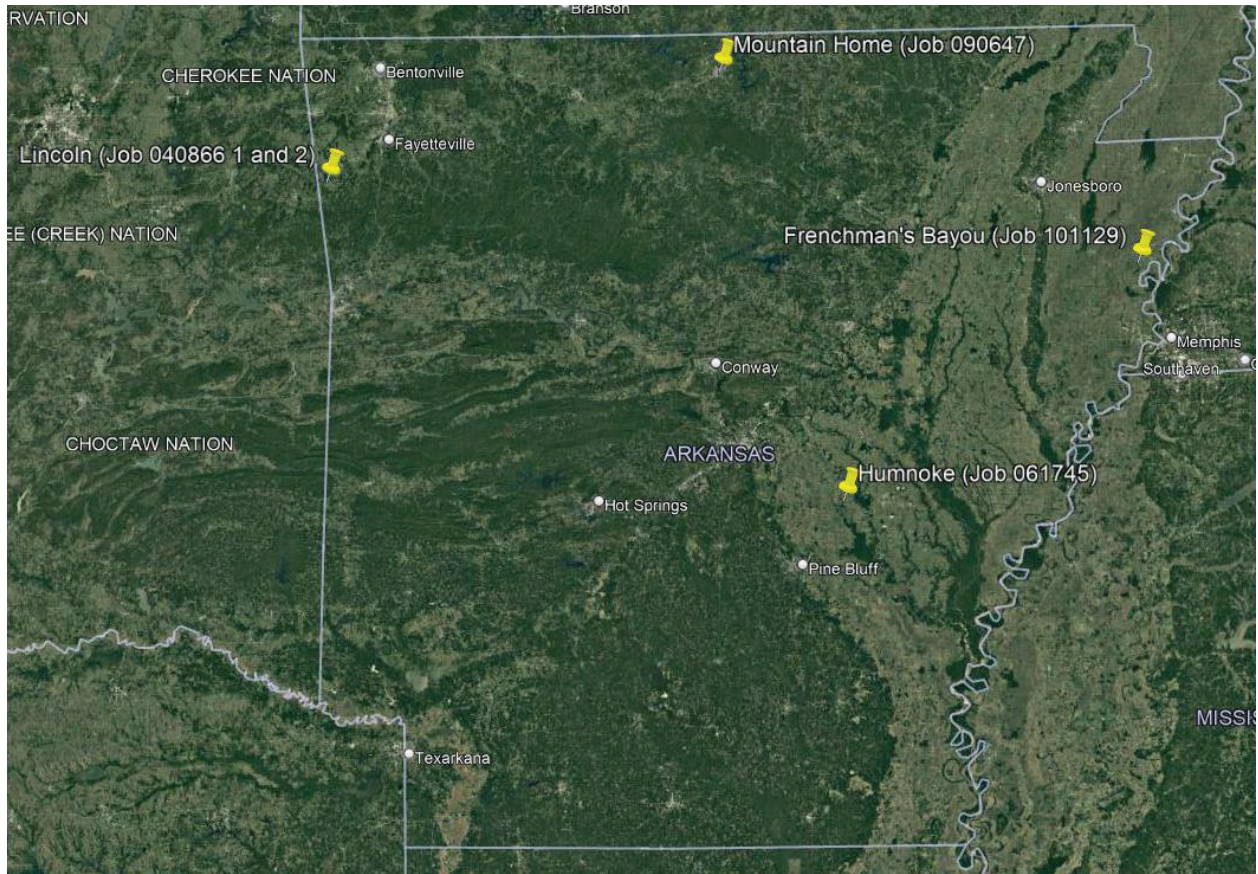| Site Number	Location	Project ID	Latitude	Longitude	LiDAR Data Collection Date	Conventional Survey Data Collection Date
1)	Lincoln, Washington County, AR	Job 040866 Bridge 1 (east)	35.872446	-94.457282	December 20, 2021	December 20, 2021
2)	Lincoln, Washington County, AR	Job 040866 Bridge 2 (west)	35.877001	-94.468389	January 13, 2022	January 13, 2022
3)	Humnoke, Lonoke County, AR	Job 061745	34.486621	-91.758741	January 24, 2022	January 24, 2022
4)	Frenchman, Mississippi County, AR	Job 101129	35.468304	-90.181926	February 14, 2022	February 14, 2022
5)	Mountain Home, AR	Job 090647	36.332779	-92.370756	April 22, 2022	March 14, 2022

LINCOLN BRIDGE 1 (EAST) JOB 040866

UAS LiDAR and conventional surveys were conducted at the Lincoln Bridge 1 (East) site on December 20, 2021. The UAS flight path at the site is shown in Figure 10. In Figure 11, the raw LiDAR data from the survey are shown and colored based on elevation. A picture of the site is provided in Figure 12; the grass along the road was relatively short at the time of the survey. Figure 13 provides pictures of the UAS LiDAR and GNSS survey setup for the project. The checkpoints for each surface classification are tabulated in Table 2, and the location of the checkpoints at this site are provided in Figure 14. A total of 120 checkpoints were collected at the site, with 81 soft surface points, 37 hard surface points, and two control points. To collect checkpoints at this site, only GNSS conventional surveying was conducted.

Figure 10. Flight Path for Lincoln Bridge 1 (East) (Job 040866)

Figure 11. Raw LiDAR Data Colored by Elevation, Collected at Lincoln Bridge 1 (East) (Job 040866)

Figure 12. Photo of Lincoln Bridge 1 (East) (Job 040866)

Figure 13. LiDAR and GNSS Being Setup for Lincoln Bridge 1 (East) (Job 040866)

Table 2. Checkpoint Types Surveyed at Lincoln Bridge 1 (East) (Job 040866)

Type of Points at the Lincoln East Bridge	No. of Points	Total
Soft Surface (Grass) comparison with GNSS RTK	71	
Soft Surface (Tree) comparison with GNSS RTK	10	
Total Soft Surface Survey Points		81
Hard Surface (Road) with GNSS RTK	37	
Total Hard Surface Survey Points		37
Control Points with GNSS at Lincoln East Bridge	2	2
Total Survey Points		**120**
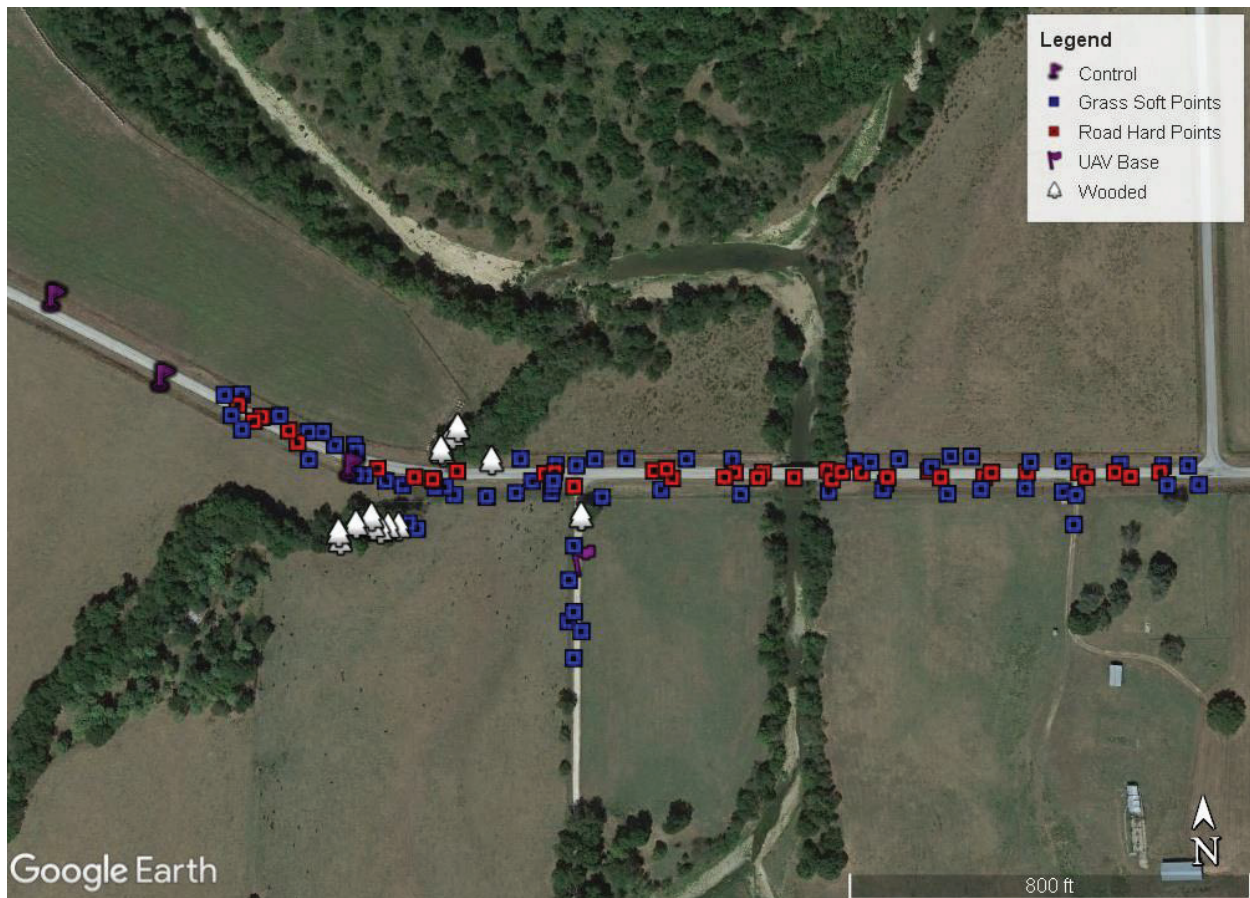
Figure 14. GNSS Checkpoints and Their Classification for Lincoln Bridge 1 (East) (Job 040866)

LINCOLN BRIDGE 2 (WEST), JOB 040866

UAS LiDAR and conventional surveys were conducted at the Lincoln Bridge 2 (West) site on January 13, 2022. The flight path at this site is shown in Figure 15 below. In Figure 16, the raw LiDAR data from the survey are shown and colored based on elevation. A picture of the site is provided in Figure 17; the grass along the road was relatively short at the time of this survey. Trees located to the south of the road were surveyed using conventional surveying. Figure 18 displays images of the UAS LiDAR and GNSS survey being setup for the project. The checkpoints for each surface classification are tabulated in Table 3, and the location of the checkpoints at the site are provided in Figure 19. A total of 246 checkpoints were collected at the site, with 183 soft surface points, 60 hard surface points, and three control points. To collect checkpoints for the project at this site, GNSS and total station conventional surveying was conducted.
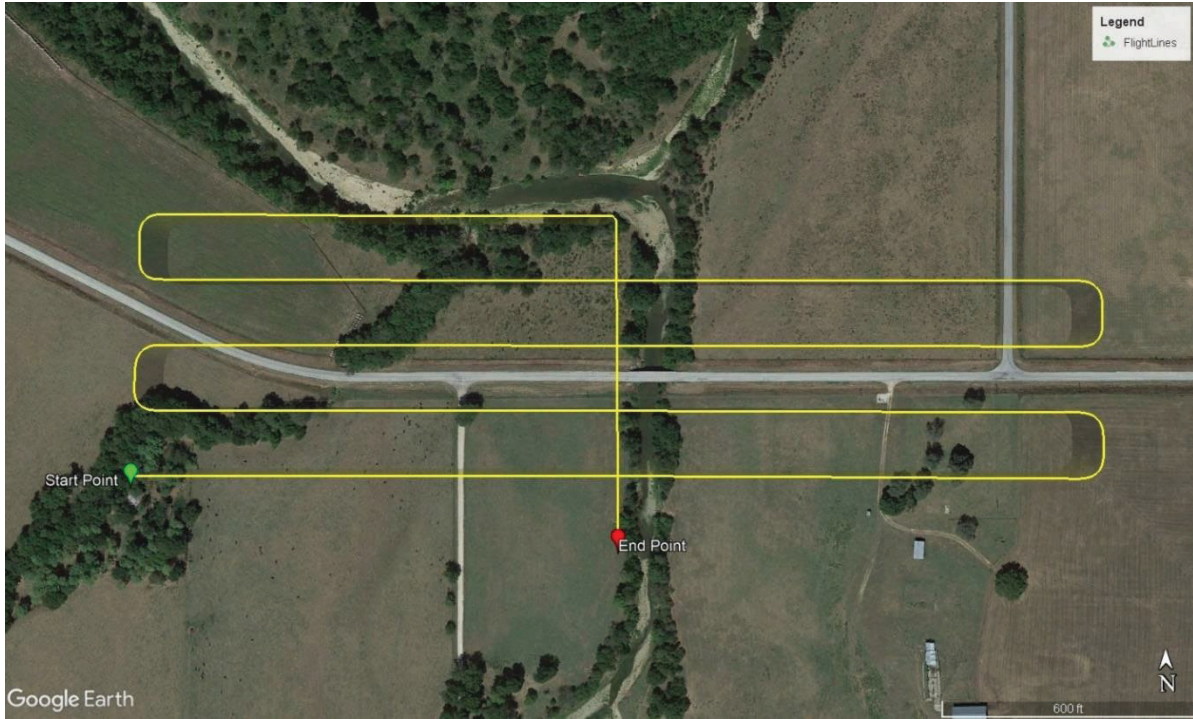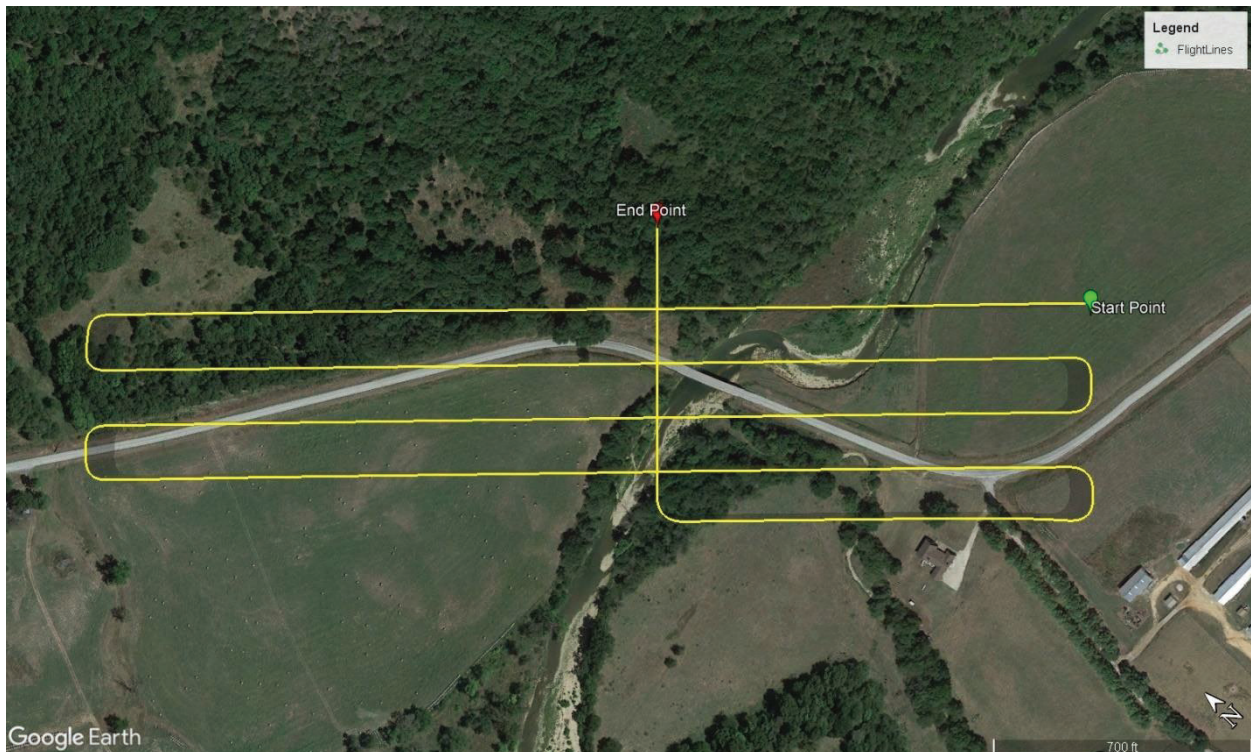

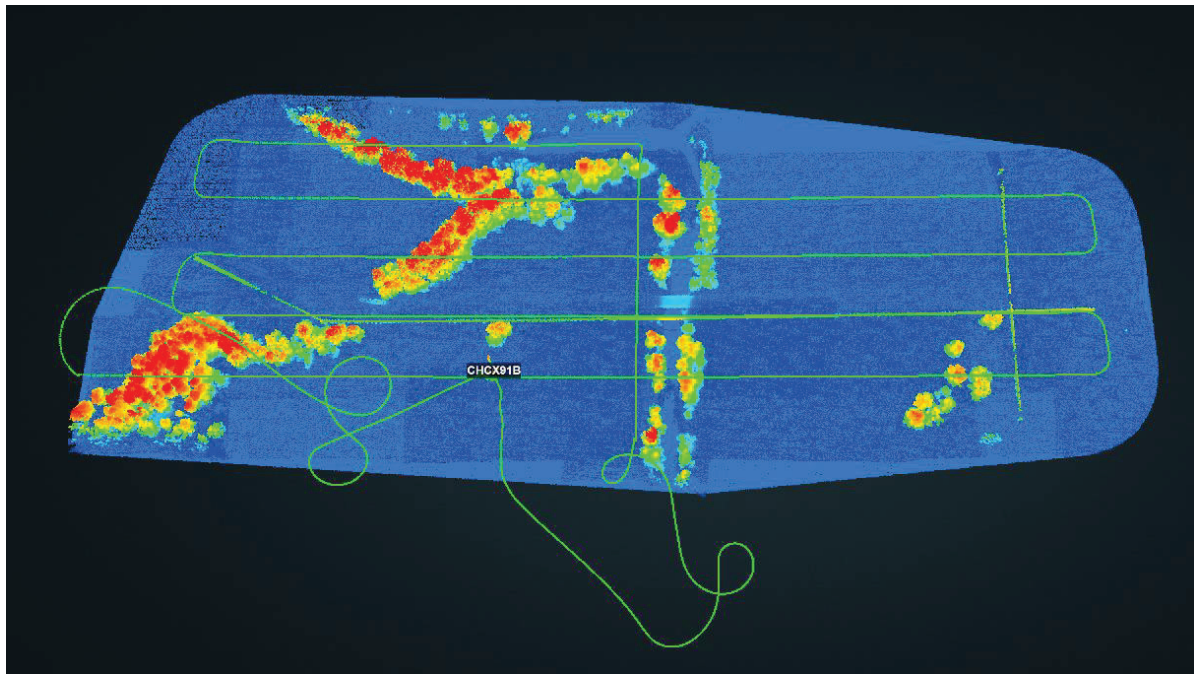**Figure 15. Flight Path for Lincoln Bridge 2 (West) (Job 040866)**
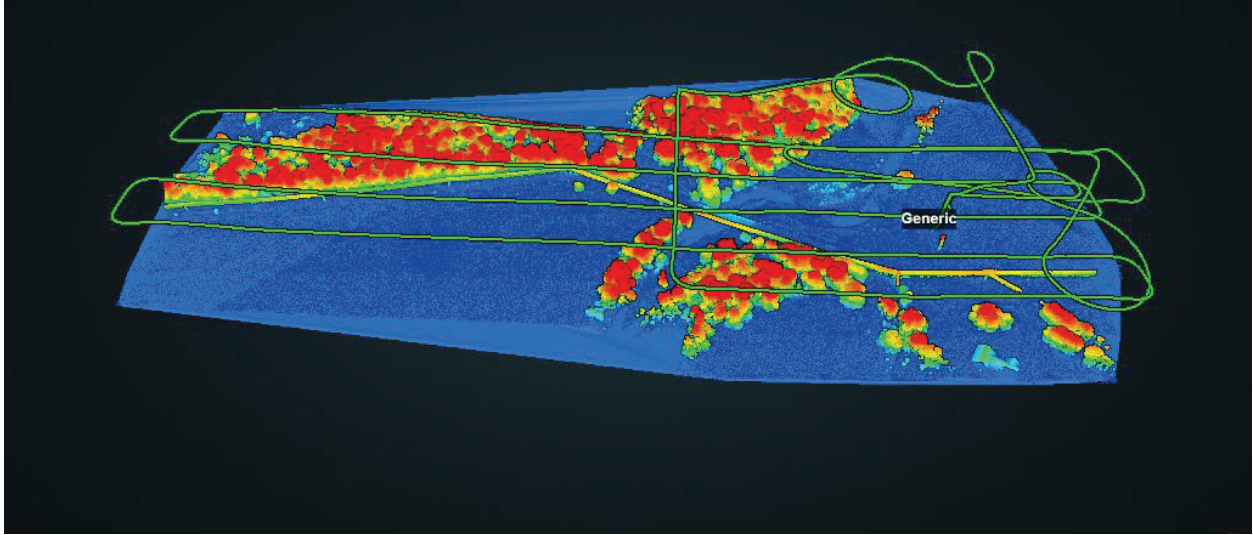
Figure 16. Raw LiDAR Data Colored by Elevation, Collected at Lincoln Bridge 2 (West) (Job 040866)

Figure 17. A Photo of Lincoln Bridge 2 (West) (Job 040866)
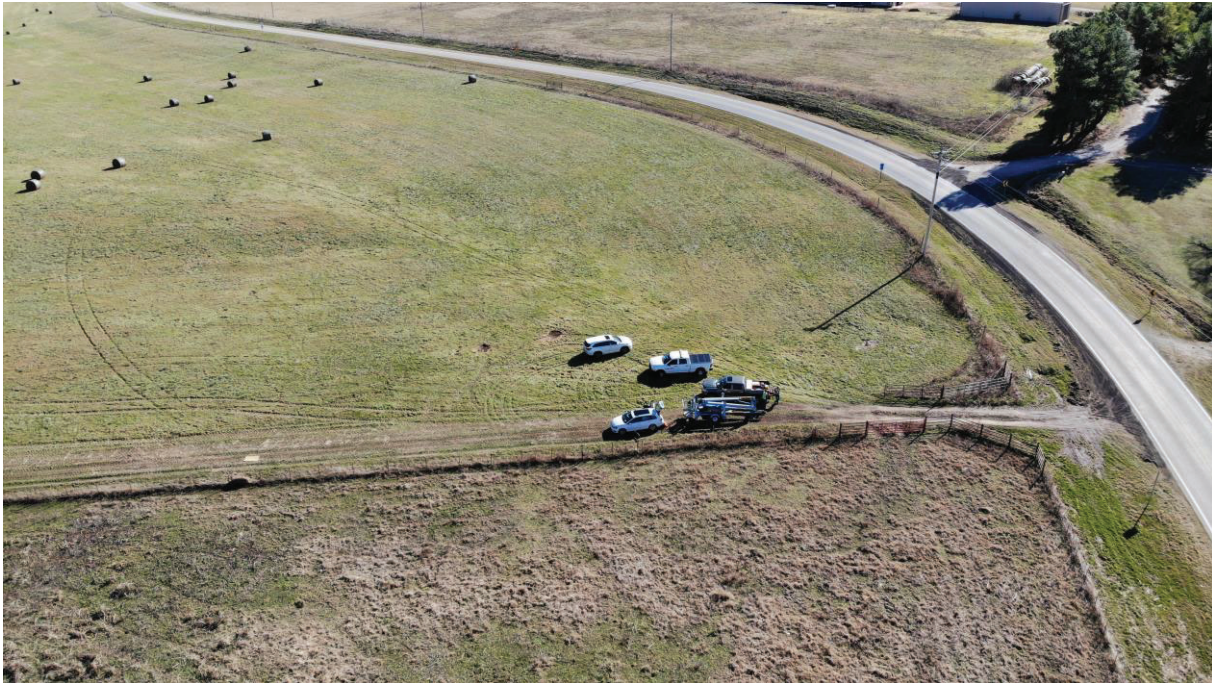
Figure 18. LiDAR and GNSS Setup at Lincoln Bridge 2 (West) (Job 040866)

Table 3. Checkpoint types Surveyed at Lincoln Bridge 2 (West) (Job 040866)

Type of Point at Lincoln West Bridge	No of Points	Total
Soft Surface (Grass) comparison with GNSS	122	
Soft Surface (Grass) comparison with Total Station	34	
Soft Surface (Tree) comparison with Total Station	24	
Total Soft Surface Survey Points		183
Hard Surface (Road) comparison with GNSS RTK	53	
Hard Surface (Road) comparison with Total Station	7	
Total Hard Surface Survey Points		60
Control Points with GNSS at Humnoke Bridge	3	3
Total Survey Points		**246**
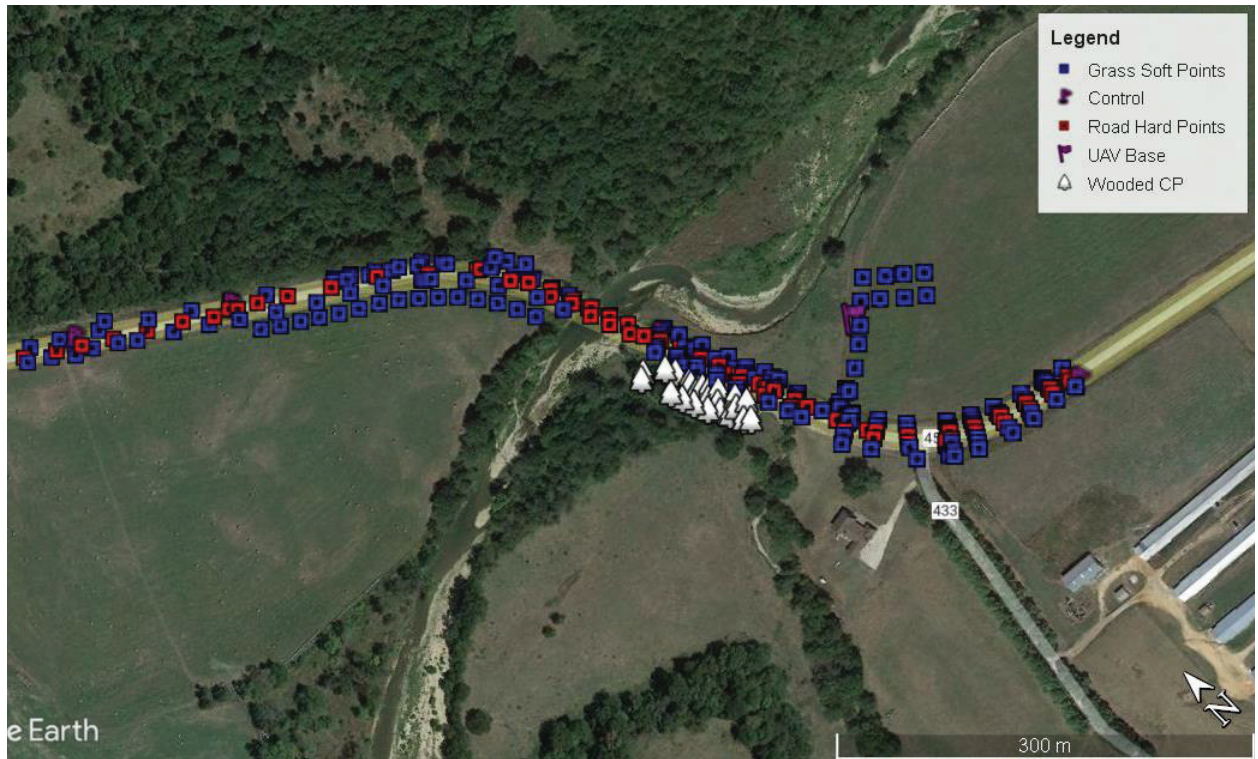
Figure 19. GNSS/Total Station Checkpoints and Their Classification at Lincoln Bridge 2 (West) (Job 040866)

HUMNOKE, ARKANSAS JOB 061745

UAS LiDAR and conventional surveys were conducted at the Humnoke site on January 24, 2022. The flight path at the site is shown in Figure 20 below, and the raw LiDAR data from the survey are shown in Figure 21, colored based on elevation. Two separate flights were utilized for this site due to the turn in the road. A picture of the site is provided in Figure 22, which shows the surface conditions at the site; the grass along the road was medium height at the time of the survey. However, tall grass existed along areas of the road, and trees were located in some parts of the site. All these surface types were surveyed using conventional surveying. Figure 23 provides pictures of the UAS LiDAR and GNSS survey setup for the project. In Table 4, the checkpoints for each surface classification are tabulated, and in Figure 24, the location of the checkpoints at the site are provided. A total of 274 checkpoints were collected at this site, with 147 soft surface points, 114 hard surface points, and 13 control points. For checkpoint collection at this site, GNSS and total station conventional surveying were conducted. In addition, ARDOT collected UAS LiDAR data at this site independent of this project. Their data will be compared to the UARK LiDAR data collected in this project.
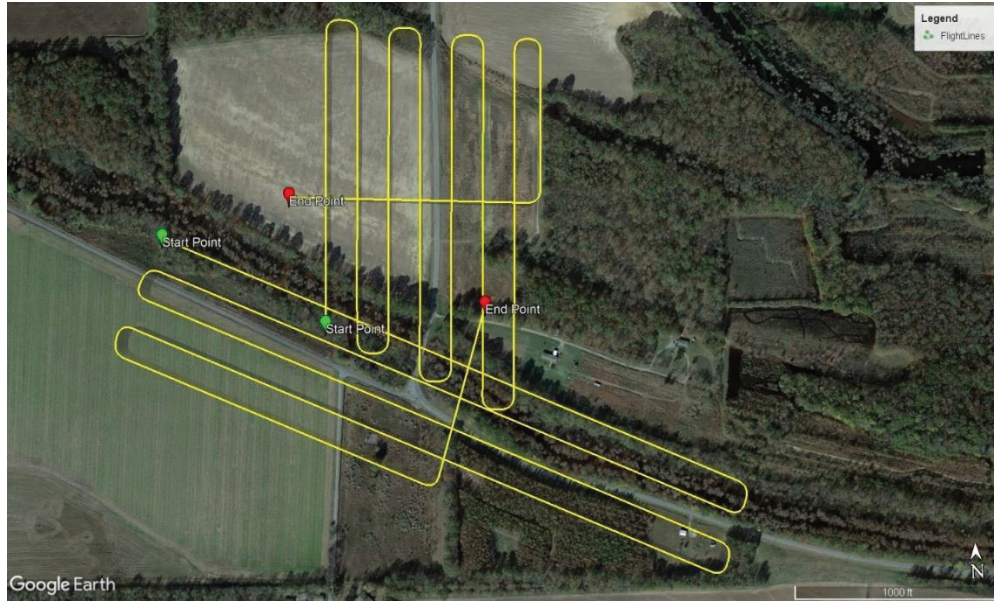
Figure 20. Flight Path at the Humnoke Site (Job 061745)
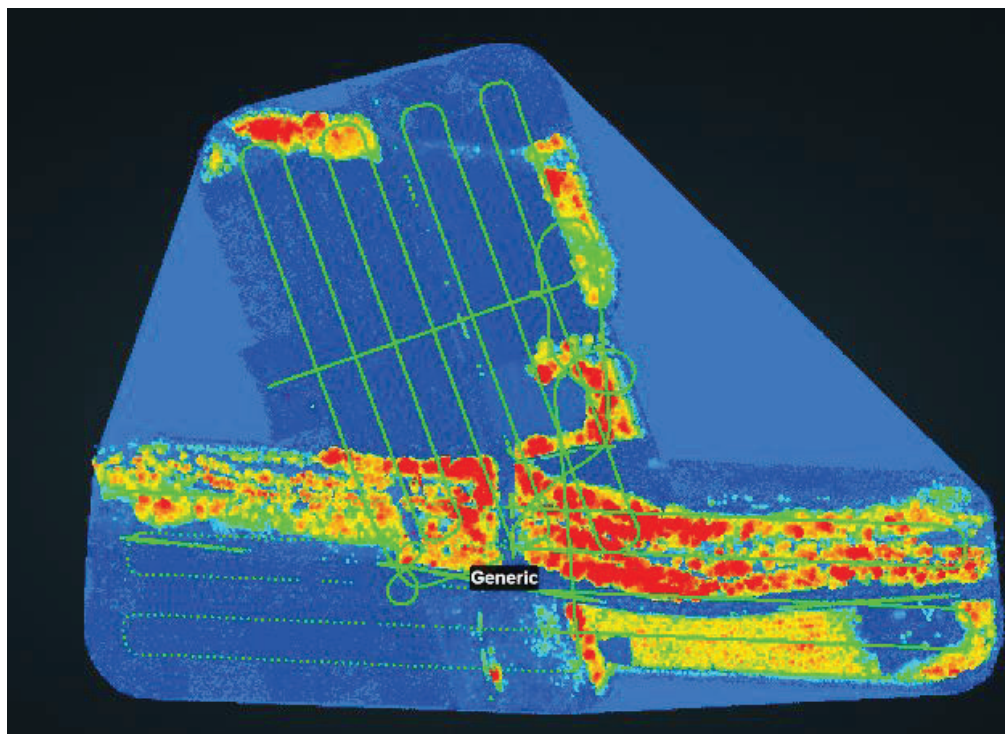
Figure 21. Raw LiDAR Data Colored by Elevation, Collected at the Humnoke Site (Job 061745)

Figure 22. Example of Surface Conditions at the Humnoke Site (Job 061745)

Figure 23. UAS with LiDAR System (Right Image) and Manlift to Elevate Drone Pilot (Left Image) at the Humnoke Site (Job 061745)

Table 4. Checkpoints Types Surveyed at the Humnoke Site, Job 061745

Type of Points at Humnoke Bridge	No. of Points	Total
Soft Surface (Grass) comparison with GNSS	103	
Soft Surface (Tall Grass) comparison with GNSS	18	
Soft Surface (Tall Grass) comparison with Total Station	4	
Soft Surface (Tree) comparison with Total Station	16	
Total Soft Surface Survey Points		141
Hard Surface (Road) comparison with GNSS RTK	57	
Hard Surface (Road) comparison with Total Station	3	
Hard Surface (Gravel) comparison with GNSS RTK	50	
Total Hard Surface Survey Points		110
Control Points with GNSS at Humnoke Bridge	7	
Control Points with Total Station at Humnoke Bridge	6	
Total Control Survey Points		13
Total Survey Points		264

Figure 24. GNSS/Total Station Checkpoints and Their Classification at the Humnoke Site

36

FRENCHMAN'S BAYOU, ARKANSAS JOB 101129

UAS LiDAR and conventional surveys were conducted at the Frenchman's Bayou site on February 14, 2022. The flight path at this site is shown in Figure 25 below. In Figure 26, the raw LiDAR data from the survey are shown and colored based on elevation. A picture of the site is provided in Figure 27, showing examples of the surface conditions at the site. The grass along the road was relatively short at the time of the survey. However, tall grass/weeds existed along areas of the road and stands of trees were located in parts of the site. All these surface types were surveyed using conventional surveying. Figure 28 provides pictures of the UAS LiDAR and GNSS survey setup for the project. In Table 5, the checkpoints for each surface classification are tabulated, and in Figure 29, the location of the checkpoints at the site are shown. A total of 213 checkpoints were collected at the site, with 130 soft surface points, 77 hard surface points, and six control points. For checkpoint collection at this site, GNSS and total station conventional surveying were conducted. Additionally, Helicopter LiDAR data were collected independent of this project. These data will be compared to the UARK LiDAR data collected in this project.
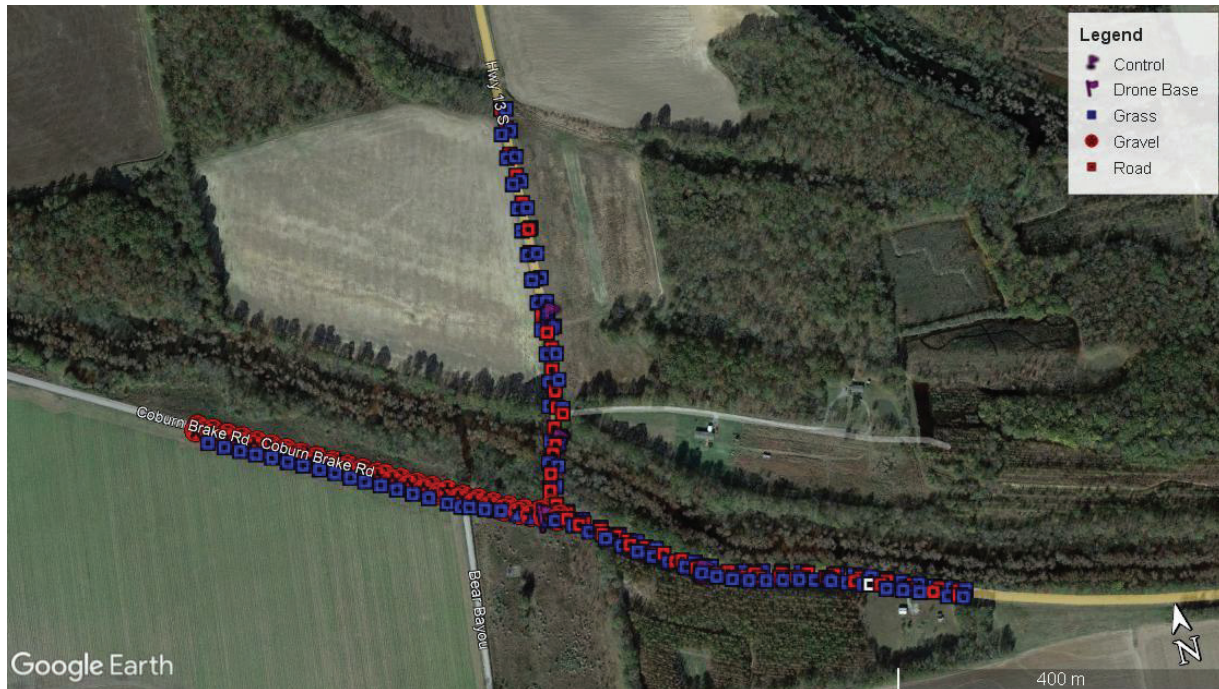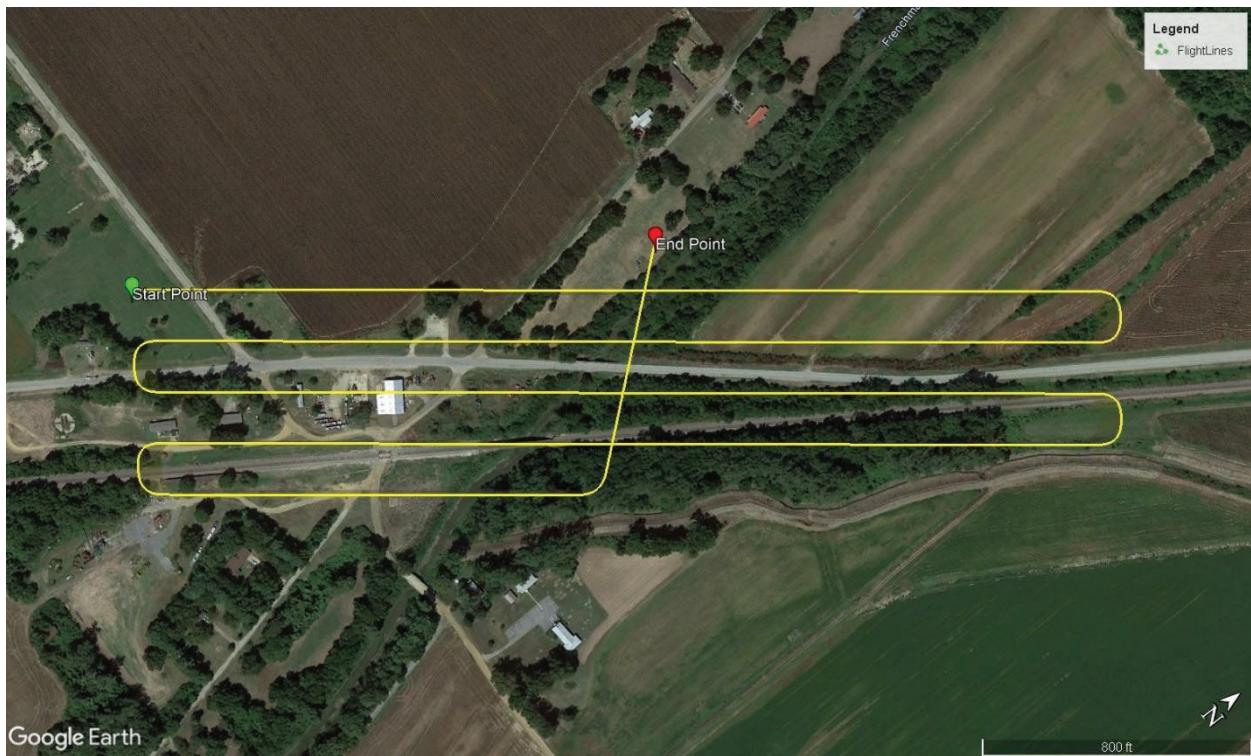

Figure 25. Flight Path at Frenchman's Bayou (Job 101129)
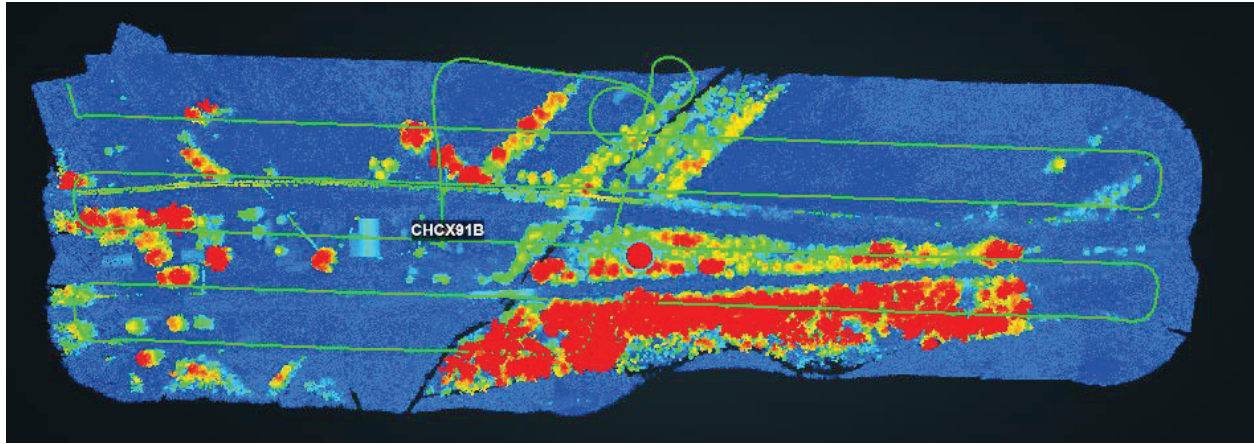
Figure 26. Raw LiDAR Data Colored by Elevation, Collected at the Frenchman's Bayou Site (Job 101129)

Figure 27. Example of Surface Conditions at Frenchman's Bayou

Figure 28. UAS LiDAR Being Setup at Frenchman's Bayou

Table 5. Checkpoint Types Surveyed at Frenchman's Bayou

Type of Points at the Frenchman Bridge	No. of Points	Total
Soft Surface (Grass) comparison with GNSS	68	
Soft Surface (Grass) comparison with Total Station	9	
Soft Surface (Tall Grass) comparison with GNSS	22	
Soft Surface (Tall Grass) comparison with Total Station	14	
Soft Surface (Tree) comparison with Total Station	17	
Total Soft Surface Survey Points		**130**
Hard Surface (Road) comparison with GNSS RTK	56	
Hard Surface (Road) comparison with Total Station	9	
Hard Surface (Gravel) comparison with GNSS RTK	12	
Total Hard Surface Points		**77**
Control Points with GNSS at the Frenchman Bridge	1	
Control Points with Total Station at the Frenchman Bridge	5	
Total Control Survey Points		**6**
Total Survey Points		**213**

Figure 29. GNSS/Total Station Checkpoints and Their Classification at Frenchman's Bayou

MOUNTAIN HOME, ARKANSAS JOB 090647

UAS LiDAR was conducted at the Mountain Home site on April 22, 2022, and conventional surveying was conducted on March 14, 2022. There were problems with the UAS LiDAR, which prevented the collection of LiDAR and conventional surveying data on the same day. The grass had started to grow and trees had begun to leaf out during the April 22 survey. Because of heavy traffic on the roadway, no asphalt hard surface points were collected at this site. Instead, parking lot and other hard surface points were collected. The flight path at this site is shown in Figure 30 below. In Figure 31, the raw LiDAR data from the survey are shown and colored based on elevation. The grass along the road was relatively short at the time of the survey. However, tall grass/weeds existed in areas along the bridge. All these surface types were surveyed using conventional surveying. In Table 6, the checkpoints for each surface classification are tabulated, and in Figure 32, the location of the checkpoints at this site are shown. A total of 129 checkpoints were collected at the site, with 89 soft surface points, 37 hard surface points, and three control points. For checkpoint collection at this site, only GNSS conventional surveying was conducted. In addition, ARDOT collected UAS LiDAR at this site independent of this project. These data will be compared to the UARK LiDAR data collected in this project.
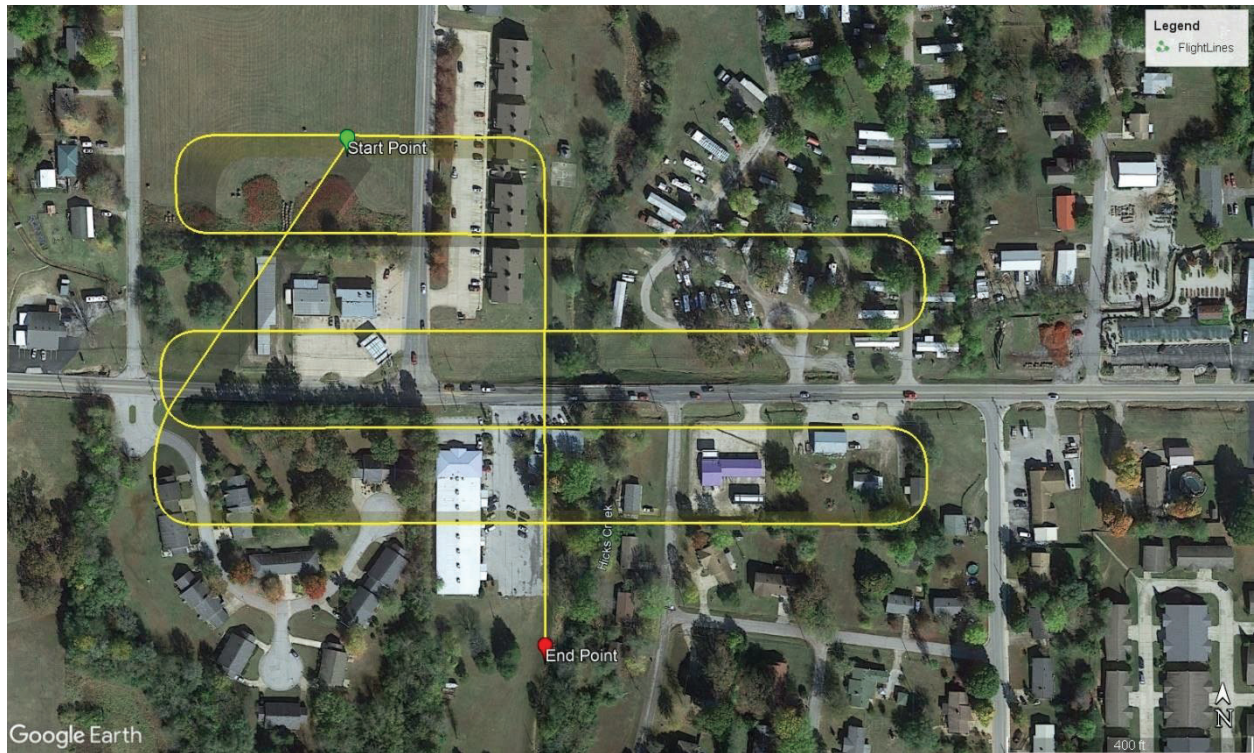
**Figure 30. Flight Path at Mountain Home (Job 090647)**
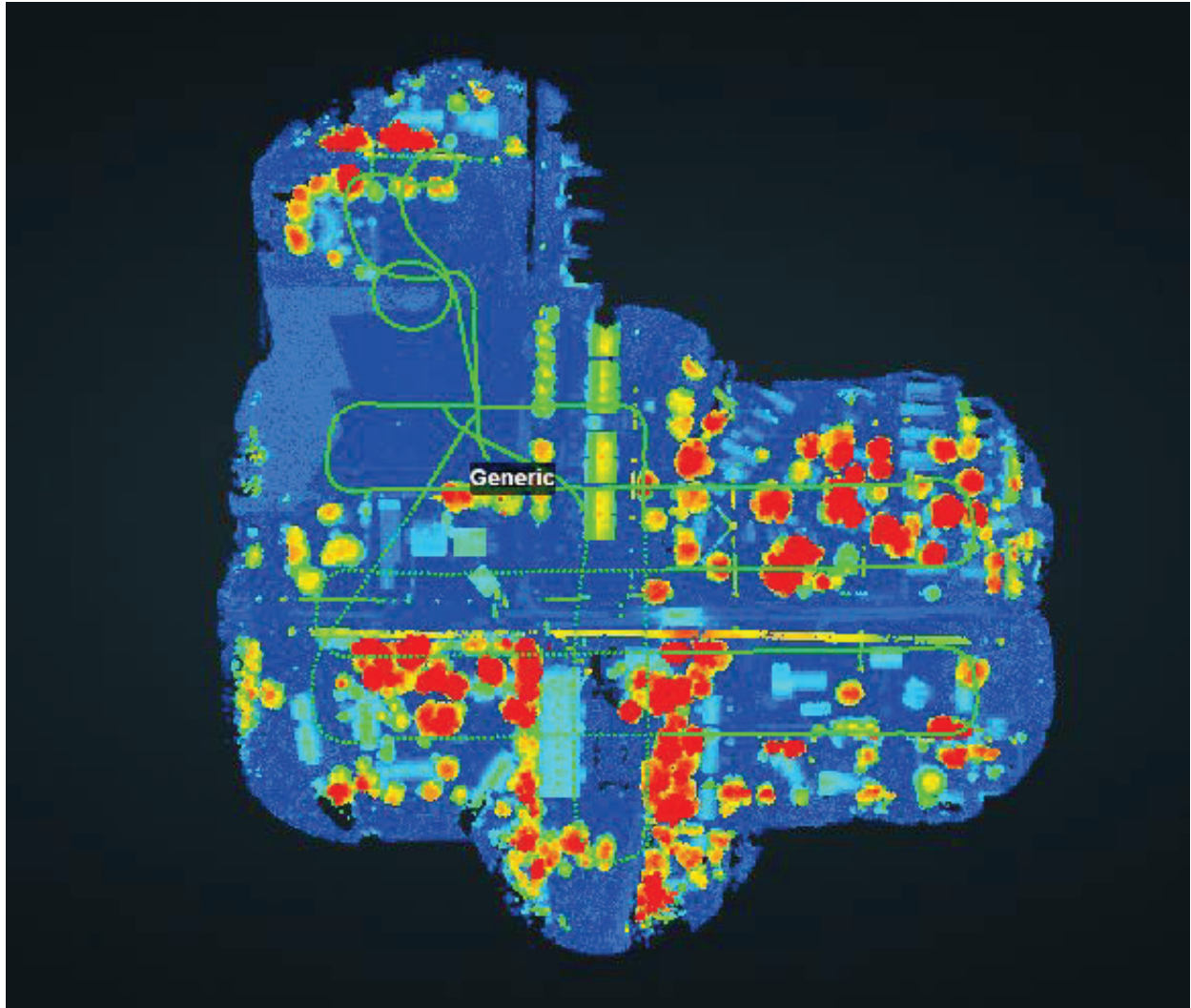
Figure 31. Raw LiDAR Data Colored by Elevation, Collected at the Mountain Home Site (Job 090647)

Table 6. Checkpoint Type Surveyed at the Mountain Home Site (Job 090647)

Type of Points at Mountain Home Bridge	No. of Points	Total
Soft Surface (Grass) comparison with GNSS	84	
Soft Surface (Tree) comparison with GNSS	5	
Total Soft Surface Survey Points		89
Hard Surface (Pavement) comparison with GNSS RTK	33	
Hard Surface (Parking) comparison with GNSS RTK	4	
Total Hard Surface Survey Points		37
Control Points with GNSS at Mountain Home Bridge	3	3
Total Survey Points		**129**

Figure 32. GNSS Checkpoints and Their Classification at the Mountain Home Site (Job 090647)

CHAPTER 4. RESULTS OF INDIVIDUAL SITE SURVEYS

This chapter assesses the accuracy of the LiDAR-measured elevations using the GNSS and total station measurements and other LiDAR measurements for each site. For clarity, LiDAR data collected for this project are labeled as UARK LiDAR, while LiDAR measurements made for or by A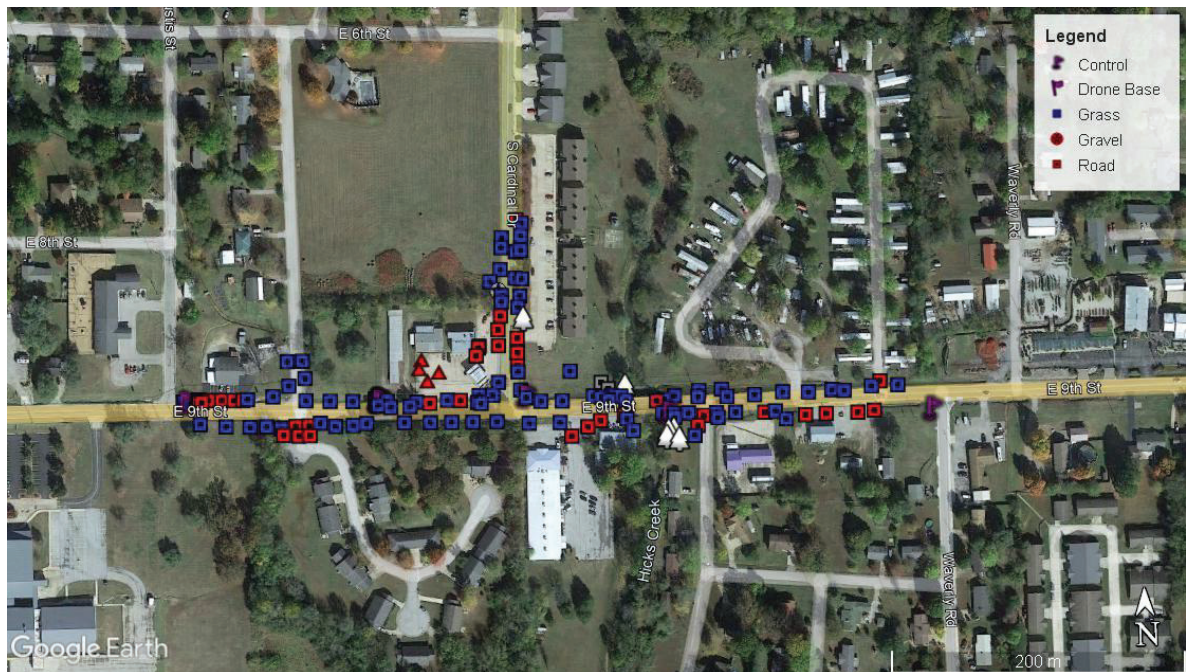RDOT are labeled as ARDOT LiDAR. All checkpoints in this project were collected by UARK, so they are simply labeled as GNSS or total station measurements. For all five bridge project sites, the GNSS and total station checkpoints were compared with the elevation data from the DEM raster produced from the LiDAR measurements at each site. In general, the comparisons were split into hard and soft surface areas and further subdivided based on specific surface type. To estimate the error in the LiDAR data, the elevation of the GNSS and total station survey checkpoints were subtracted from the LiDAR raster elevations (orthometric height determined by LiDAR). Therefore, for points with a negative error, LiDAR underestimated the elevation at that point, and for points with a positive error, LiDAR overestimated the elevation at that point. The difference in US inches with respect to different surface types have been plotted and compared in aerial images, box plots, and box-whisker graphs, and raster comparisons have been made where possible. The difference in elevation between checkpoints is discussed for each of the sites. In general, accuracy bins have been provided for every inch, with the maximum/minimum set at "less than -3 inches" to "greater than +3 inches". The range -1.0 in to +1.0 is generally considered to be within the accuracy limits of the measurements, and accuracy was not assessed tighter than this limit for general assessments.

LINCOLN BRIDGE 1 (EAST) JOB 040866

 For the Lincoln Bridge 1 (East) site, the error between the UARK LiDAR and GNSS for hard surface checkpoints is shown in an aerial photo of the site in Figure 33. For the hard surface checkpoints, about half of the data are within the +1.0 inch to -1.0 inch (green) range, indicating good accuracy. However, the other checkpoints are between -2.0 inches and -1.0 inch (light blue), indicating a slight underestimation of the elevation in some locations. In Figure 34, the error between the UARK LiDAR and GNSS for soft surface checkpoints is shown in an aerial photo of the site. Many of the grass checkpoints near the road are within the +1.0 inch to -1.0 inch (green) range, indicating good accuracy. However, for other points, the LiDAR generally overestimates the elevation, with many checkpoints falling between +1.0 inch and +2.0 inches (yellow) and some higher error points falling between +2.0 inches and +3.0 inches (orange) and even greater than +3.0 inches (red). This is generally expected given that the grass in the area was generally 3 inches+ tall, but not overgrown. For the checkpoints under tree cover, LiDAR is either accurate to within +1.0 inch to -1.0 inch (green) or underestimating the elevation.

Figure 33. Aerial Image Showing the Comparison of UARK LiDAR Raster Elevations with GNSS Checkpoints for Hard Surfaces at Lincoln Bridge 1 (East) (Job 040866)
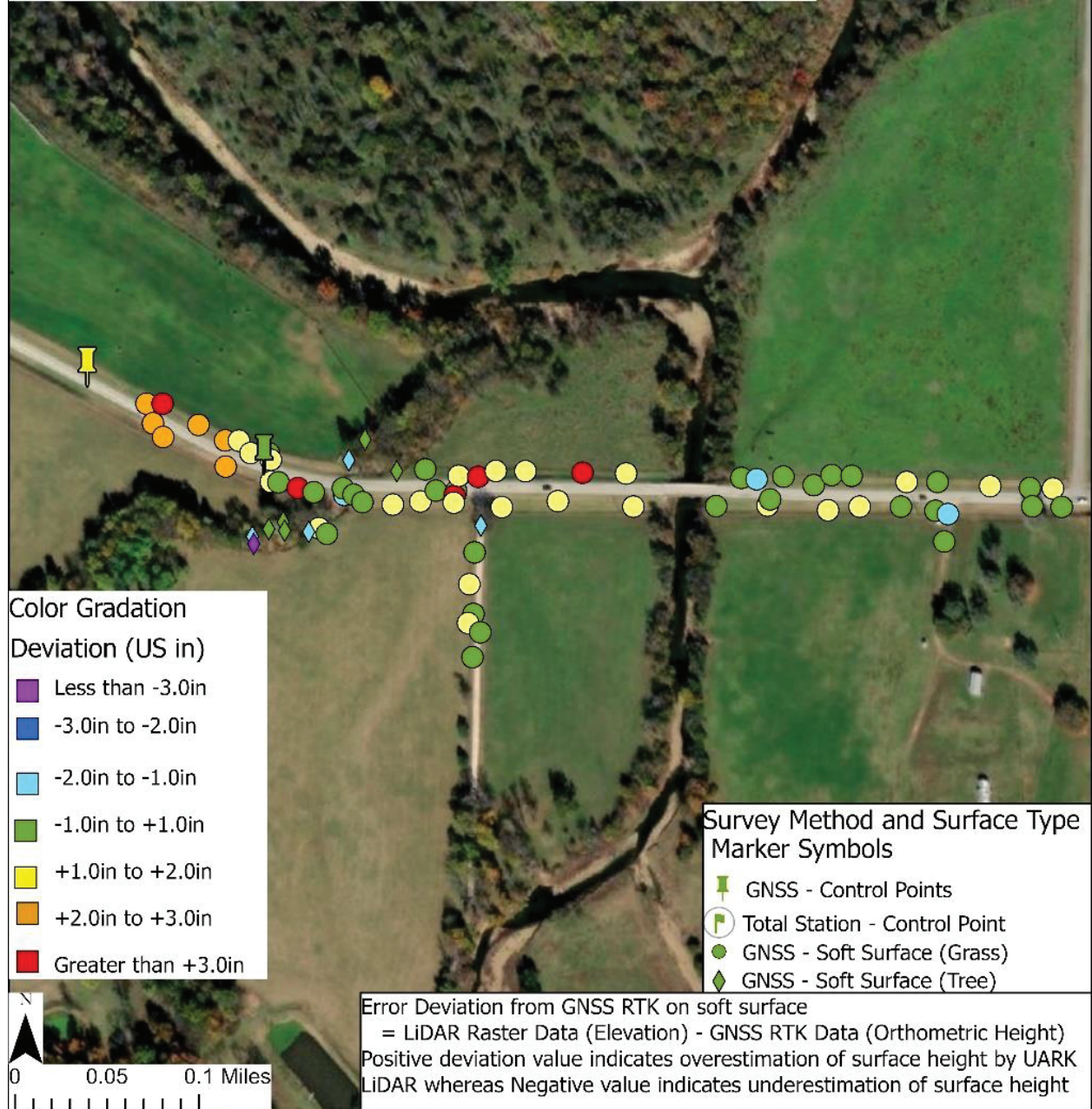
Figure 34. Aerial Image Showing the Comparison of UARK LiDAR Raster Elevations with GNSS Checkpoints for Soft Surfaces at Lincoln Bridge 1 (East) (Job 040866)

To aid a better understanding of the distribution of the error for each surface type at the Lincoln Bridge 1 (East) site, the quantity of points in each error class for each surface type and between the UARK LiDAR raster elevations and GNSS checkpoints is shown in Figure 35. Most of the points, regardless of surface type, fell within the +1.0 inch to -1.0 inch range, indicating good accuracy for each surface type. For grass, the error tended to be on the positive side (LiDAR overestimated the elevation), which is expected given the grass height at the site. The hard surface and tree checkpoints tended to have errors on the negative side (LiDAR underestimated the elevation).

Figure 36 is a box and whisker plot of the error between the UARK LiDAR raster elevations and the GNSS checkpoint elevations for the different surface types. Similar to the other plots for the Lincoln Bridge 1 (East) site, most of the checkpoints fell within the +1.0 inch to -1.0 inch range, with the soft surface points having significantly more variability than the hard surface points.
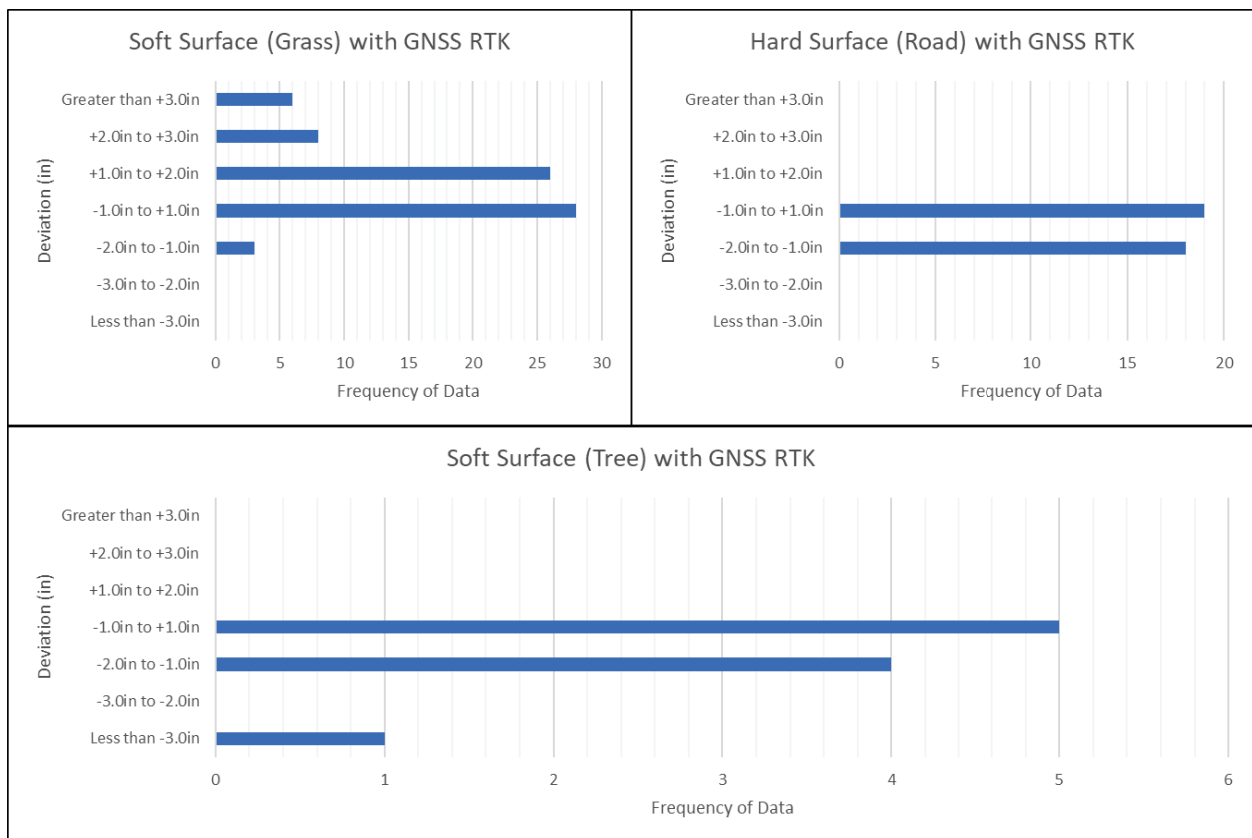

Figure 35. Data Frequency Bar Graph Comparison of UARK LiDAR Raster Elevation and GNSS Checkpoints for Hard and Soft Surfaces at Lincoln Bridge 1 (East) (Job 040866)
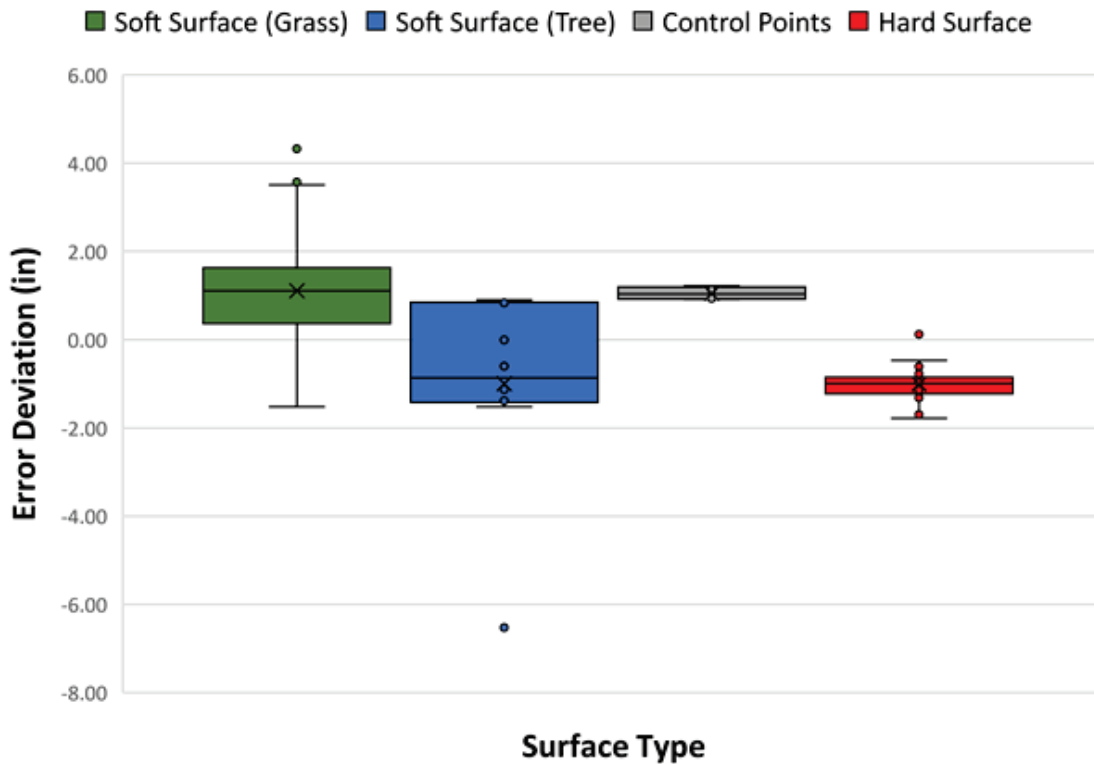
Figure 36. Box and Whisker Plot Comparison of UARK LiDAR Raster Elevation and GNSS Checkpoints for Hard and Soft Surfaces at Lincoln Bridge 1 (East) (Job 040866)

LINCOLN BRIDGE 2 (WEST) JOB 040866

For the Lincoln Bridge 2 (West) site, the error between the UARK LiDAR and GNSS/total station for hard surface checkpoints is shown in an aerial photo of the site in Figure 37. For the hard surface checkpoints, three quarters of the data is within +1.0 inch to -1.0 inch (green), indicating good accuracy. However, one quarter of the data is between -2.0 inches and -1.0 inch (light blue), indicating a slight underestimation of the elevation in some locations. This is very similar to the results for the Lincoln Bridge 1 (East) site. The error between the UARK LiDAR and GNSS/total station for soft surface checkpoints is shown in an aerial photo of the site in Figure 38. Many of the grass checkpoints near the road were within the +1.0 inch to -1.0 inch (green), indicating good accuracy. However, for other points, the LiDAR generally overestimated the elevation, with many checkpoints falling between +1.0 inch and +2.0 inches (yellow) and some higher error points falling between +2.0 inches and +3.0 inches (orange) and even greater than +3.0 inches (red). This was generally expected given that the height of grass in the area was generally 3 inches+, but not overgrown. For the tree checkpoints, the accuracy tended to be both positive and negative, indicating more uncertainty in the results under these conditions.

48

Figure 37. Aerial Image Showing the Comparison Between UARK LiDAR Raster Elevations and GNSS/Total Station Checkpoints for Hard Surfaces at Lincoln Bridge 2 (West) (Job 040866)
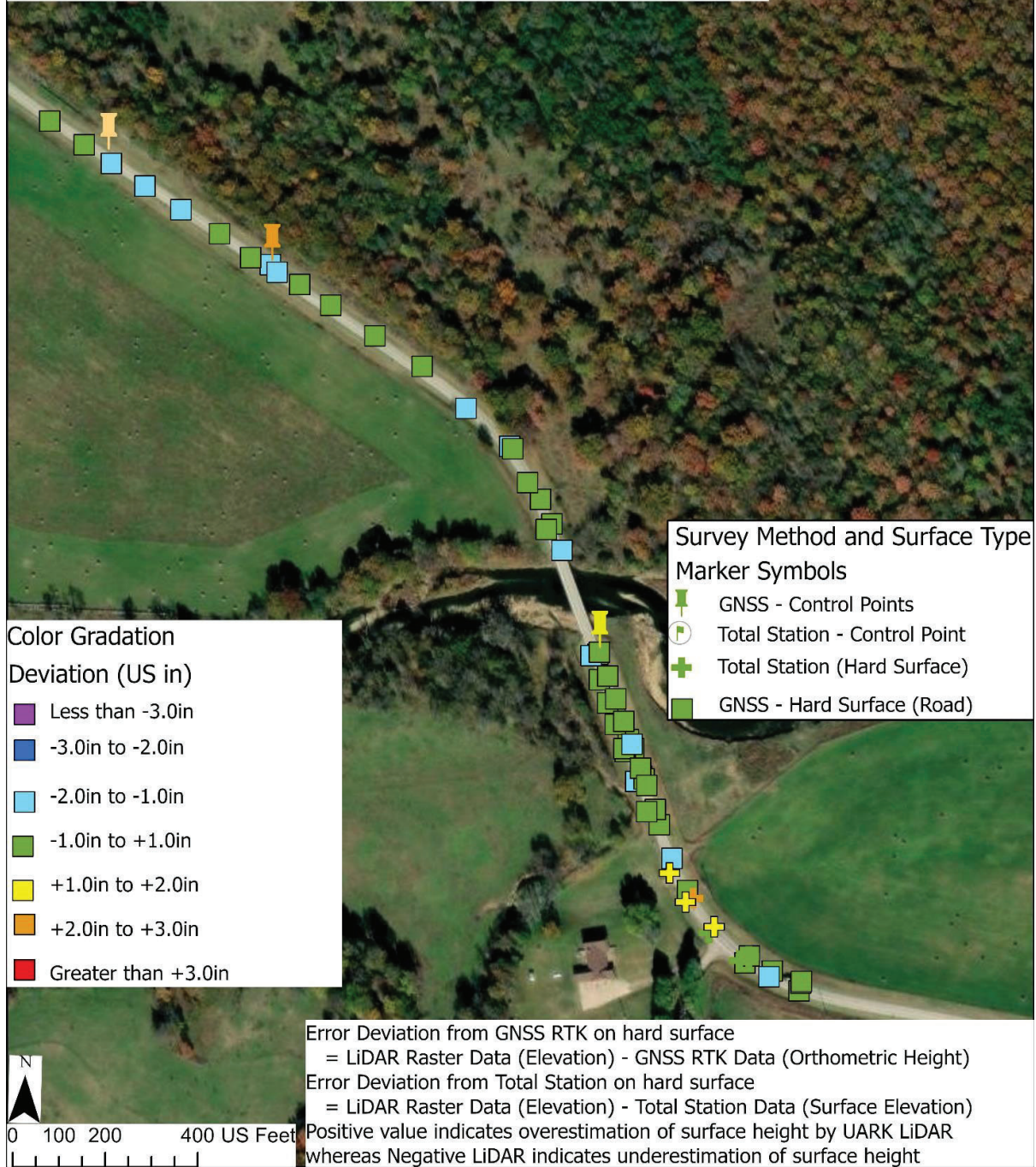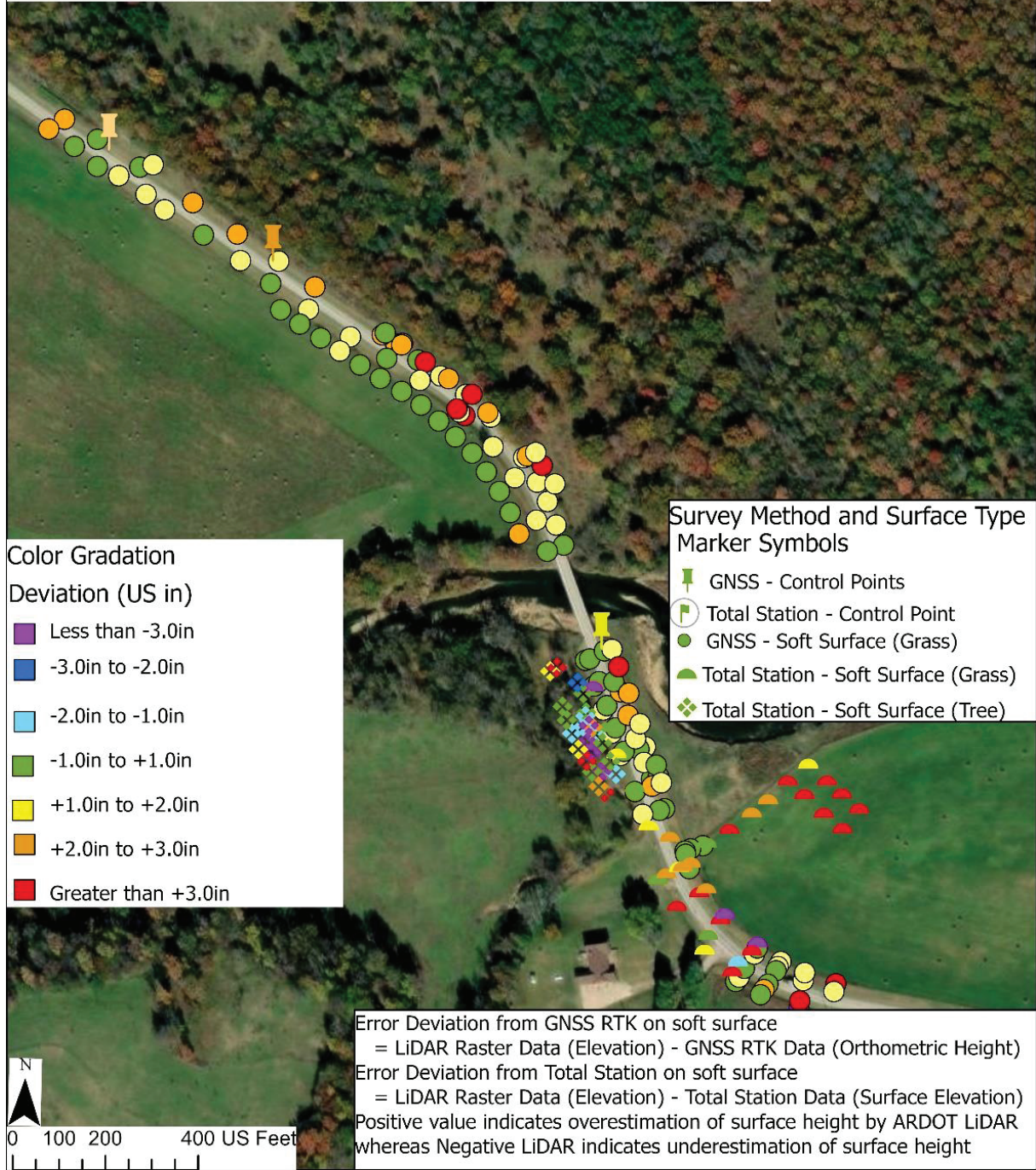
Figure 38. Aerial Image Showing the Comparison Between UARK LiDAR Raster Elevations and GNSS/Total Station Checkpoints for Soft Surfaces at Lincoln Bridge 2 (West) (Job 040866)

To aid a better understanding of the distribution of the error for each surface type at the Lincoln Bridge 2 (West) site, the quantity of points in each error class for each surface type and between the UARK LiDAR raster elevations and GNSS/total station checkpoints is shown in Figure 39. Most of the points, regardless of surface type, fell within the +1.0 inch to -1.0 inch range, indicating good accuracy for each surface type. For grass points using the total station, the error tended to be on the positive side (LiDAR overestimated the elevation), with many of the points having errors of more than 3 inches. Many of the total station grass points tended to be in hay fields far from the road which have taller grass and as such would be expected to have their elevations more significantly overestimated by LiDAR (Figure 38). As observed previously, the tree checkpoints tended to have the largest variability with both positive and negative errors.

A box and whisker plot of the error between the UARK LiDAR raster elevations and GNSS/total station checkpoint elevations for the different surface types is shown in Figure 40. Similar to the other plots for the Lincoln Bridge 2 (West) site, most of the checkpoints fell near the +1.0 inch to -1.0 inch range, with the soft surface points (grass and trees) having significantly more variability than the hard surface points. The variability of the total station soft surface points was large compared to the other categories. As discussed, this is likely because the total station was used to survey more challenging surface types, unlike the GNSS system.
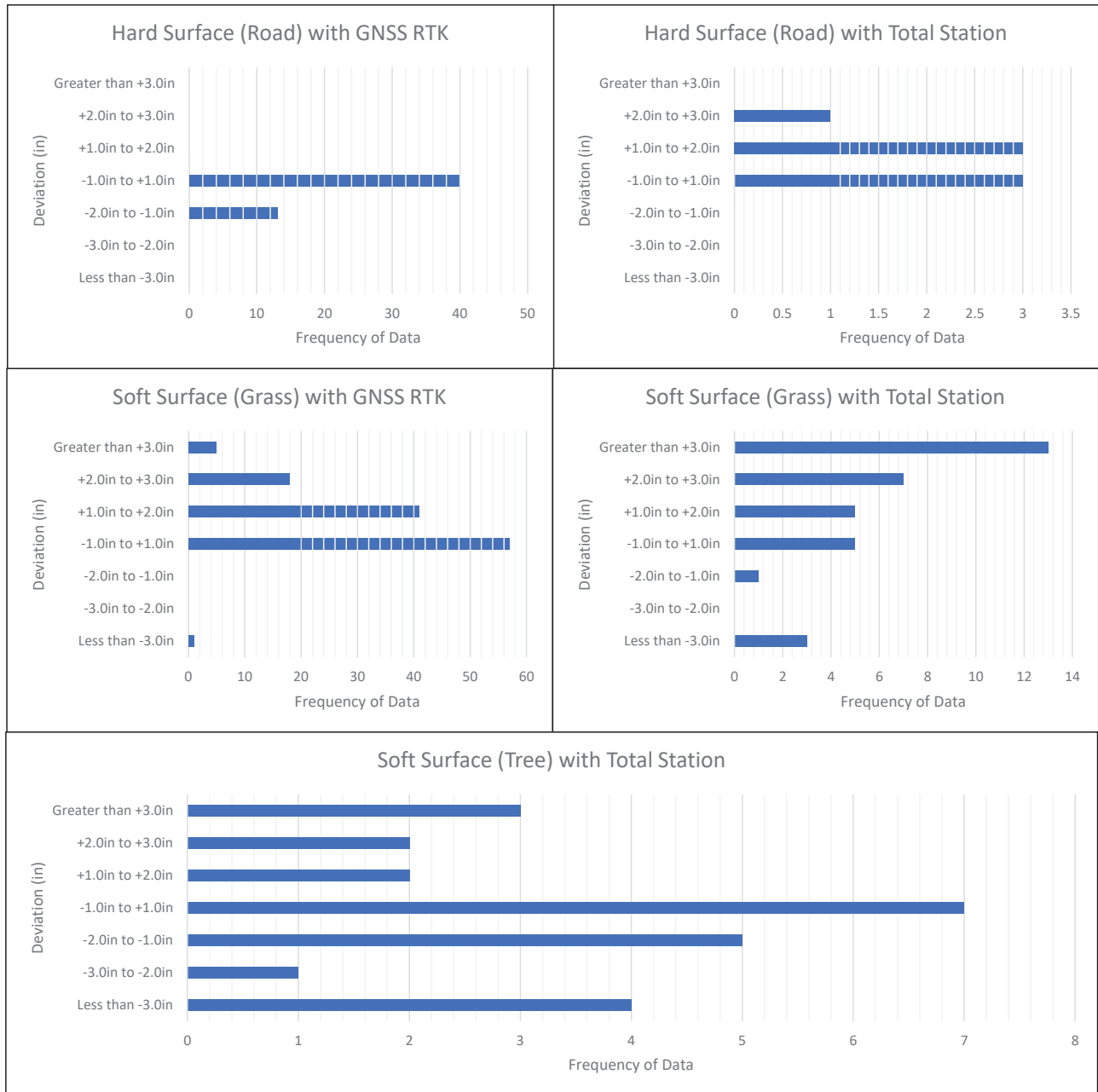
Figure 39. Data Frequency Bar Graph Comparison of UARK LiDAR Raster Elevations with GNSS/Total Station Checkpoints for Hard and Soft Surfaces at Lincoln Bridge 2 (West) (Job 040866)

Lincoln West Bridge UARK LIDAR Data comparison with GNSS RTK and Total Station
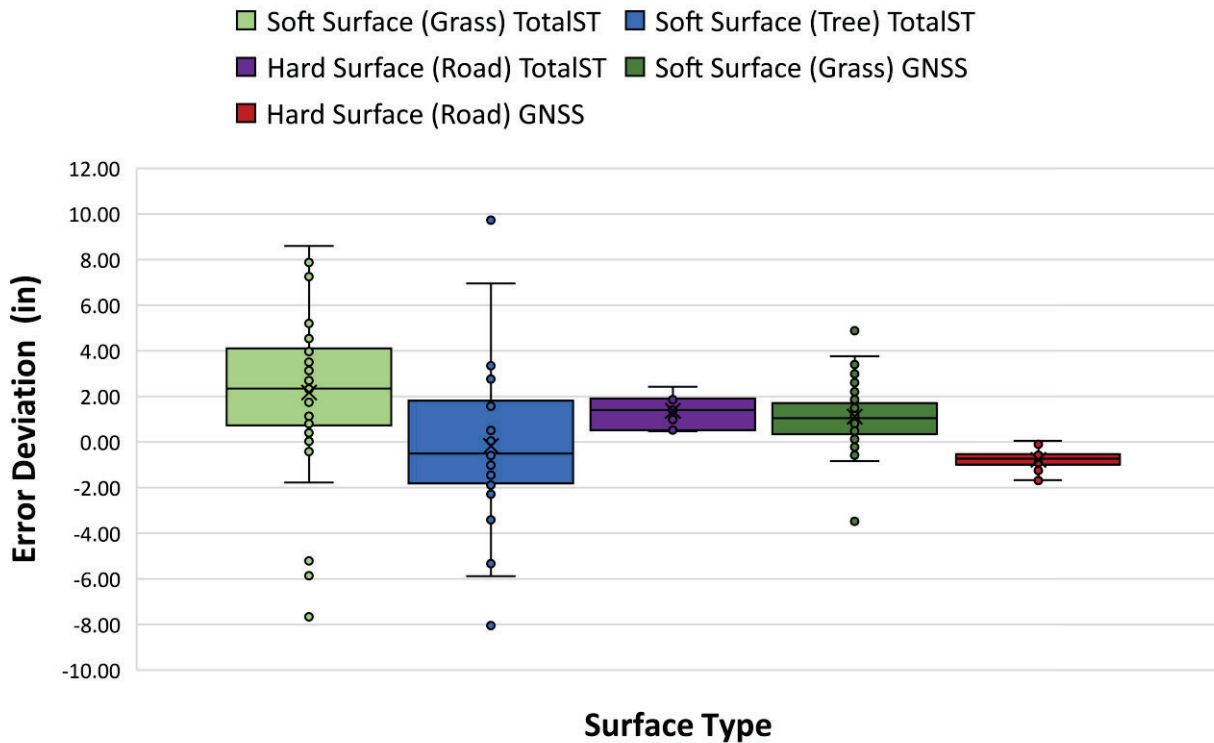

Figure 40. Box and Whisker Plot Comparison of UARK LiDAR Raster Elevations with GNSS/Total Station Checkpoints for Hard and Soft Surfaces at Lincoln Bridge 2 (West) (Job 040866)

HUMNOKE, ARKANSAS JOB 061745

For the Humnoke site, the error between the UARK LiDAR and GNSS/total station for hard surface checkpoints is shown in an aerial photo of the site in Figure 41. For the hard surface checkpoints, about half of the data is within +1.0 inch to -1.0 inch (green), indicating good accuracy. However, the other half is within +1.0 inch to +2.0 inches (yellow), indicating a slight overestimation of the elevation in some locations. This is in contrast to the results for the Lincoln sites where the error for hard surfaces was generally on the negative side. The error between the UARK LiDAR and GNSS/total station for soft surface checkpoints is shown in an aerial photo of the site in Figure 42. Many of the grass checkpoints near the road had overestimated elevations, with many checkpoints at +3.0 inches (red) and many falling between +2.0 inches and +3.0 inches (orange), as well as between +1.0 inch and +3.0 inches (yellow). Some points were within the standard +1.0 inch to -1.0 inch (green) range. This higher error was expected given the height of grass in the area was generally 3 inches+. For the tree checkpoints, the accuracy tended to be both positive and negative, indicating similar errors under these conditions.

Figure 41. Aerial Image Showing the Comparison of UARK LiDAR Raster Elevations with GNSS/Total Station Checkpoints for Hard Surfaces at Humnoke (Job 061745)

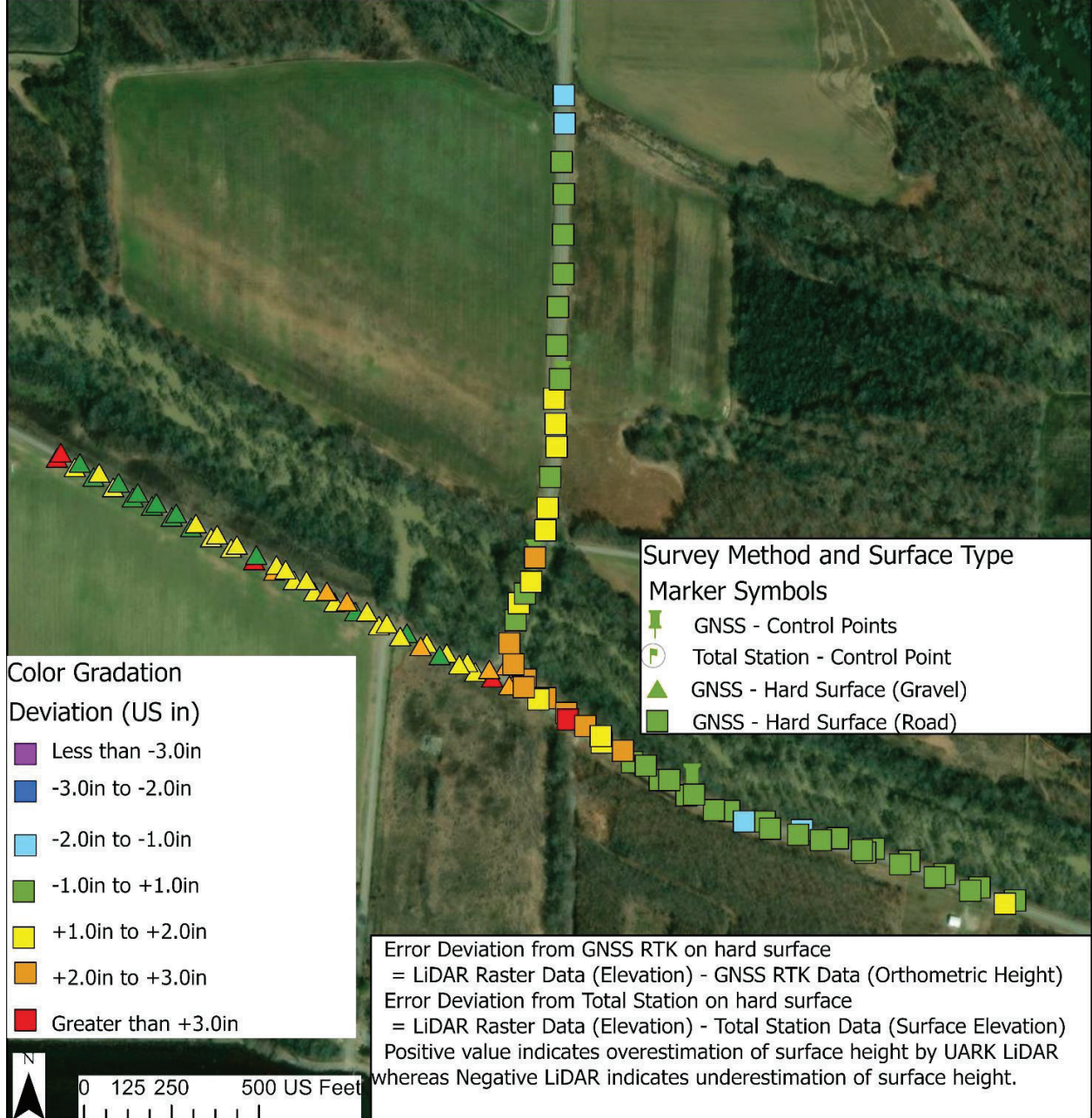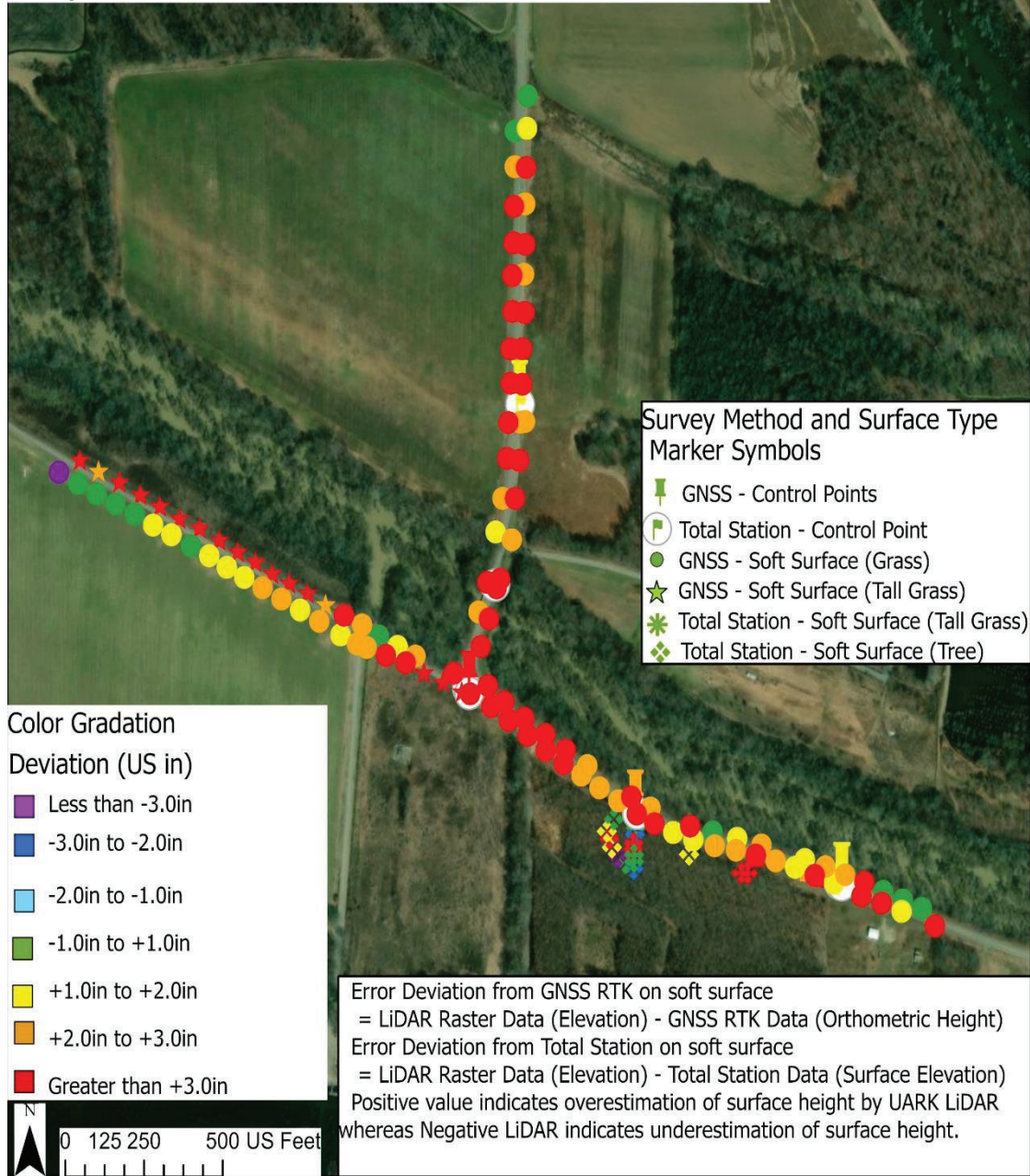**Figure 42. Aerial Image Showing the Comparison of UARK LiDAR Raster Elevations with GNSS/Total Station Checkpoints for Soft Surfaces at Humnoke (Job 061745)**

To aid a better understanding of the distribution of the error for hard surface points at the Humnoke site, the quantity of points in each error class for hard surface types and between the UARK LiDAR raster elevations and the GNSS/total station checkpoints is shown in Figure 43. Most of the points, regardless of the hard surface type, fell within the +1.0 inch to -1.0 inch range, indicating good accuracy. The errors tended to be on the positive side (LiDAR overestimated the elevation [high]). The quantity of points in each error class for soft surface types and between the UARK LiDAR raster elevations and GNSS/total station checkpoints is shown in Figure 44. For grass points, the error tended to be on the positive side (LiDAR overestimated the elevation), with many of the points having errors above 3 inches. At the Humnoke site, the grass (especially taller grass sections) tended to be at least 3+ inches. This larger positive error was expected. As observed previously, the tree checkpoints tend to have the largest variability, with both positive and negative errors.

A box and whisker plot of the error between the UARK LiDAR raster elevations and GNSS/total station checkpoint elevations for the different surface types is shown in Figure 45. Similar to the other plots for the Humnoke site, most of the hard surface checkpoints (both positive and negative) fell near the +1.0 inch to -1.0 inch range. The soft surface points (grass and trees) had significantly more variability than the hard surface points, and the variability of the total station soft surface points was quite large compared to the other categories. As discussed, this is likely because the total station was used to survey more challenging surface types compared to the GNSS system.

Figure 43. Data Frequency Bar Graph Showing the Comparison of UARK LiDAR Raster Elevations with GNSS/Total Station Checkpoints for Hard Surfaces at Humnoke (Job 061745)
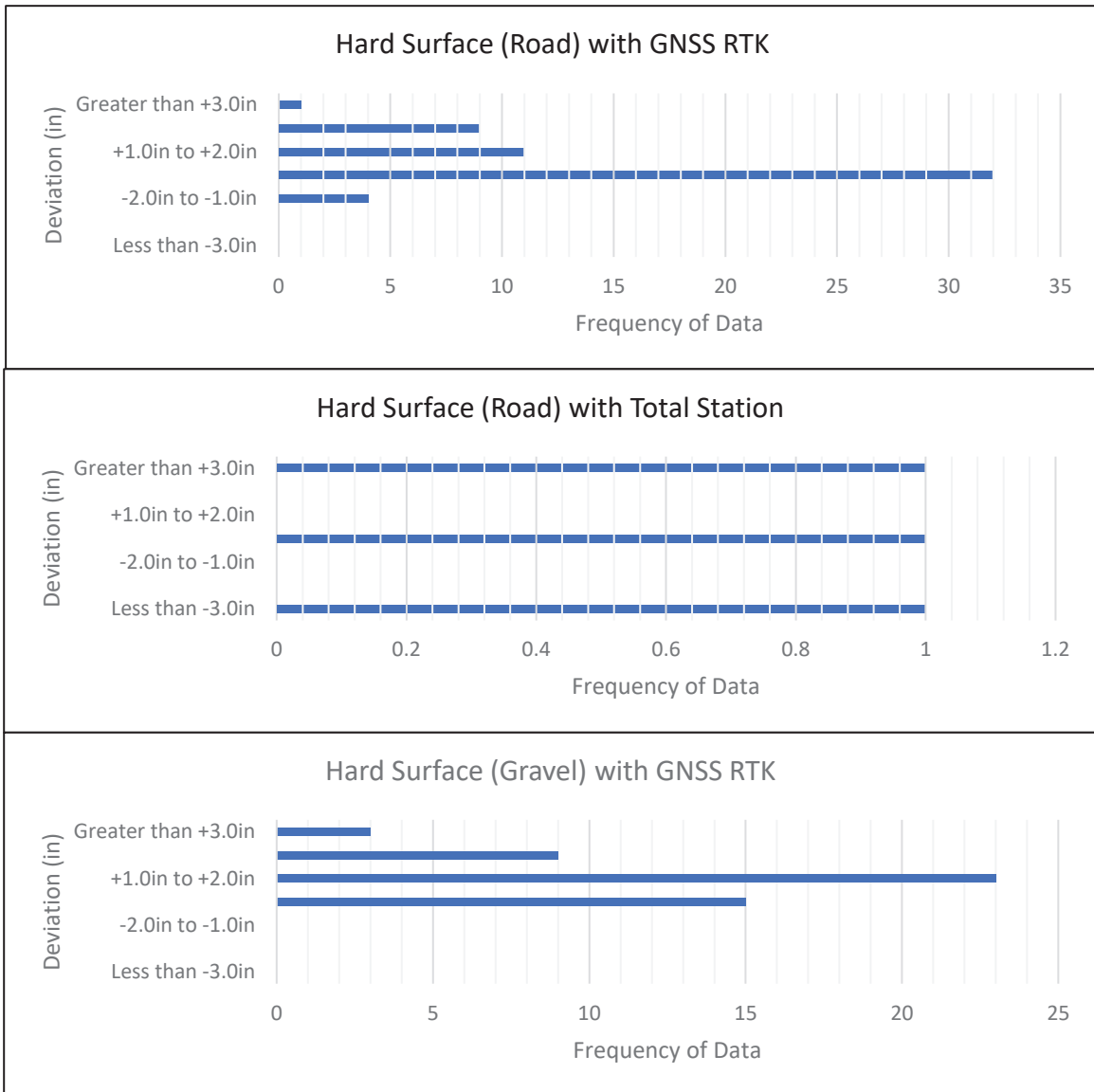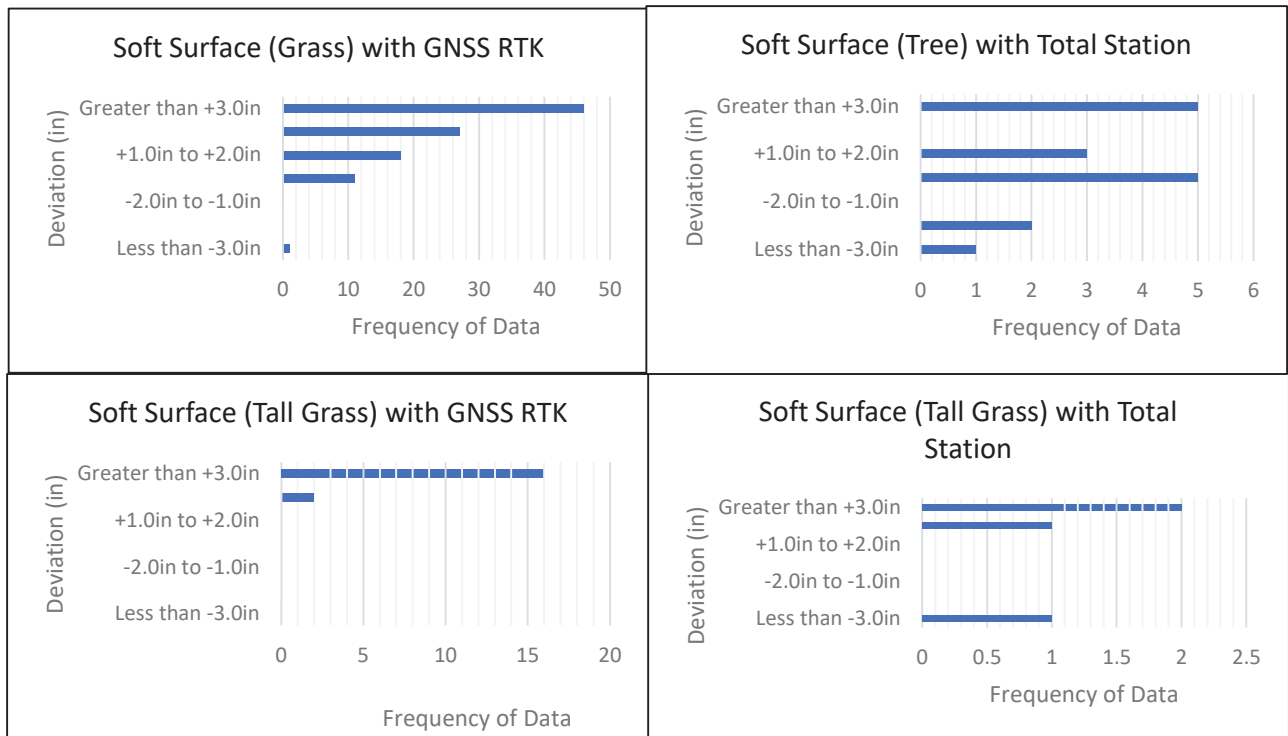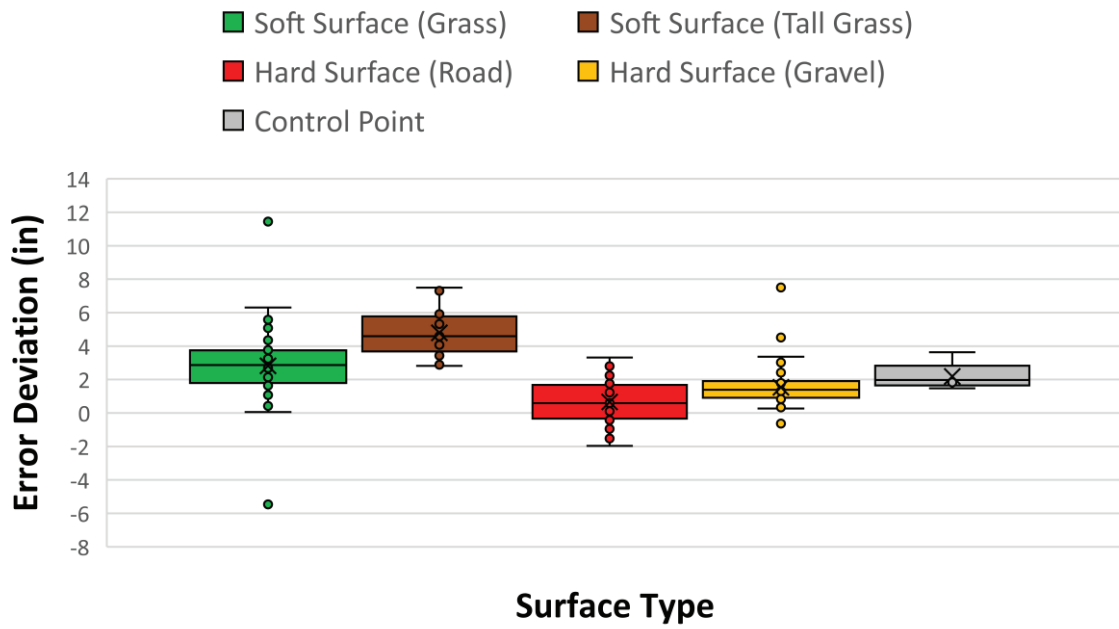
Figure 44. Data Frequency Bar Graph Showing the Comparison of UARK LiDAR Raster Elevations with GNSS/Total Station Checkpoints for Soft Surfaces at Humnoke (Job 061745)
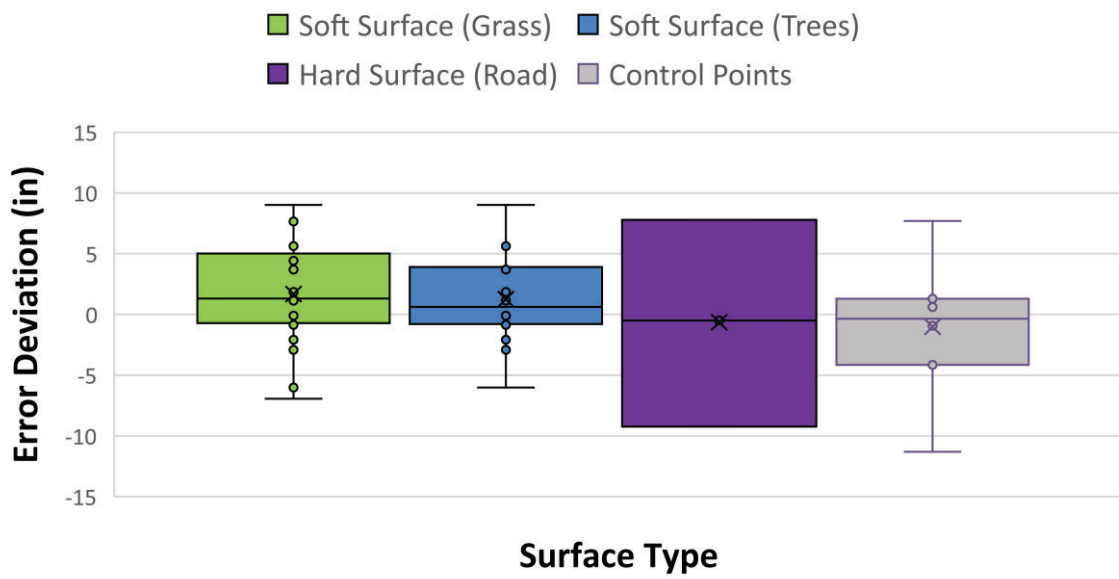
Figure 45. Box and Whisker Plot of the Comparison of UARK LiDAR Raster Elevation with GNSS (Top)/Total Station (Bottom) Checkpoints for Hard and Soft Surfaces at Humnoke (Job 061745)

For the Humnoke site, the error between the ARDOT LiDAR and GNSS/total station for hard surface checkpoints is shown in an aerial photo of the site in Figure 46. For the hard surface checkpoints, more than half of the data fell within the +1.0 inch to -1.0 inch (green) range, indicating good accuracy. However, the other portion fell between +1.0 inch to +2.0 inches (yellow) and -2.0 inches to -1.0 inch (light blue), suggesting a general uncertainty in the measurements rather than a bias. This is different from the UARK measurements at the Humnoke site, which tended to only have errors on the positive side. The error between the ARDOT LiDAR and GNSS/total station for soft surface checkpoints is shown in an aerial photo of the site in Figure 47. Approximately half of the grass checkpoints near the road were within the +1.0 inch to -1.0 inch (green) error level. Most of the other checkpoints indicate an overestimation of the elevation, with some checkpoints falling between +1.0 inch to +2.0 inch (yellow) and others falling between +2.0 inches and +3.0 inches (orange) and greater than +3.0 inches (red). This was expected since the height of grass in the area was generally 3 inches+, but not overgrown. For the tree checkpoints, the accuracy tended to be positive, with many points being in the +3.0 inches (red) range.

Figure 46. Aerial Image Showing the Comparison of ARDOT LiDAR Raster Elevations with GNSS/Total Station Checkpoints for Hard Surfaces at Humnoke (Job 061745)
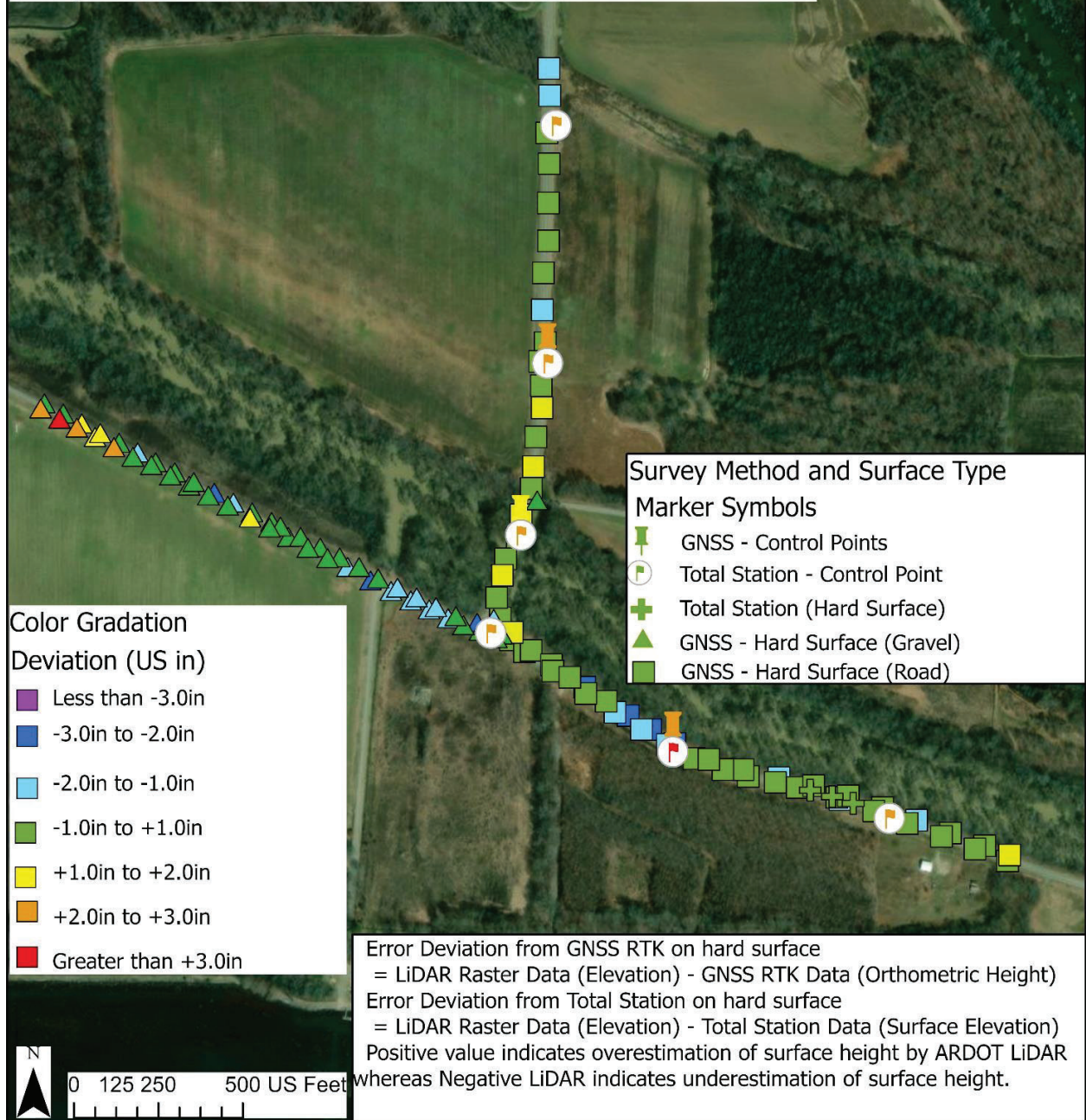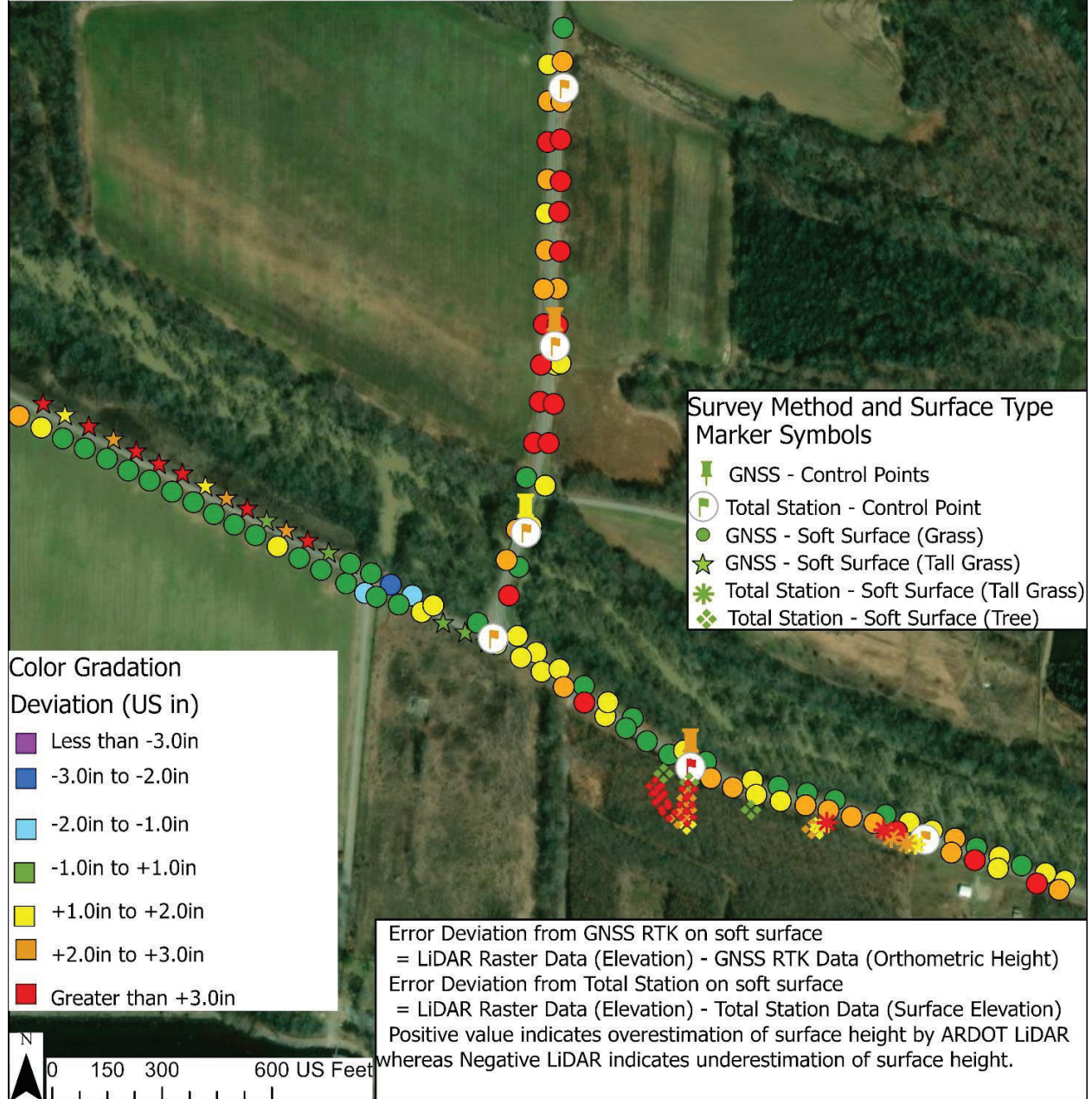
Figure 47. Aerial Image Showing the Comparison of ARDOT LiDAR Raster Elevations with GNSS/Total Station Checkpoints for Soft Surfaces at Humnoke (Job 061745)

To aid a better understanding of the distribution of the error for each surface type for the ARDOT LiDAR data at the Humnoke site, the quantity of points in each error class for each surface type between the ARDOT LiDAR raster elevations and GNSS/total station checkpoints is shown in Figure 48. Most of the points, regardless of the surface type, fell within the +1.0 inch to -1.0 inch range, indicating good accuracy for each surface type. There tended to be both positive and negative errors for the hard surface points. The quantity of points in each error class for soft surface types between the UARK LiDAR raster elevations and GNSS/total station checkpoints is shown in Figure 49. For grass points, the error tended to be in the +1.0 inch to -1.0 inch range or on the positive error side (LiDAR overestimated the elevation), with many of the points having errors above 3 inches. At the Humnoke site, the grass (especially taller grass sections) tended to be at least 3+ inches tall; therefore, this larger positive error was expected. For grass points obtained using the total station, the error tended to be on the positive side (LiDAR overestimated the elevation), with many of the points having errors above 3 inches. As observed previously, the tree checkpoints tend to have the largest variability, with both positive and negative errors.

Box and whisker plots of the error of the UARK LiDAR raster elevations and GNSS/total station checkpoint elevations for the different surface types is shown in Figure 50. Similar to the other plots for the Humnoke site, most of the hard surface checkpoints fell near the +1.0 inch to -1.0 inch range, with the soft surface checkpoints (grass and trees) having significantly more variability than the hard surface points. The soft surface checkpoints tended to have positive errors, with values above +2.0 inches. The variability of the total station soft surface points was large compared to that of the other categories. As discussed, this is likely because the total station was used to survey more challenging surface types than the GNSS system and because fewer points were surveyed using the total station.

The DEM for the UARK LiDAR was subtracted from the DEM for the ARDOT LiDAR at the Humnoke site (Figure 51). This allowed for the visualization of the differences between the LiDAR elevations over the entire measurement area at once. In the overall map, the ARDOT LiDAR tends to have a similar elevation (-1.0 inch to +1.0 inch, green) for much of the map, with some areas (both soft and hard surfaces) having a slightly higher elevation in the ARDOT LiDAR data (+1.0 inch to +3.0 inches, yellow, brown) compared to the UARK LiDAR. For the grass areas, some differences were expected, as the grass height was not the same at each survey time. The areas with the largest differences tended to be areas of standing water (i.e., creeks and low areas on the map) located at the center of the map. These areas had both under- and over-estimates.

Figure 48. Data Frequency Bar Graph Showing the Comparison of ARDOT LiDAR Raster Elevations with GNSS/Total Station Checkpoints for Hard Surfaces at Humnoke (Job 061745)

Figure 49. Data Frequency Bar Graph Showing the Comparison of ARDOT LiDAR Raster Elevations with GNSS/Total Station Checkpoints for Soft Surfaces at Humnoke (Job 061745)
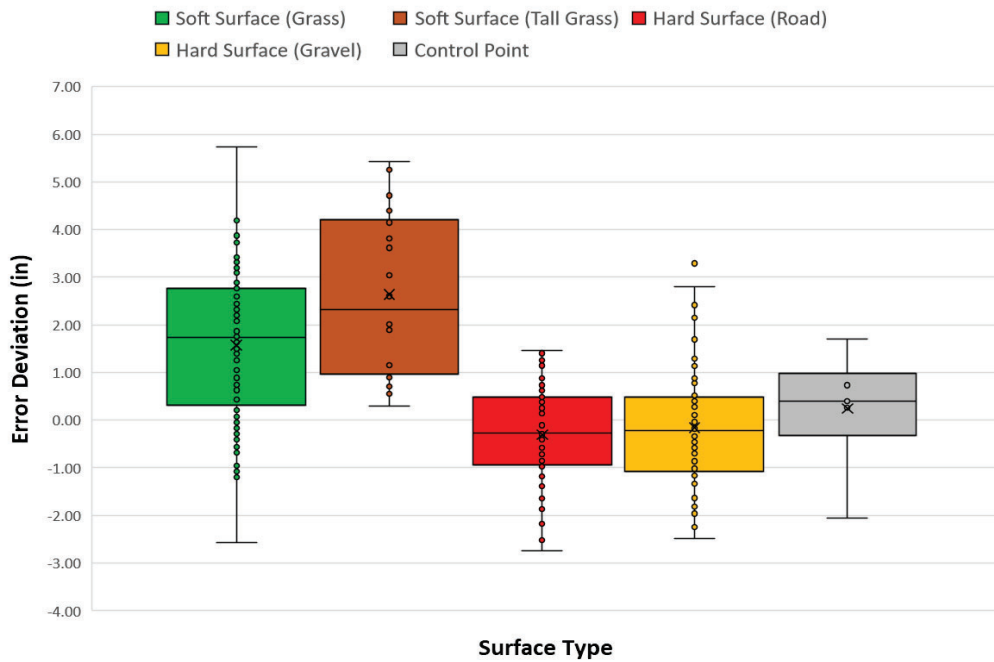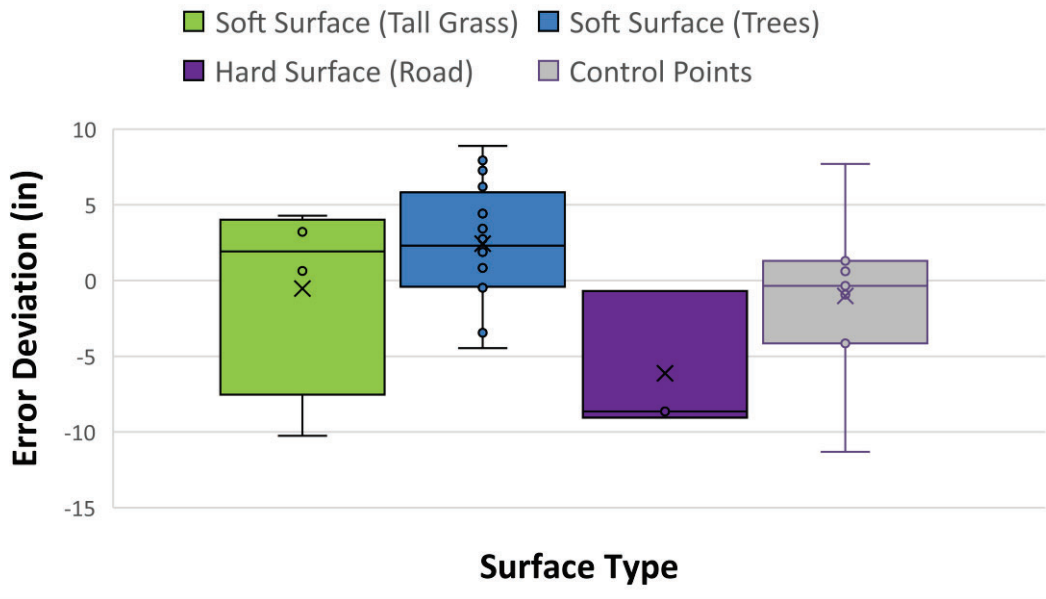
Figure 50. Box and Whisker Plot Showing the Comparison of ARDOT LiDAR Raster Elevations with GNSS (Top)/Total Station (Bottom) Checkpoints for Hard and Soft Surfaces at Humnoke (Job 061745)
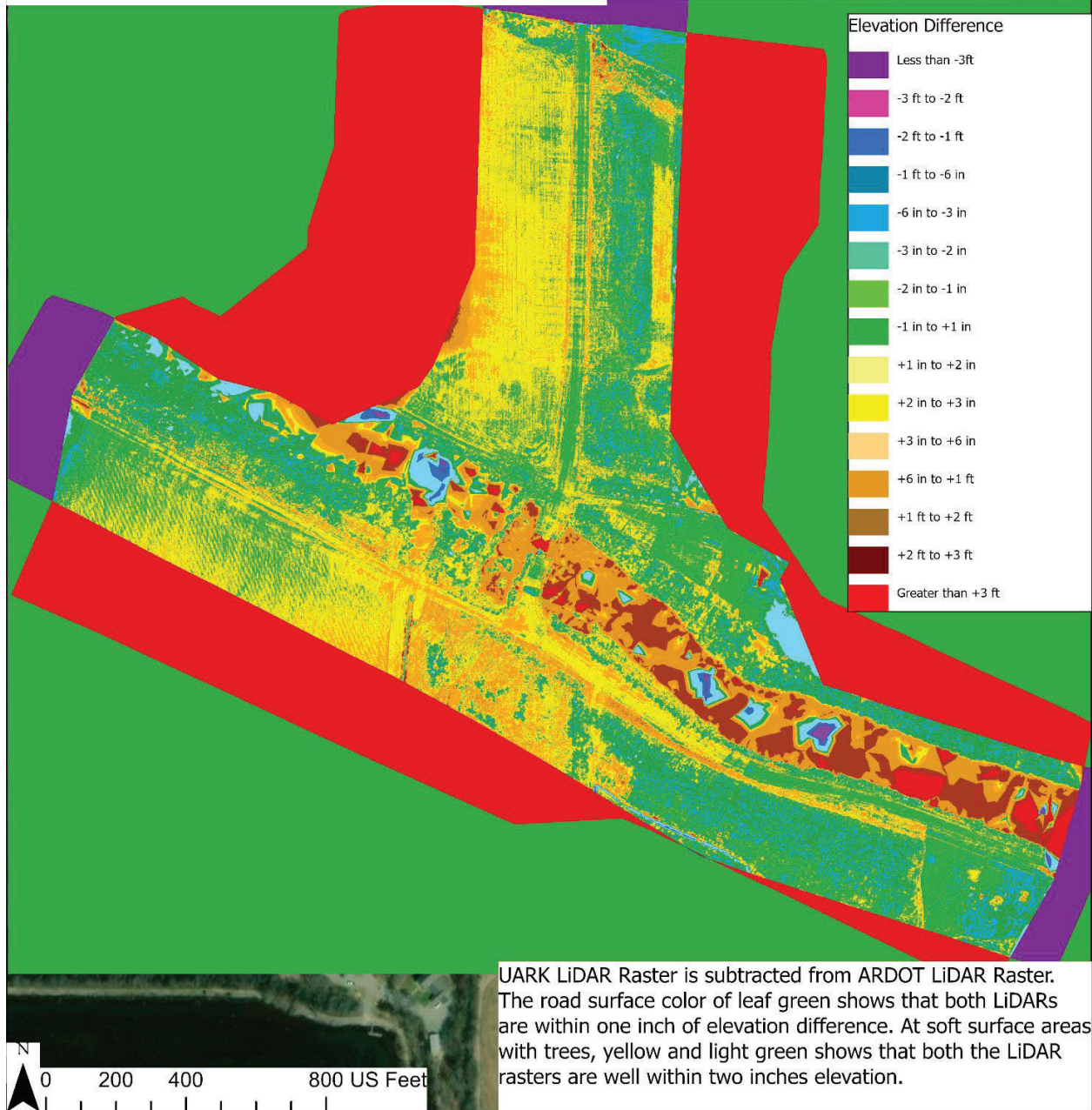
Figure 51. ARDOT LiDAR DEM Subtracted from UARK LiDAR DEM at Humnoke (Job 061745)

FRENCHMAN'S BAYOU, ARKANSAS JOB 101129

For the Frenchman's Bayou site, the error of the UARK LiDAR and GNSS/total station for hard surface checkpoints is shown in an aerial photo of the site in Figure 52. For the hard surface checkpoints, about three quarters of the data was within the +1.0 inch to -1.0 inch range (green), indicating good accuracy. However, the other portion was between -2.0 inches and -1.0 inch (light blue), indicating a slight underestimation of the elevation in some locations. This is similar to the results gotten at the Lincoln sites but in contrast to the Humnoke results. The error of the UARK LiDAR and GNSS/total station for soft surface checkpoints is shown in an aerial photo of the site in Figure 53. Similar to the hard surface checkpoints, most of the soft surface checkpoints were within the +1.0 inch to -1.0inch range (green), indicating good accuracy. However, some of the tall grass checkpoints tended to overestimate the elevation, with many tall grass checkpoints falling between +1.0 inch and +2.0 inches (yellow) and some higher error points falling between +2.0 inches to +3.0 inches (orange) and even greater than +3.0 inches (red). This was generally expected since the height of grass in the area was generally 3 inches+. For the tree checkpoints, the accuracy tended to be on the positive side, with many points near or greater than +3 inches.

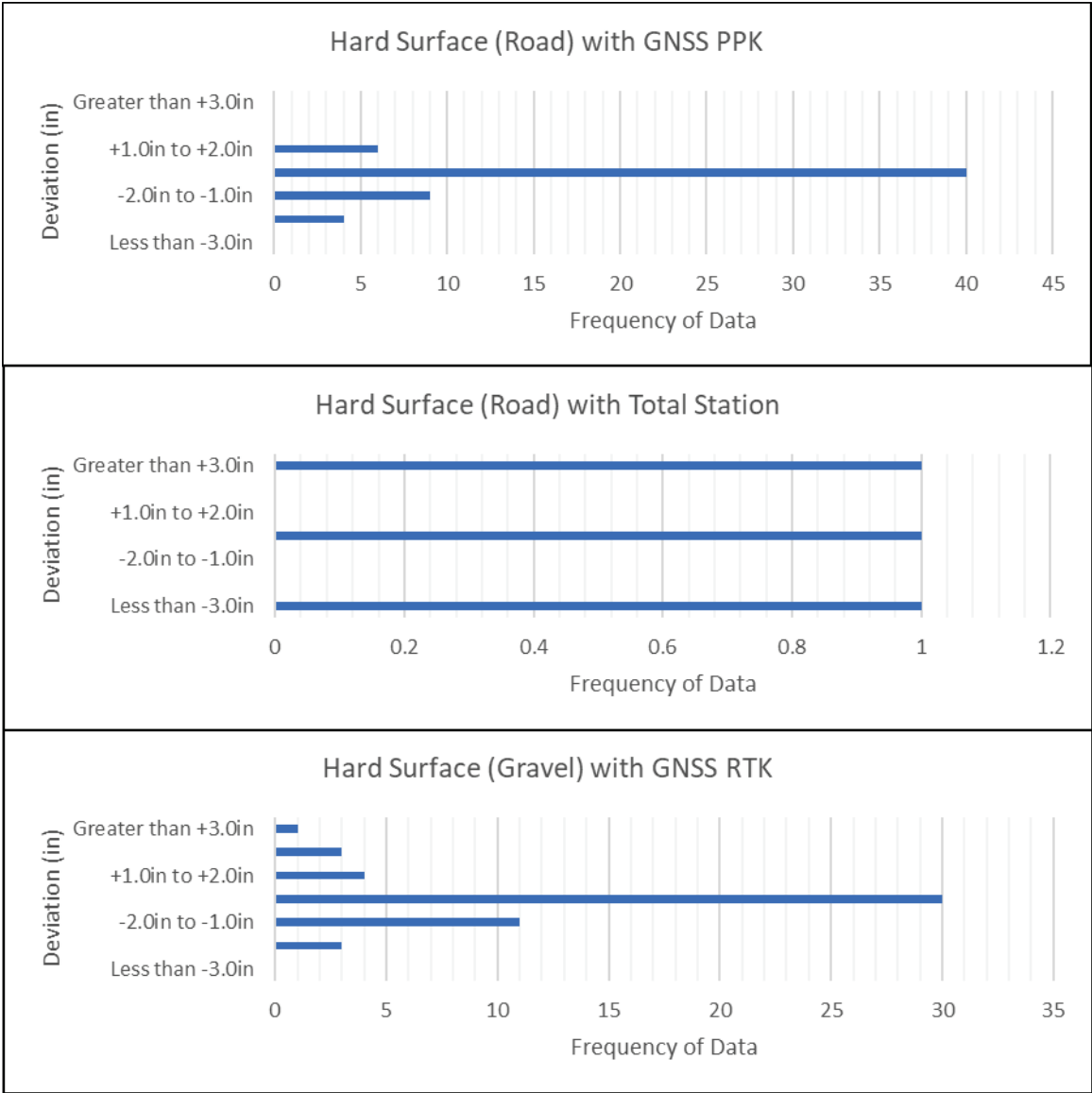**Figure 52. Aerial Image Showing the Comparison of UARK LiDAR Raster Elevations with GNSS/Total Station Checkpoints for Hard Surfaces at Frenchman's Bayou (Job 101129)**
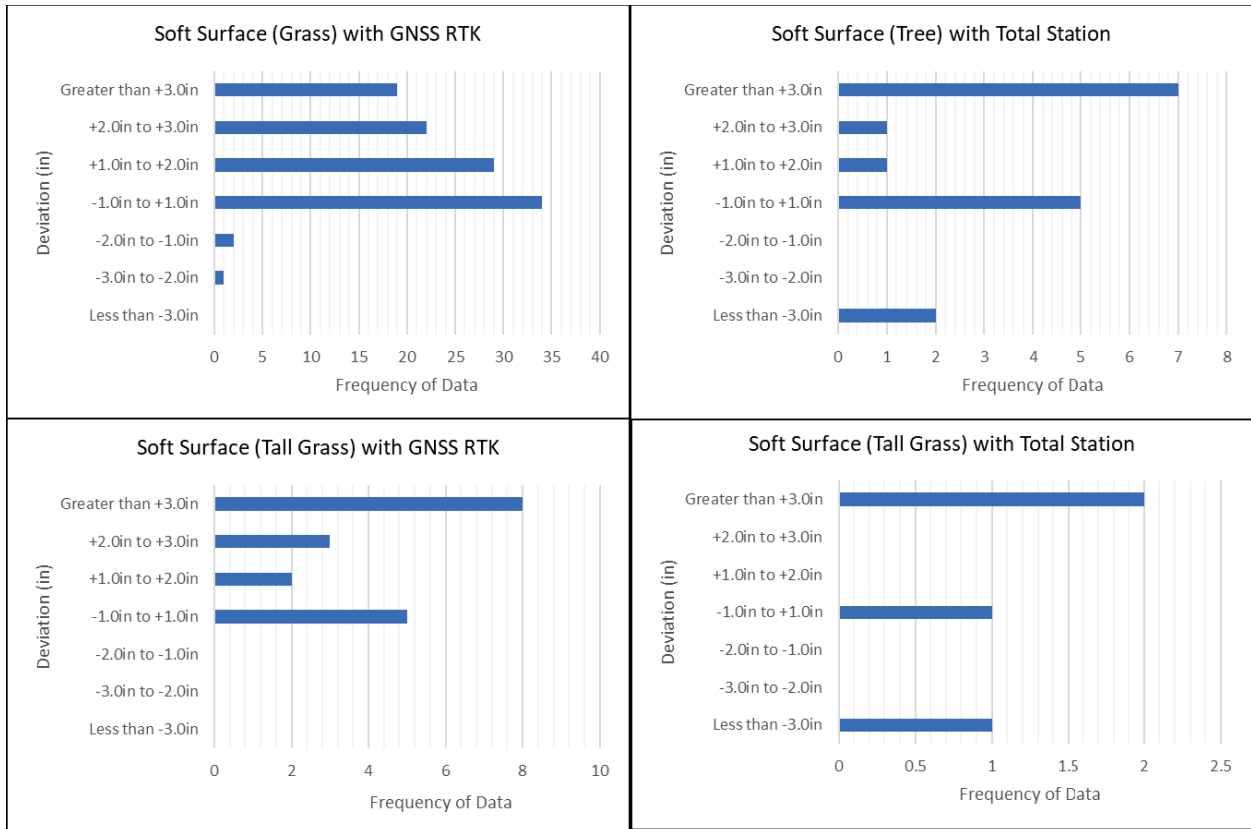
Figure 53. Aerial Image Showing the Comparison of UARK LiDAR Raster Elevations with GNSS/Total Station Checkpoints for Soft Surfaces at Frenchman's Bayou (Job 101129)

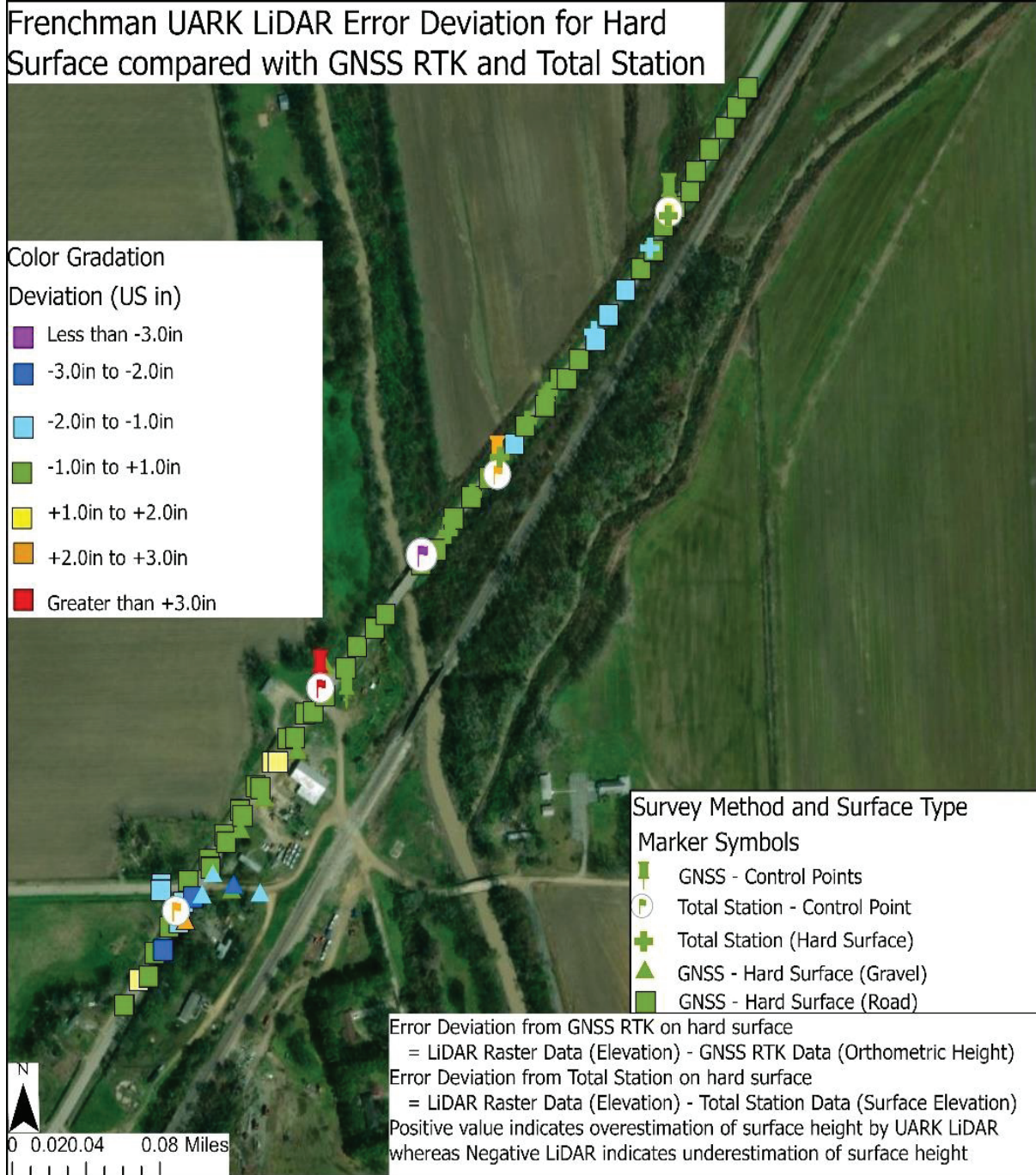To aid a better understanding of the distribution of the error for each surface type for the UARK LiDAR data at the Frenchman's Bayou site, the quantity of points in each error class for hard surface types and between the UARK LiDAR raster elevations and GNSS/total station checkpoints is shown in Figure 54. Most of the points, regardless of surface type, fell within the +1.0 inch to -1.0 inch range, indicating good accuracy for each surface type. Figure 55 shows the quantity of points in each error class for soft surface types and between the UARK LiDAR raster elevations and GNSS/total station checkpoints. For grass points, the error tended to be in the +1.0 inch to -1.0 inch range, with errors on both sides. The tall grass and tree points tended to be on the positive side, with many points falling between the +1.0 inch to -1.0 inch range, and some points approaching or exceeding the 3+ inches error range. These large errors were especially true for the tree checkpoints.

A box and whisker plot of the error between the UARK LiDAR raster elevations and GNSS/total station checkpoint elevations for the different surface types is shown in Figure 56. Similar to the other plots for the Frenchman's Bayou site, most of the hard surface checkpoints fell near the +1.0 inch to -1.0 inch range, with the soft surface points (grass and trees) having significantly more variability than the hard surface points. The tall grass checkpoints tended to have positive errors, with a mean error of around 1.0 inch to 2.0 inches, which varied up to 4.0 inches. The tree points have the most variability, with the mean error being around +4.0 inches and even +6.0 inches in some cases.

Figure 54. Data Frequency Bar Graph Showing the Comparison of UARK LiDAR Raster Elevations with GNSS/Total Station Checkpoints for Hard Surfaces at Frenchman's Bayou (Job 101129)
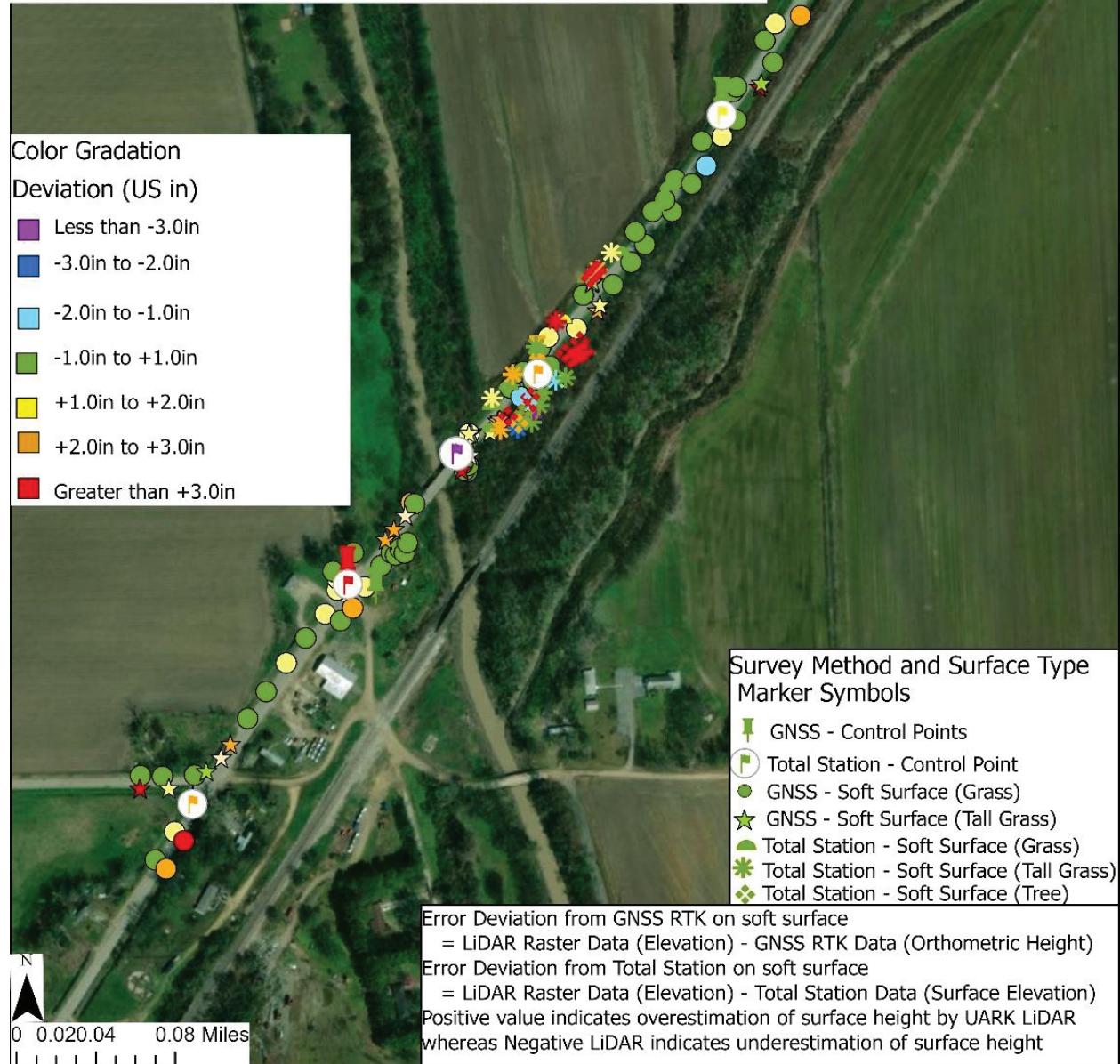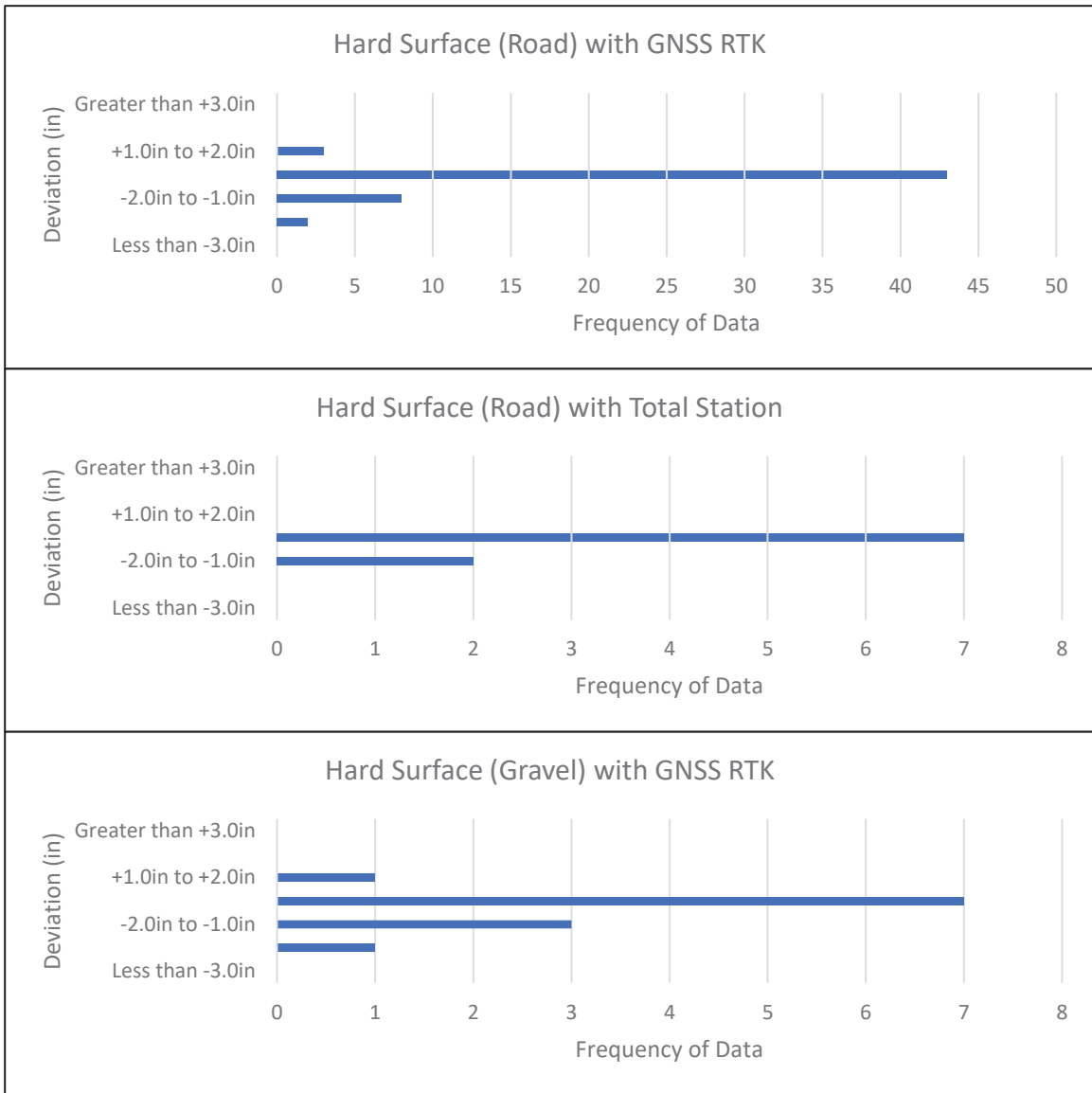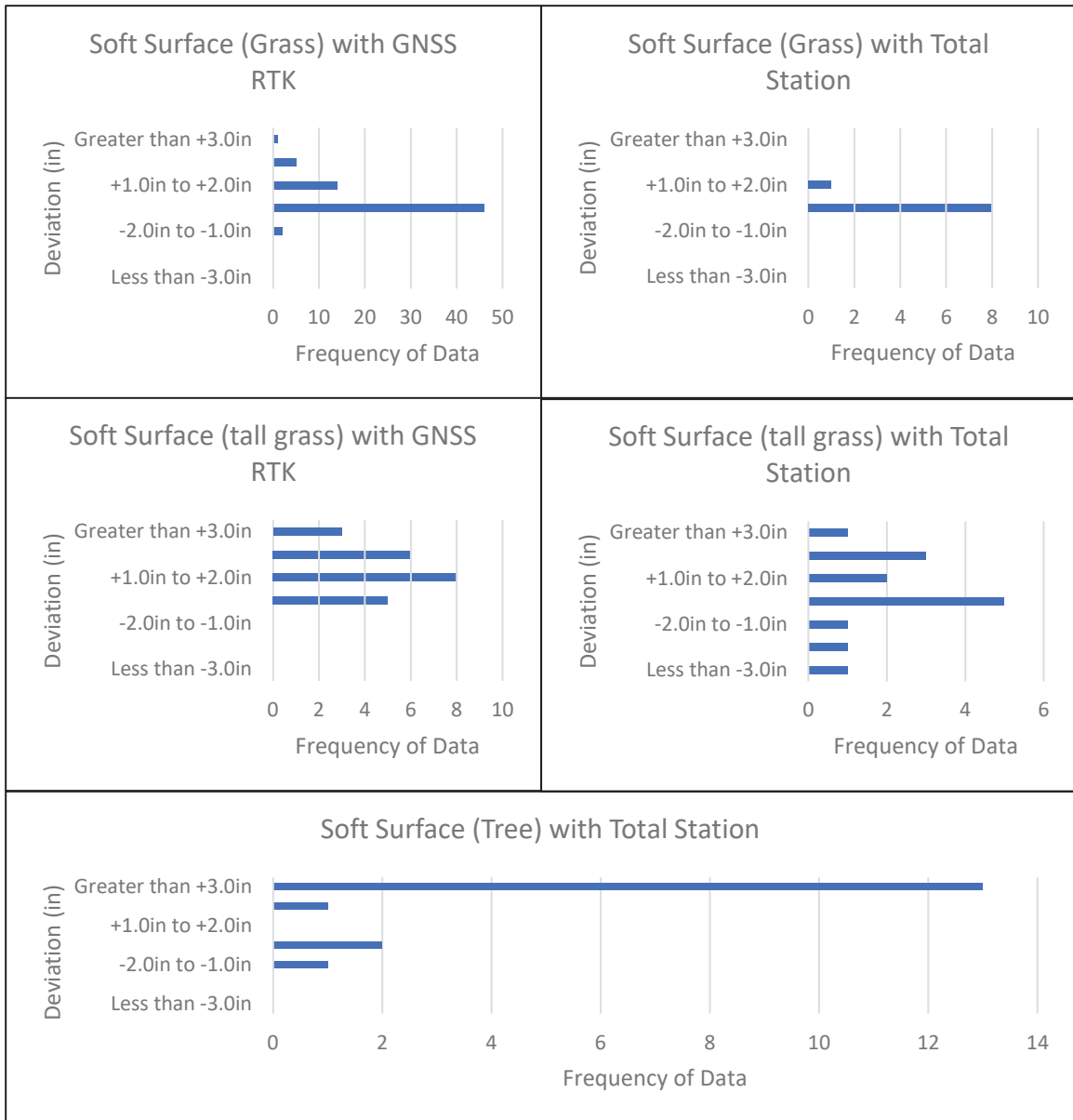
Figure 55. Data Frequency Bar Graph Showing the Comparison of UARK LiDAR Raster Elevations with GNSS/Total Station Checkpoints for Soft Surfaces at Frenchman's Bayou (Job 101129)
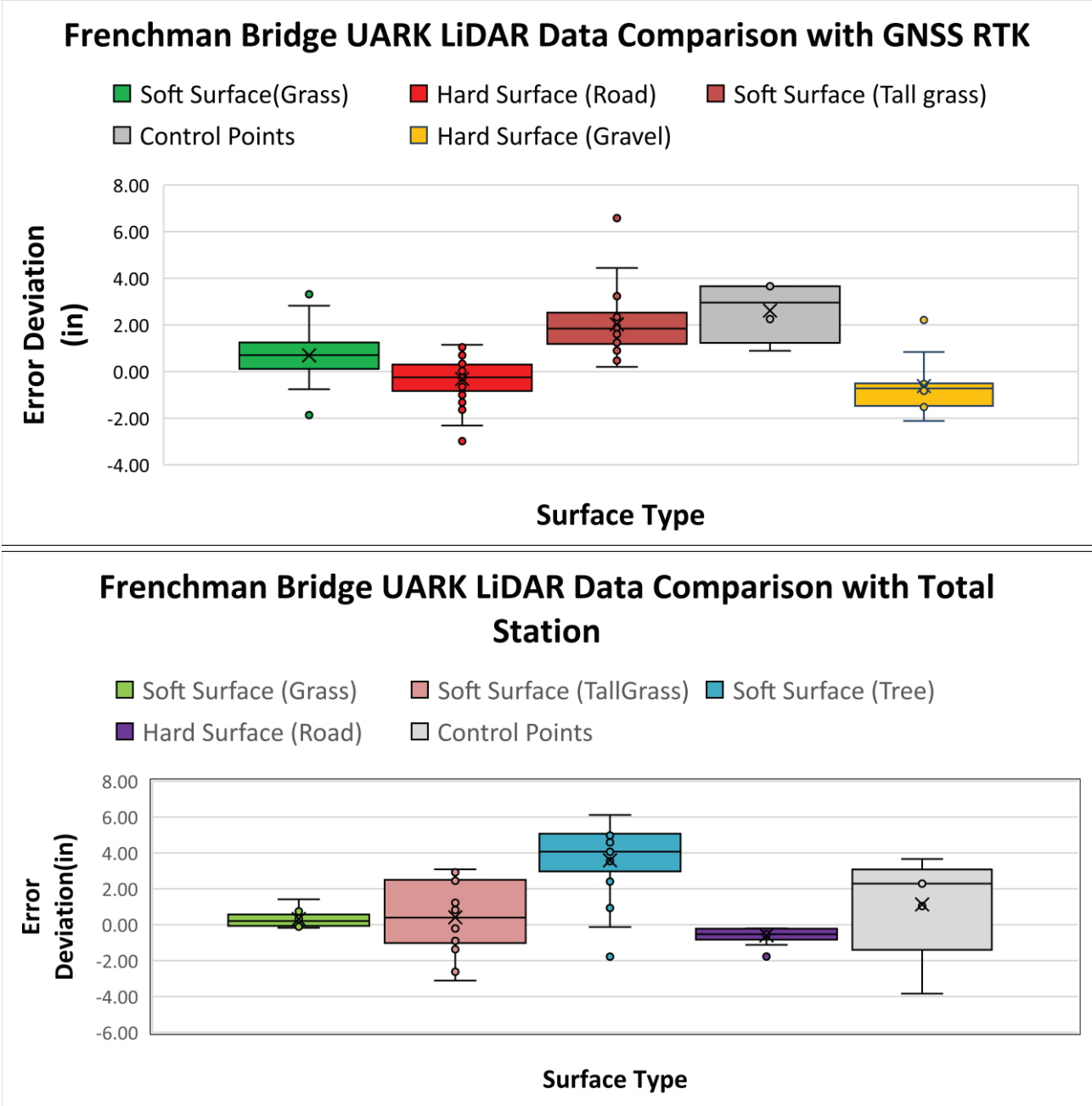
Figure 56. Box and Whisker Plot Showing the Comparison of UARK LiDAR Raster Elevations with GNSS (Top)/Total Station (Bottom) Checkpoints for Hard and Soft Surfaces at Frenchman's Bayou (Job 101129)

For Frenchman's Bayou, the error of the ArDOT LiDAR and the GNSS/total station for hard surface checkpoints is shown in an aerial photo of the site in Figure 57. For the hard surface checkpoints, almost all the data were in the +1.0 inch to -1.0 inch (green) range, indicating good accuracy. Some points had underestimated elevation. In general, this is very similar to the UARK LiDAR results. The error of the ArDOT LiDAR and GNSS/total station for soft surface checkpoints is shown in an aerial photo of the site in Figure 58. About half of the soft surface checkpoints were within the +1.0 inch to -1.0 inch (green) range, indicating good accuracy. However, the other half of the grass checkpoints tended to overestimate the elevation in the +1.0 inch to +2.0 inches (yellow) range, with some exceeding this range. The tall grass and tree checkpoints tended to have errors greater than +3.0 inches (red), with some having errors less than this. This error was generally greater than observed in the UARK LiDAR data. However, the helicopter LiDAR data were collected by ArDOT more than a year before the UARK LiDAR data were collected. Therefore, the ground and grass conditions could have changed significantly in this time; so, the differences in the soft surface measurements are expected.

Figure 57. Aerial Image Showing the Comparison of ARDOT LiDAR Raster Elevations with GNSS/Total Station Checkpoints for Hard Surfaces at Frenchman's Bayou (Job 101129)

76

Figure 58. Aerial Image Showing the Comparison of ARDOT LiDAR Raster Elevations with GNSS/Total Station Checkpoints for Soft Surfaces at Frenchman's Bayou (Job 101129)

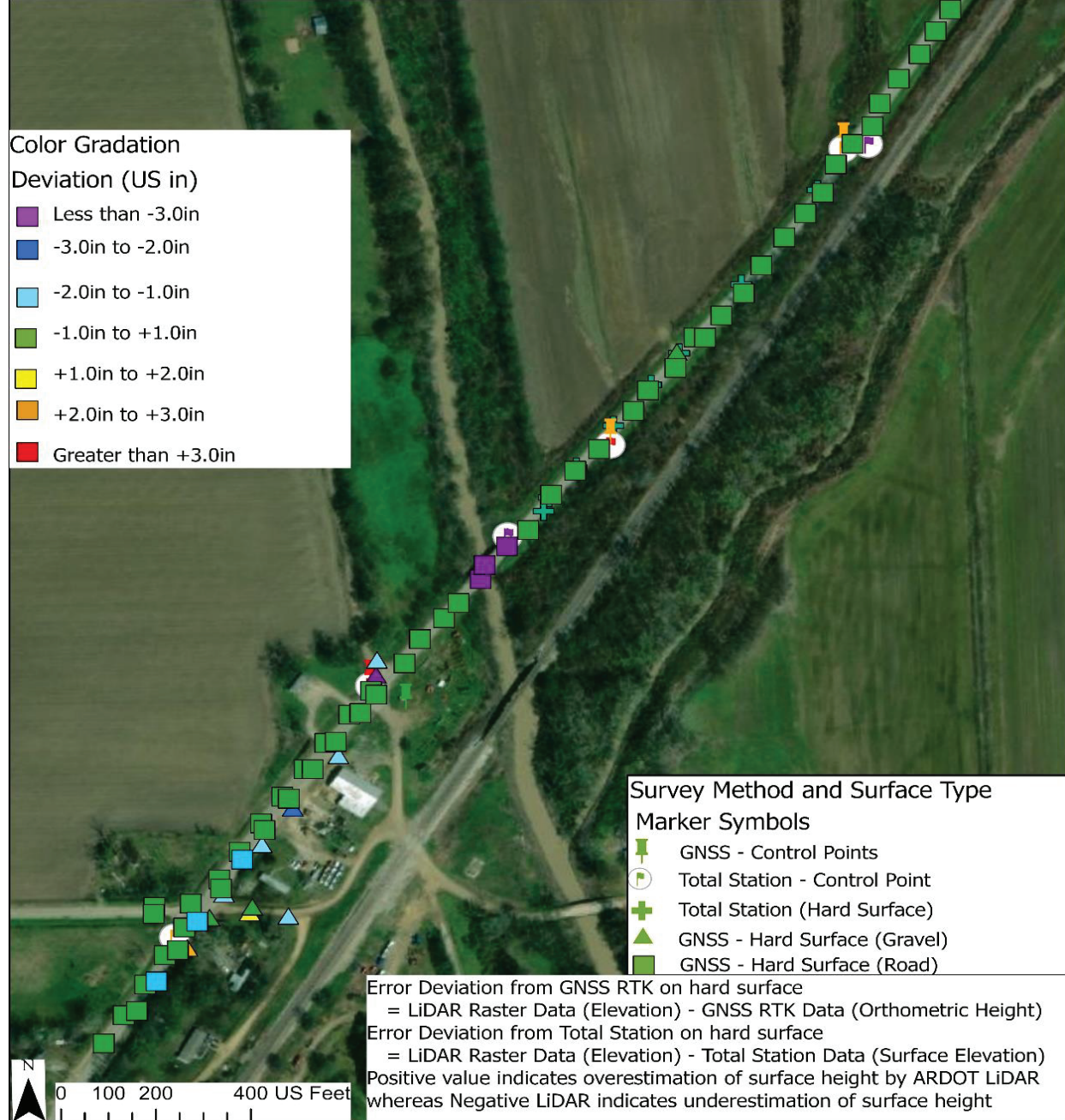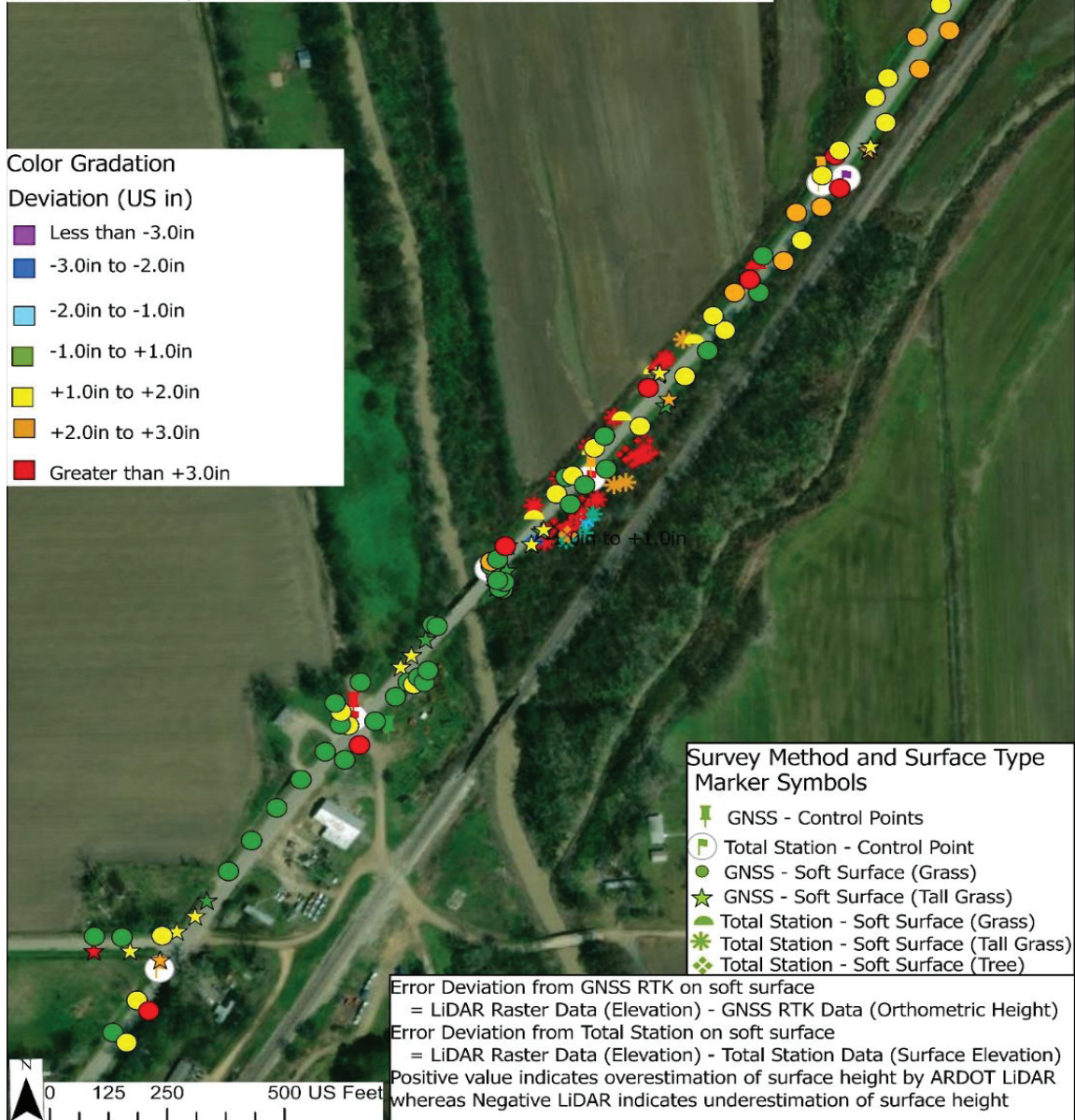To aid a better understanding of the distribution of the error for each surface type for the ArDOT LiDAR data at the Frenchman's Bayou site, the quantity of points in each error class for hard surface types and for the ArDOT LiDAR raster elevations and GNSS/total station checkpoints is shown in Figure 59. Almost all the hard surface points fell within the +1.0 inch to -1.0 inch range, indicating good accuracy for each surface type. Some variability was observed for the gravel checkpoints. Figure 60 shows the quantity of points in each error class for soft surface types and for the ArDOT LiDAR raster elevations and GNSS/total station checkpoints. For grass points, the error tended to be in the +1.0 inch to -1.0 inch range, with the errors being positive. For the tall grass and tree points, errors tended to be on the positive side, with many points in each positive-error category.

A box and whisker plot of the error in the ArDOT LiDAR raster elevations and GNSS/total station checkpoint elevations for the different surface types is shown in Figure 61. Similar to the other plots for the Frenchman's Bayou site, most of the hard surface checkpoints fell in the +1.0 inch to -1.0 inch range, with the soft surface points (grass and trees) having significantly more variability than the hard surface points. The tall grass checkpoints tended to have positive errors, with a mean of around 1.0 inch to 2.0 inches, which varied up to 4 inches. The tree checkpoints have the most variability, with a mean error of around +4.0 inches and even +6.0 inches in some cases.

The DEM for the UARK LiDAR data was subtracted from that for the ArDOT LiDAR at the Frenchman's Bayou site (Figure 62). This allowed for the visualization of the differences between the LiDAR elevations over the entire measurement area at once. The overall map shows that the ArDOT LiDAR produced a similar elevation (-1.0inch to +1.0 inch, green) for most of the map, indicating excellent agreement between the datasets. Some grass areas had a slightly higher elevation for the ArDOT LiDAR (+1.0 inch to +3.0 inches, yellow, pink) than for the UARK LiDAR. The blue underestimates on the figure are generally located where there is standing water (i.e., creeks and low areas on the map). Overall, these datasets had excellent agreement.

Figure 59. Data Frequency Bar Graph Showing the Comparison of ARDOT LiDAR Raster Elevations with GNSS/Total Station Checkpoints for Hard Surfaces at Frenchman's Bayou (Job 101129)

Figure 60. Data Frequency Bar Graph Showing the Comparison of ARDOT LiDAR Raster Elevations with GNSS/Total Station Checkpoints for Soft Surfaces at Frenchman's Bayou (Job 101129)

Figure 61. Box and Whisker Plot Showing the Comparison of ARDOT LiDAR Raster Elevations with GNSS/Total Station Checkpoints for Hard (Top) and Soft (Bottom) Surfaces at Frenchman's Bayou (Job 101129)
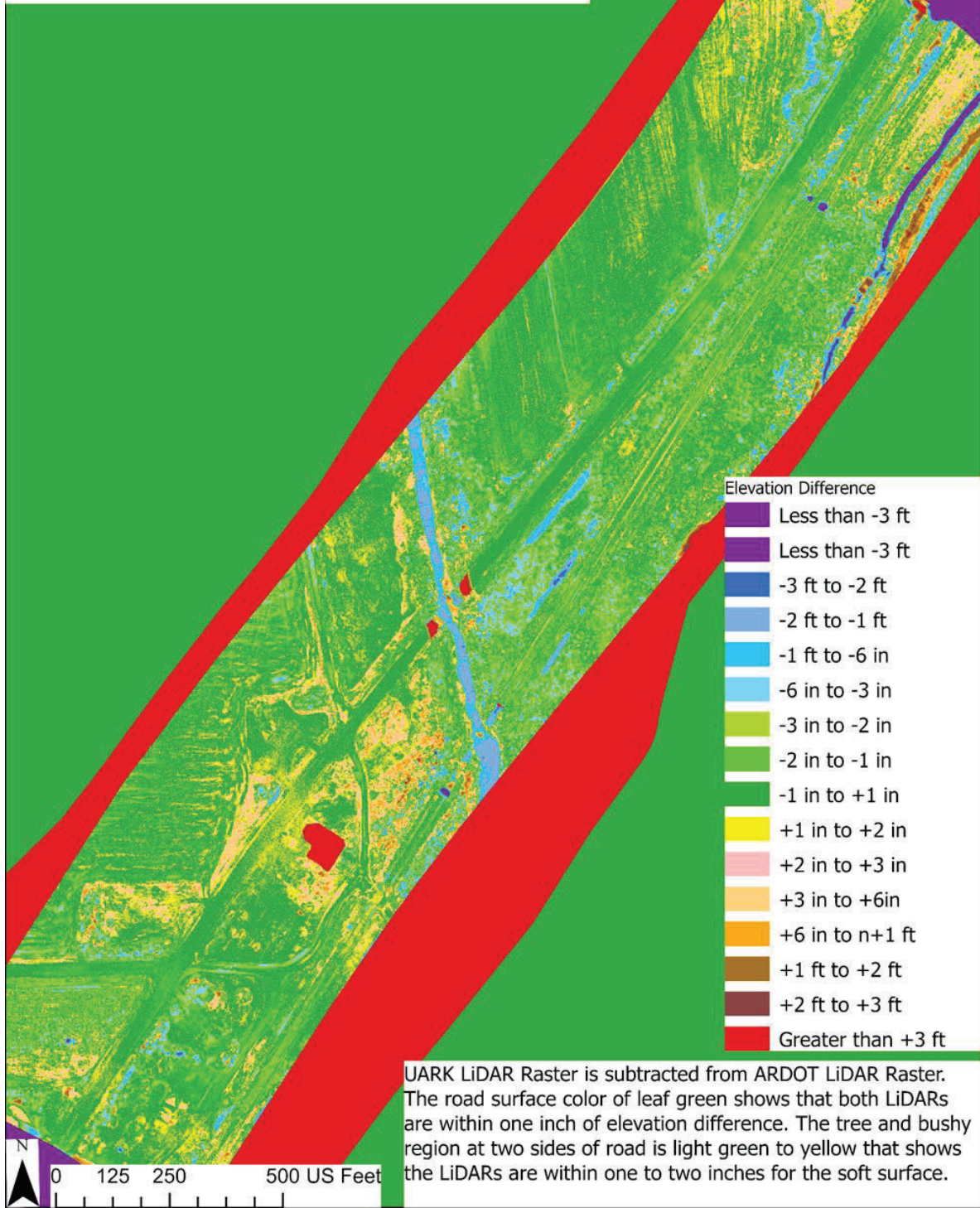
Figure 62. ARDOT LiDAR DEM Subtracted from UARK LiDAR DEM at Frenchman's Bayou (Job 101129)

MOUNTAIN HOME, ARKANSAS JOB 090647

For the Mountain Home site, the error between the UARK LiDAR and GNSS for hard surface checkpoints is shown in an aerial photo of the site in Figure 63. For the hard surface checkpoints, more than half of the data was within the +1.0 inch to -1.0 inch (green) range, indicating good accuracy. The other half slightly overestimated or underestimated the elevation. The error between the UARK LiDAR and GNSS for soft surface checkpoints is shown in an aerial photo of the site in Figure 64. Many of the grass checkpoints near the road were within the +1.0 inch to -1.0 inch (green) range, indicating good accuracy. However, for other points, LiDAR generally overestimated the elevation, with many checkpoints falling between +1.0 inch and +2.0 inches (yellow) and some higher error points falling between +2.0 inches and +3.0 inches (orange) and even greater than +3.0 inches (red). In addition, some points were in the -2.0 inches to -1.0 inch range. The overestimation was generally expected given the height of grass in the area.

Figure 63. Aerial Image Showing the Comparison of UARK LiDAR Raster Elevations with GNSS Checkpoints for Hard Surfaces at Mountain Home (Job 090647)

Figure 64. Aerial Image Showing the Comparison of UARK LiDAR Raster Elevations with GNSS Checkpoints for Soft Surfaces at Mountain Home (Job 090647)

To aid a better understanding of the distribution of the error for each surface type at the Mountain Home site, the quantity of points in each error class for each surface type and between the UARK LiDAR raster elevations and GNSS/total station checkpoints is shown in Figure 65. Most of the points for hard surface types fell within the +1.0 inch to -1.0 inch range, indicating good accuracy. For grass and tree points, the error tended to fall on the positive side (indicating that LiDAR overestimated the elevation), with many of the points having errors greater than 1.0 inch.

A box and whisker plot of the error between the UARK LiDAR raster elevations and GNSS/total station checkpoint elevations for the different surface types is shown in Figure 66. The mean error for each surface type fell within the +1.0 inch to -1.0 inch range. Much more variability was observed for the soft surface points (grass and trees) than for the hard surface points. The tree checkpoints had the most variability, with both positive and negative errors.
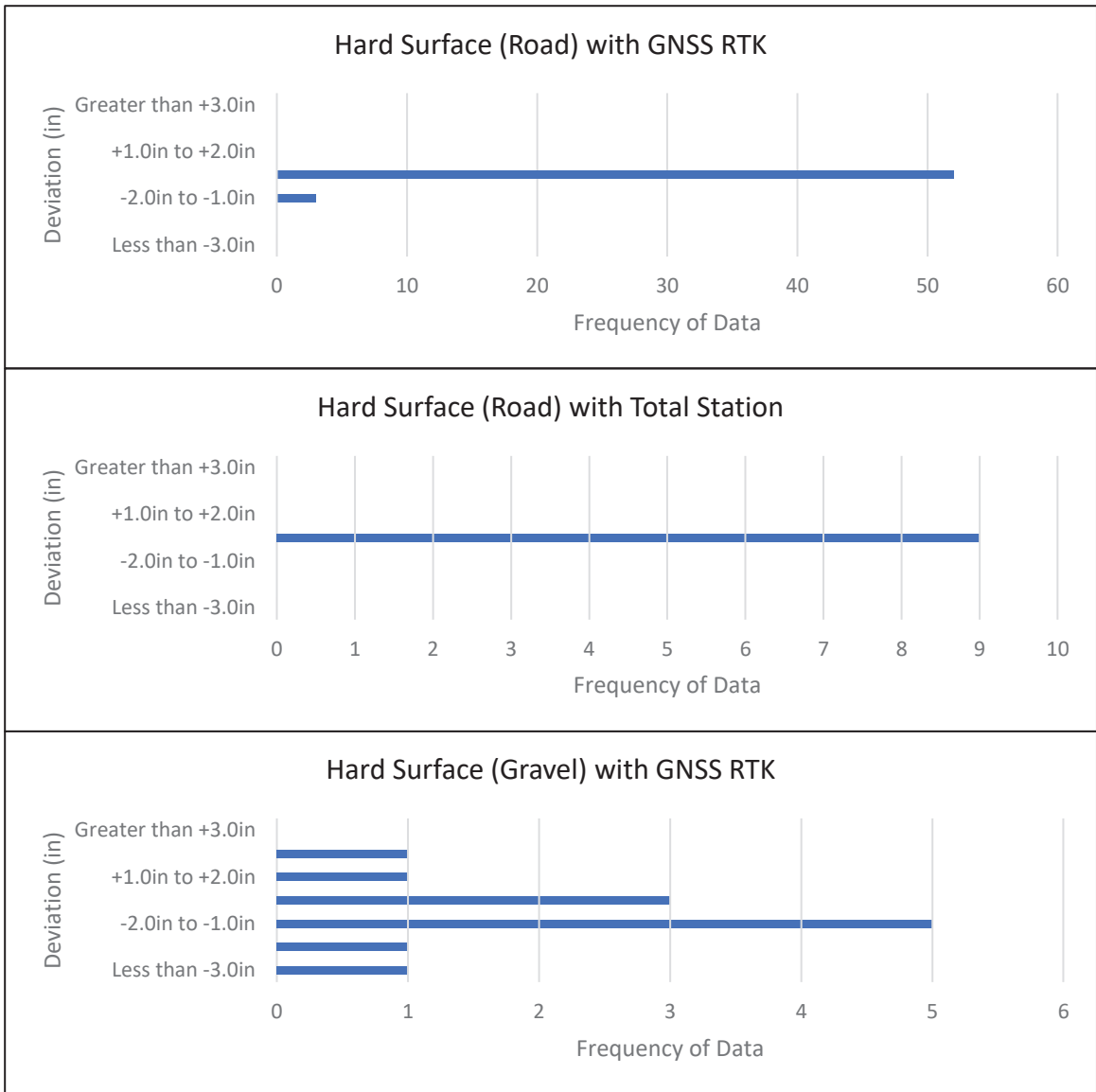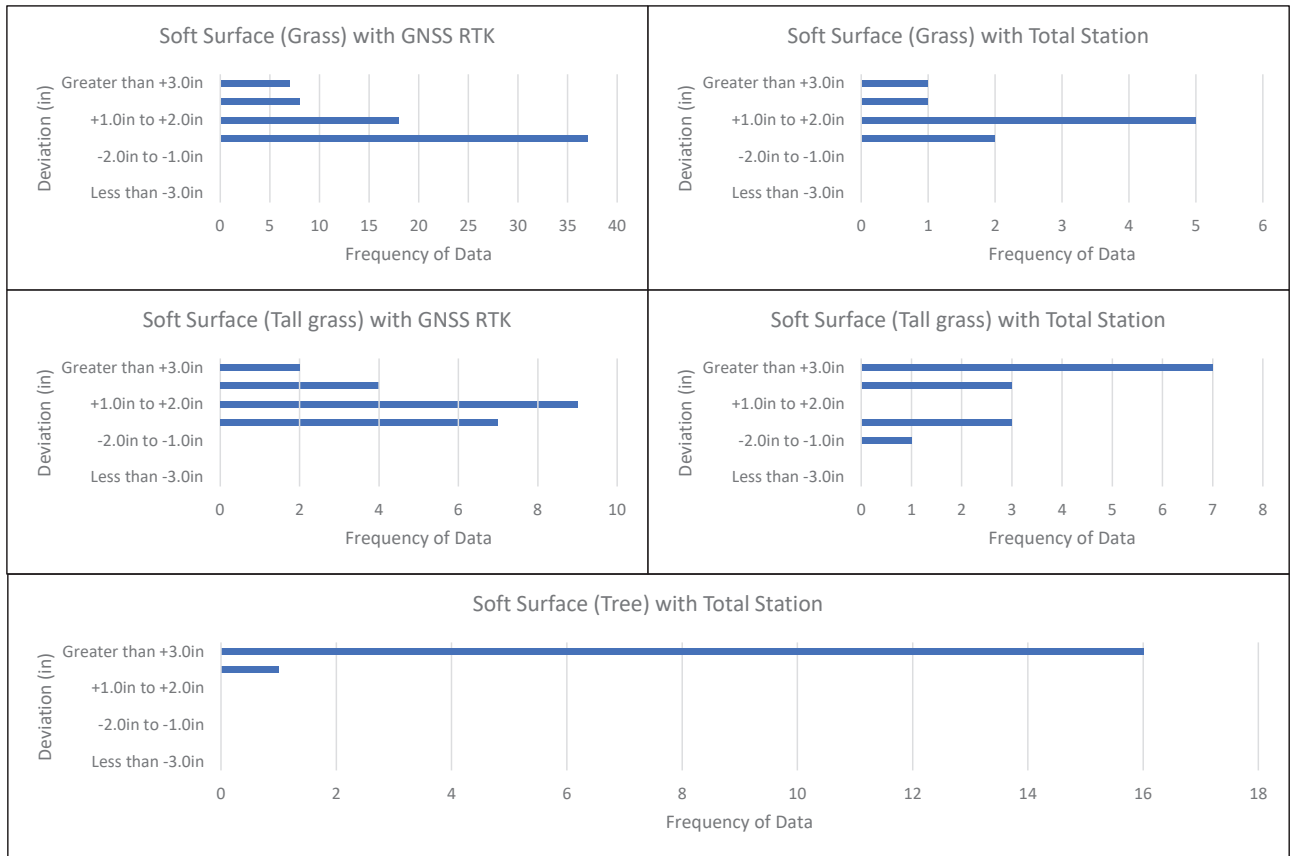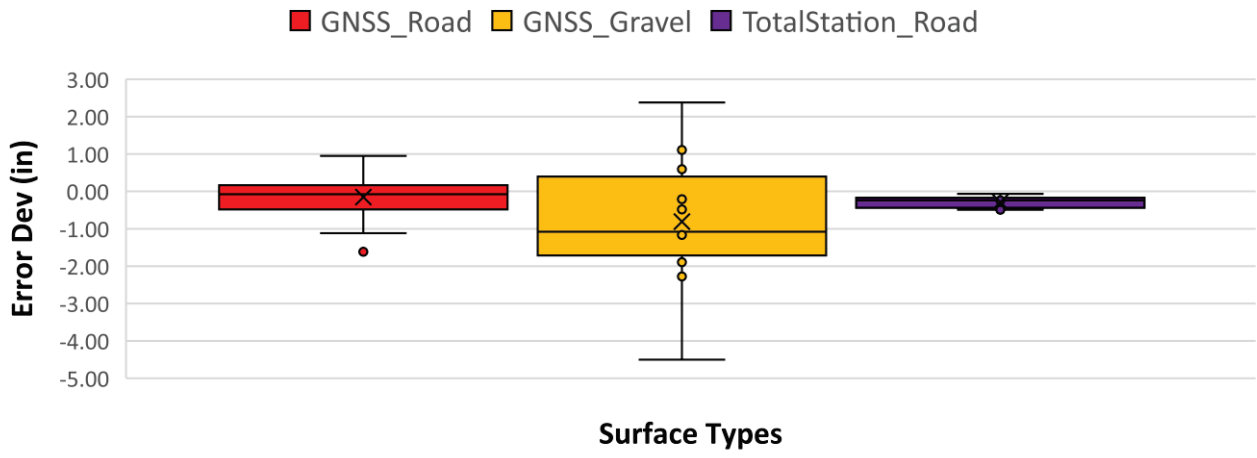
Figure 65. Data Frequency Bar Graph Showing the Comparison of UARK LiDAR Raster Elevations with GNSS/Total Station Checkpoints for Hard and Soft Surfaces at Mountain Home (Job 090647)
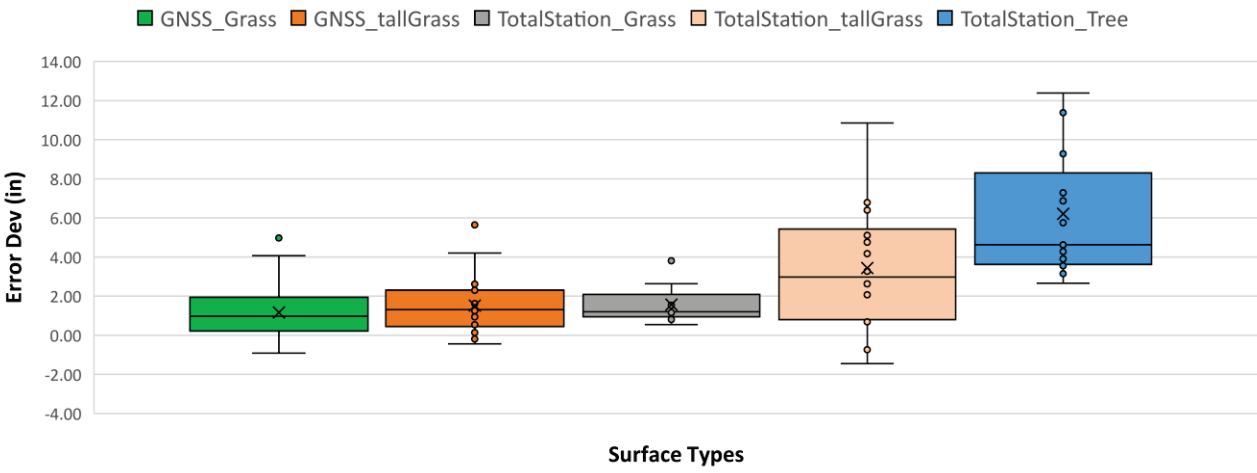
Figure 66. Box and Whisker Plot Showing the Comparison of UARK LiDAR Raster Elevations with GNSS Checkpoints for Hard and Soft Surfaces at Mountain Home (Job 090647)

For the Mountain Home site, the error in the ArDOT LiDAR and GNSS data for hard surface checkpoints is shown in an aerial photo of the site in Figure 67. For the hard surface checkpoints, most of the data was within the +1.0 inch to -1.0 inch (green), indicating good accuracy. Similar to the UARK LiDAR data at Mountain Home, the other points tended to slightly overestimated and underestimated. In Figure 68, the error between the ArDOT LiDAR and GNSS for soft surface checkpoints is shown in an aerial photo of the site. Most of the points indicate an overestimation, with errors of above +3.0 inches. This is significantly more error than observed in the UARK data. However, the ArDOT LiDAR data were collected during the summer when grass height could be much higher, leading to the errors observed in the LiDAR data for soft surface points.
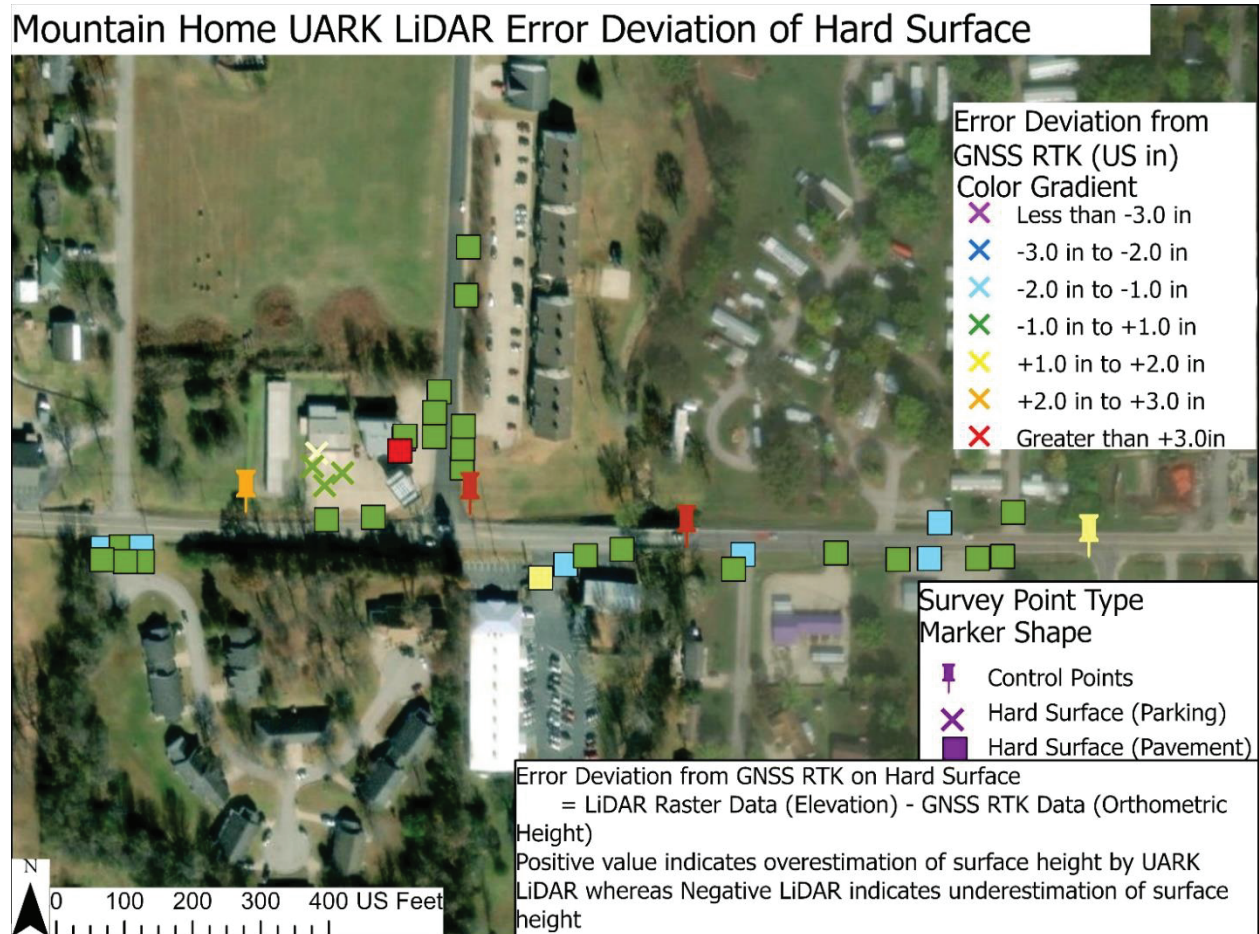
Figure 67. Aerial Image Showing the Comparison of ARDOT LiDAR Raster Elevations with GNSS Checkpoints for Hard Surfaces at Mountain Home (Job 090647)
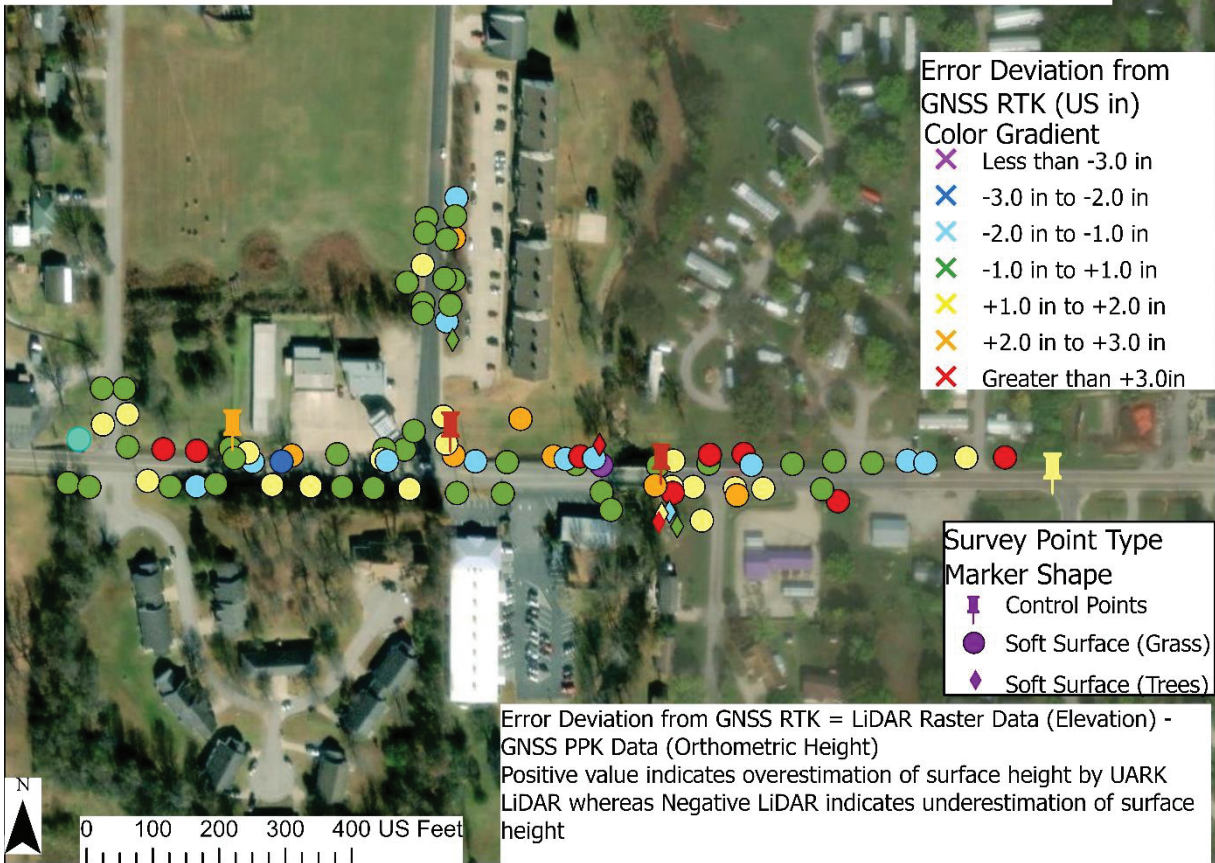

Figure 68. Aerial Image Showing the Comparison of ARDOT LiDAR Raster Elevations with GNSS Checkpoints for Soft Surfaces at Mountain Home (Job 090647)

To aid a better understanding of the distribution of the error for each surface type at the Mountain Home site, the quantity of points in each error class for each surface type and for the AʀDOT LiDAR raster elevations and the GNSS checkpoints is shown in Figure 69. Most of the points for hard surface types fell within the +1.0 inch to -1.0 inch range, indicating good accuracy. For grass and tree points, the error tended to be on the positive side (indication that LiDAR overestimated the elevation), with many of the points having errors greater than 3.0 inches.

A box and whisker plot of the error in the AʀDOT LiDAR raster elevations and GNSS/total station checkpoint elevations for the different surface types is shown in Figure 70. The mean error for hard surfaces fell within the +1.0 inch to -1.0 inch range, with generally low variability. Much more variability was observed for the soft surface points (grass and trees) than for the hard surface points. The mean error for the soft surface points was +2 inches to +3.0 inches, with errors above +3.0 inches being common. The tree checkpoints had the most variability, with both positive and negative errors.

The DEM for the UARK LiDAR was subtracted from that for the AʀDOT LiDAR (Figure 71), allowing for the visualization of the differences between the LiDAR elevations over the entire measurement area at once. On the overall map, the AʀDOT LiDAR tends to have a similar (-1.0inch to +1.0 inch, green) or a slightly higher (+1.0inch to +3.0 inches, yellow) elevation compared to the UARK LiDAR. The higher elevation occurred for both hard (roads) and soft (short grass) surfaces. For some areas with higher elevation (i.e., roof tops and trees), AʀDOT LiDAR's elevation tended to be lower by 3 inches to 2 ft; however, these types of surfaces were generally not of interest in the LiDAR surveys and this was often a processing issue rather than a measurement issue. The final area of interest was the large brown area in the north-west corner of the survey area. This is a large open field classified as tall/thick grass. For this field, the AʀDOT had a significantly higher elevation (+1 inch to 3 ft) than the UARK LiDAR. This is likely because of differences in grass height during each survey. The grass had been recently mowed prior to the UARK LiDAR and was likely significantly higher for the AʀDOT LiDAR measurements that took place in June. Therefore, grass height and measurement time can be critical to the accuracy of measuring ground elevation for tall grass areas.
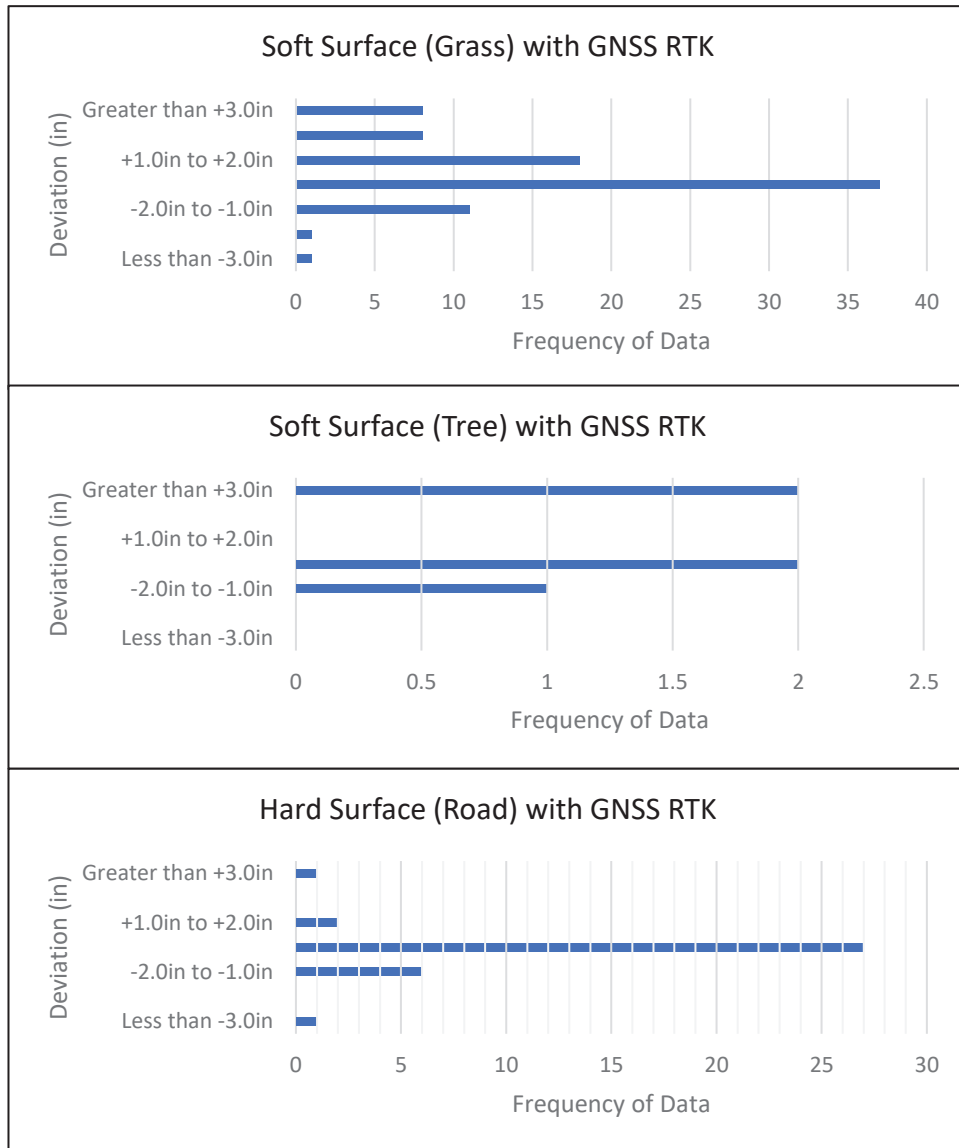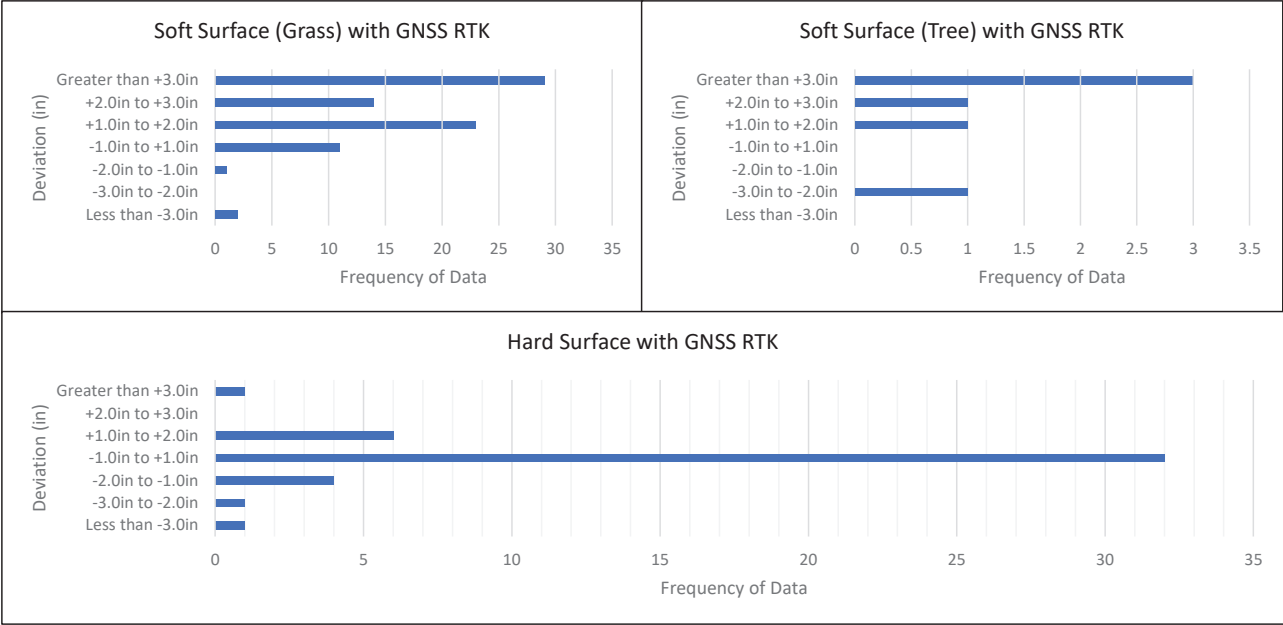
Figure 69. Data Frequency Bar Graph Showing the Comparison of ARDOT LiDAR Raster Elevation with GNSS Checkpoints for Hard and Soft surfaces at Mountain Home (Job 090647)
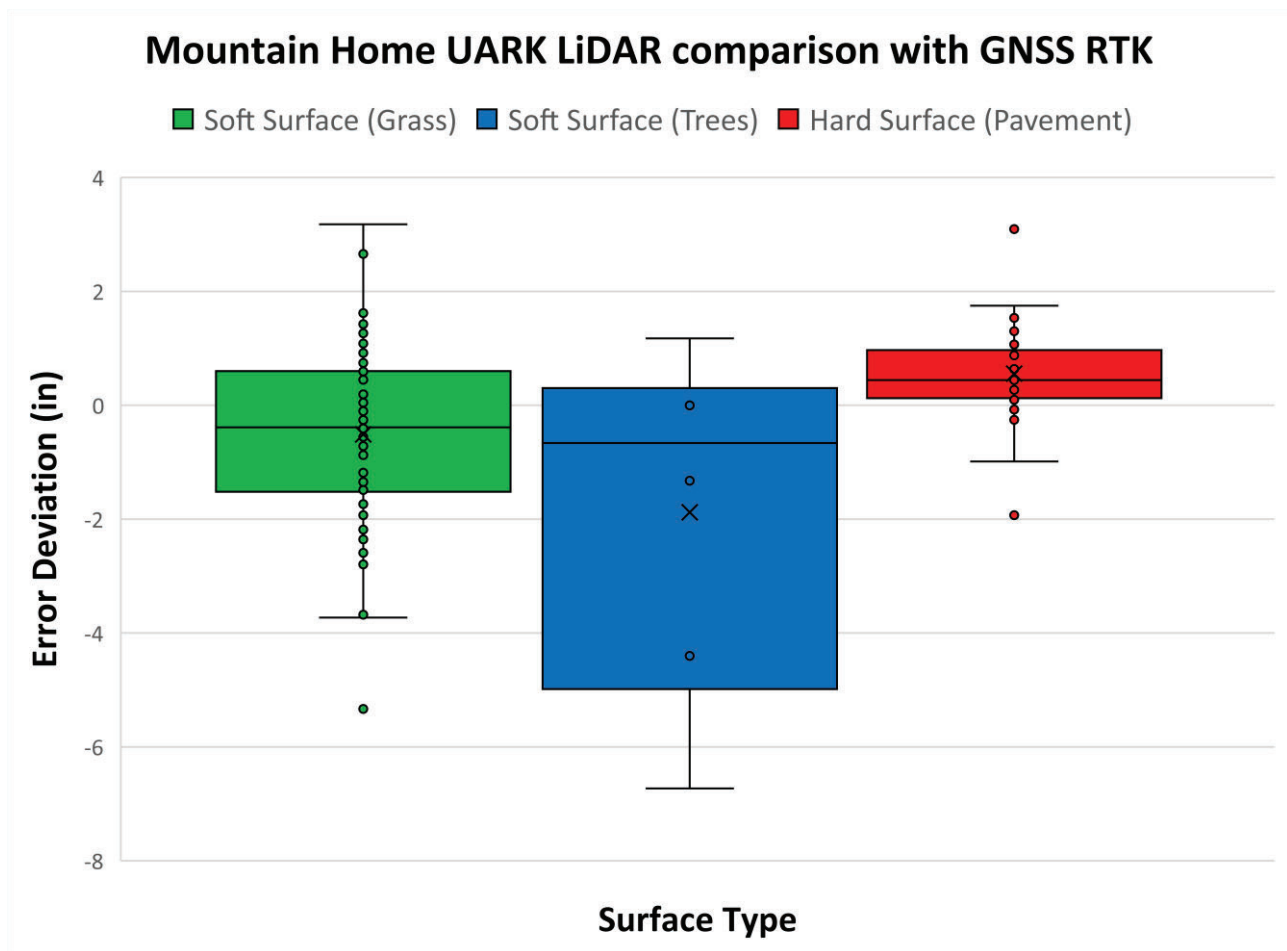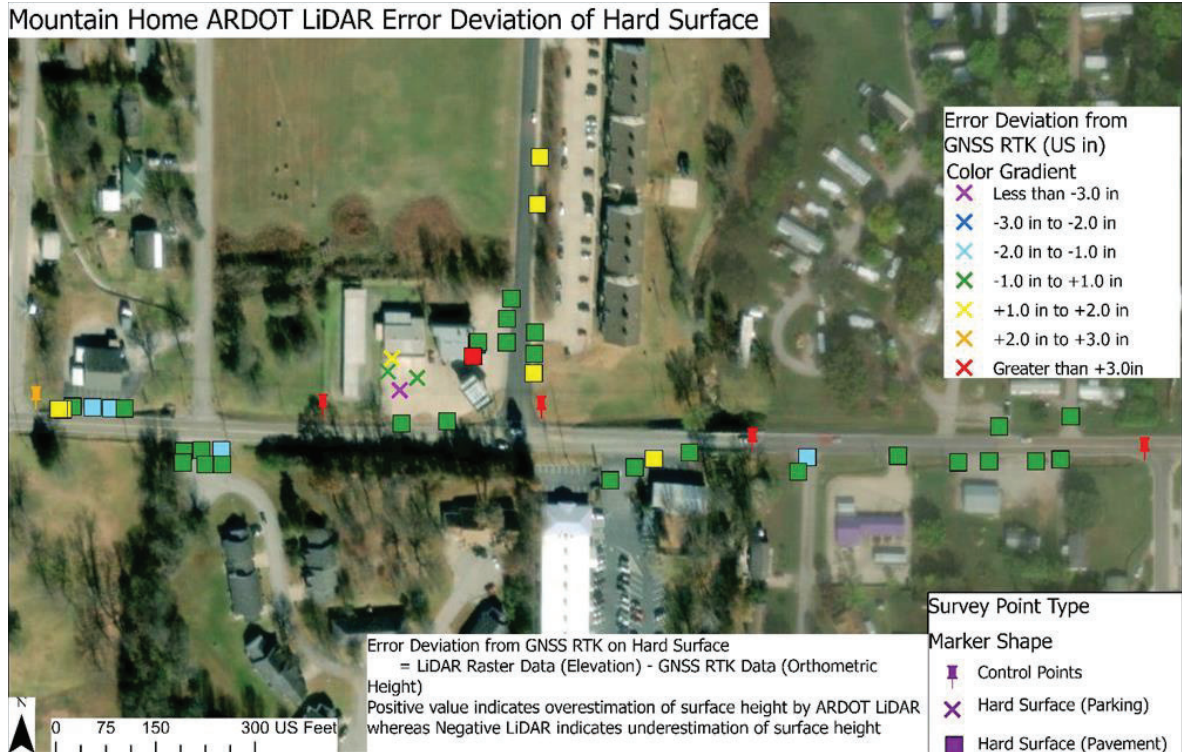
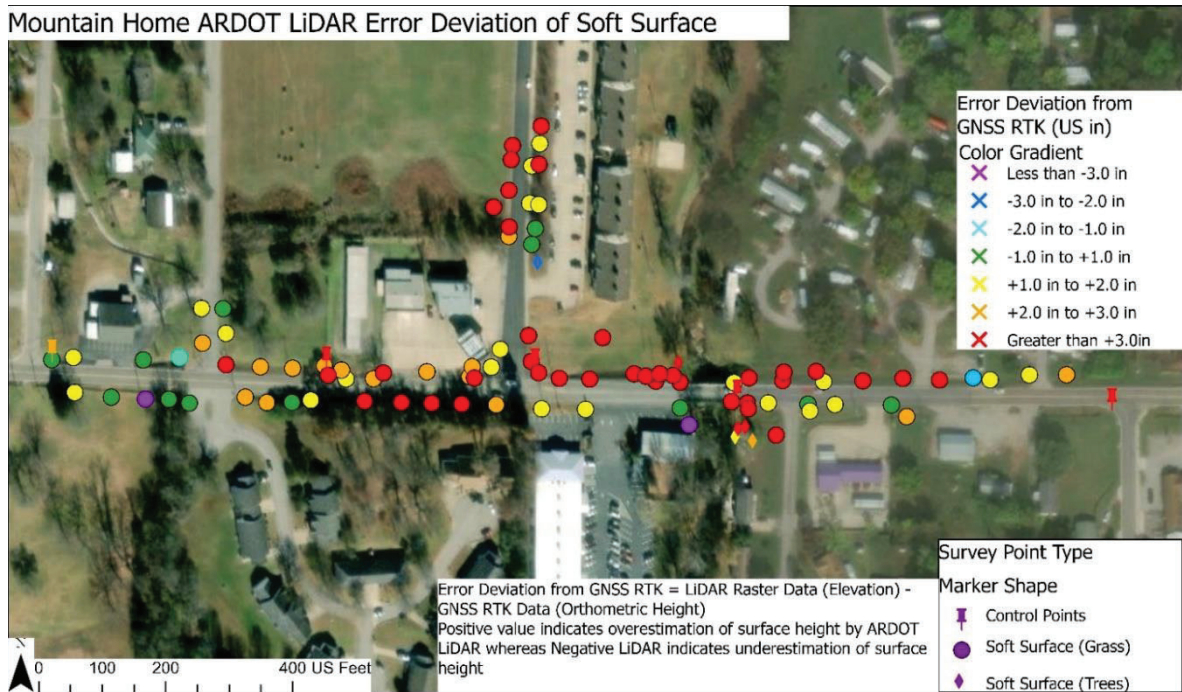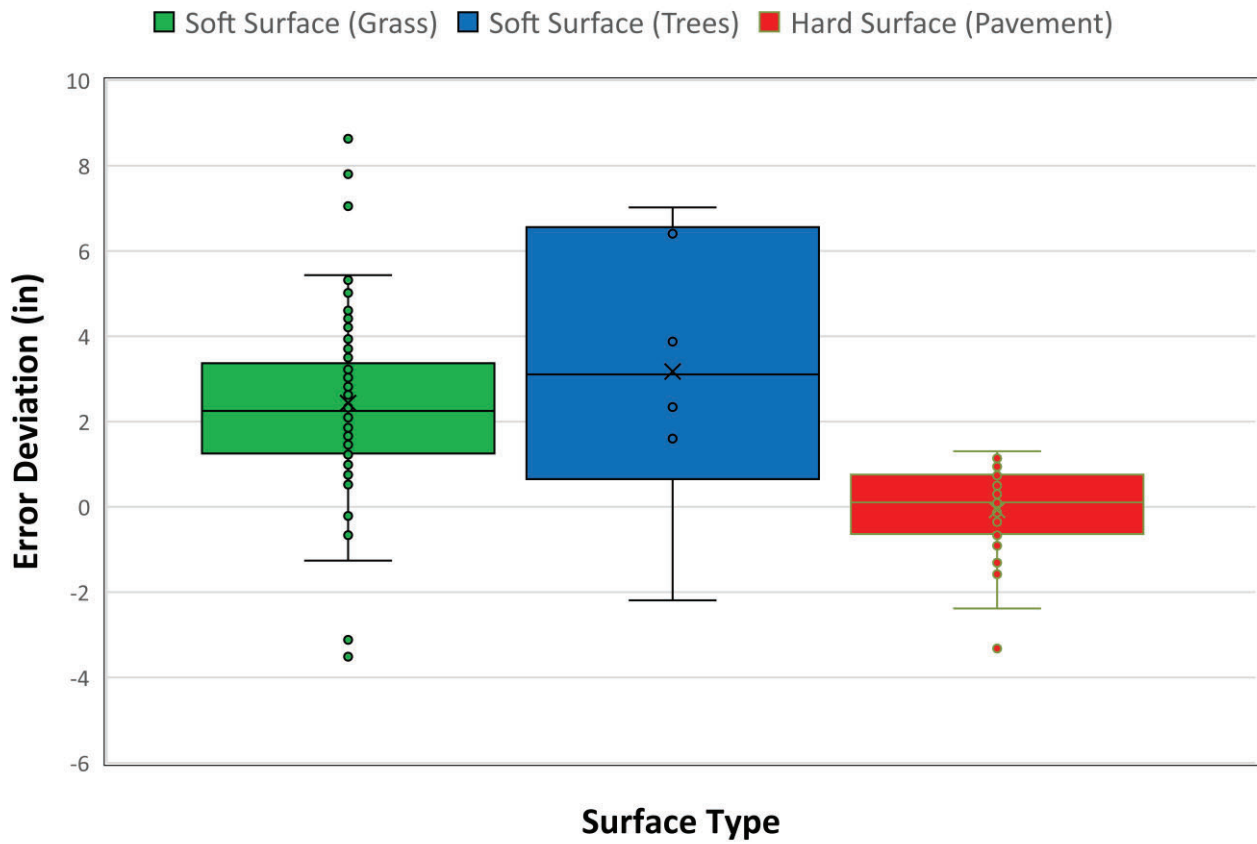**Figure 70. Box and Whisker Plot Showing the Comparison of ARDOT LiDAR Raster Elevations with GNSS Checkpoints for Hard and Soft Surfaces at Mountain Home (Job 090647)**
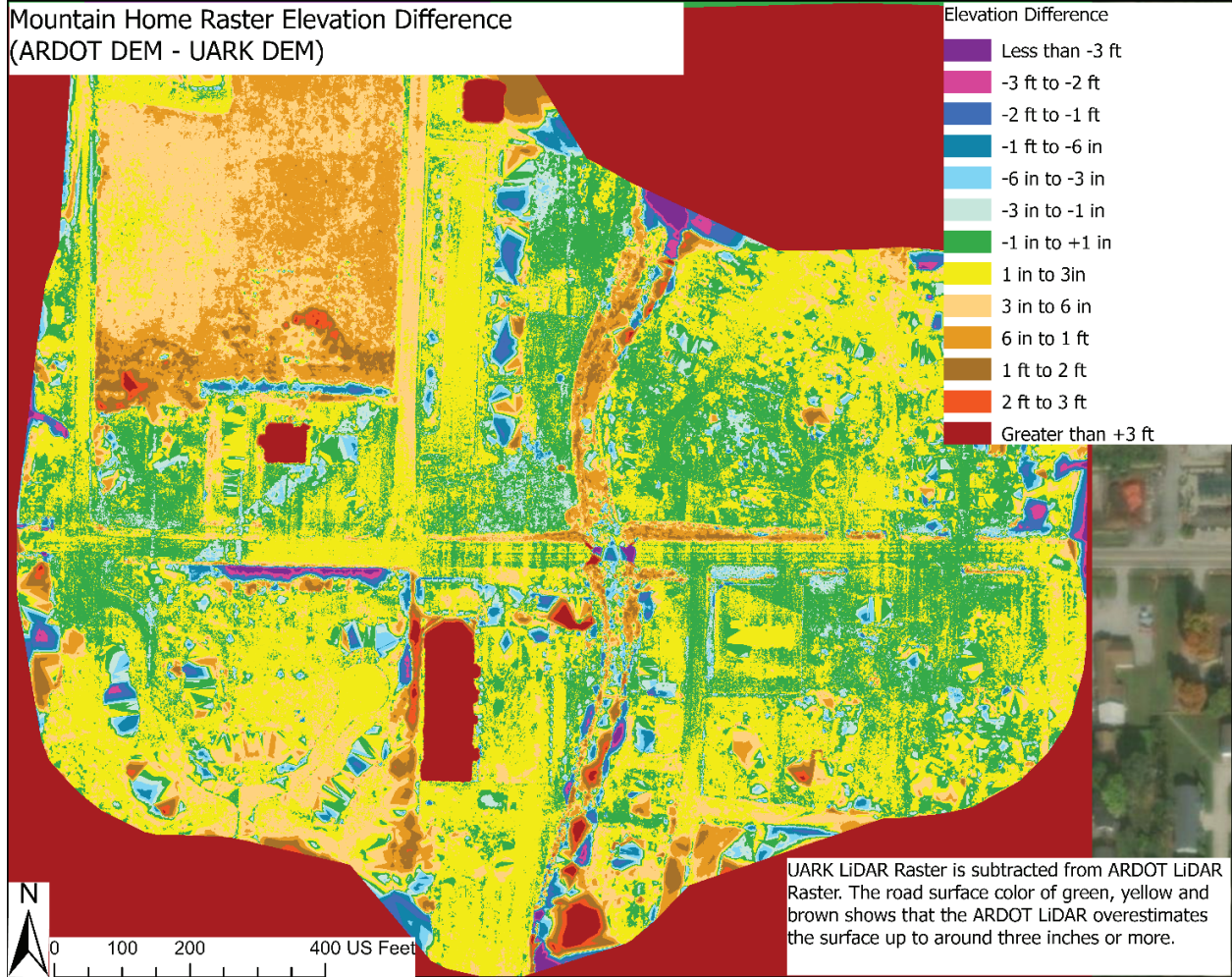
Figure 71. ARDOT LiDAR DEM Subtracted from UARK LiDAR DEM for Mountain Home (Job 090647)

CHAPTER 5. COMBINED RESULTS

This chapter compares the overall results from each site to understand the potential differences between the results of each site, as well as the expected accuracy of future surveys.

PROJECT ACCURACY COMPARISON

For each bridge site (Lincoln 1, Lincoln 2, Humnoke, Frenchman's Bayou, and Mountain Home) and LiDAR dataset (ARDOT and UARK), the root mean squared error (RMSE) was calculated for each hard surface type and is tabulated in Table 7 and visualized in Figure 72. The RMSE was calculated as the difference between the LiDAR elevation and GNSS/total station checkpoint elevation squared. The resulting values were summed and divided by the number of data points. The hard surface points were categorized as road (asphalt/concrete) and gravel (uneven rough surface) checkpoints.

For the road checkpoints measured using GNSS and a total station, an RMSE of 0.5 inches to just over 1.0 inch was observed for all sites. As observed in Chapter 4, the Frenchman's Bayou site had the highest accuracy, while the Humnoke and Mountain Home sites had the lowest. The ARDOT LiDAR data had lower error at the Frenchman's Bayou and Humnoke site, while the UARK LiDAR had a lower error at the Mountain Home site.

Table 7. RMSE for Hard Surface Checkpoints at All Sites in the Study

Site Names	Road Checkpoints RMS Error (in)	Gravel Checkpoints RMS Error (in)
Lincoln East UARK	1.06	
Lincoln West UARK	0.97	
Humnoke UARK	2.07	1.97
Humnoke ARDOT	1.80	1.28
Mountain Home UARK	1.23	
Mountain Home ARDOT	1.33	
Frenchman UARK	0.87	1.27
Frenchman ARDOT	0.53	1.86
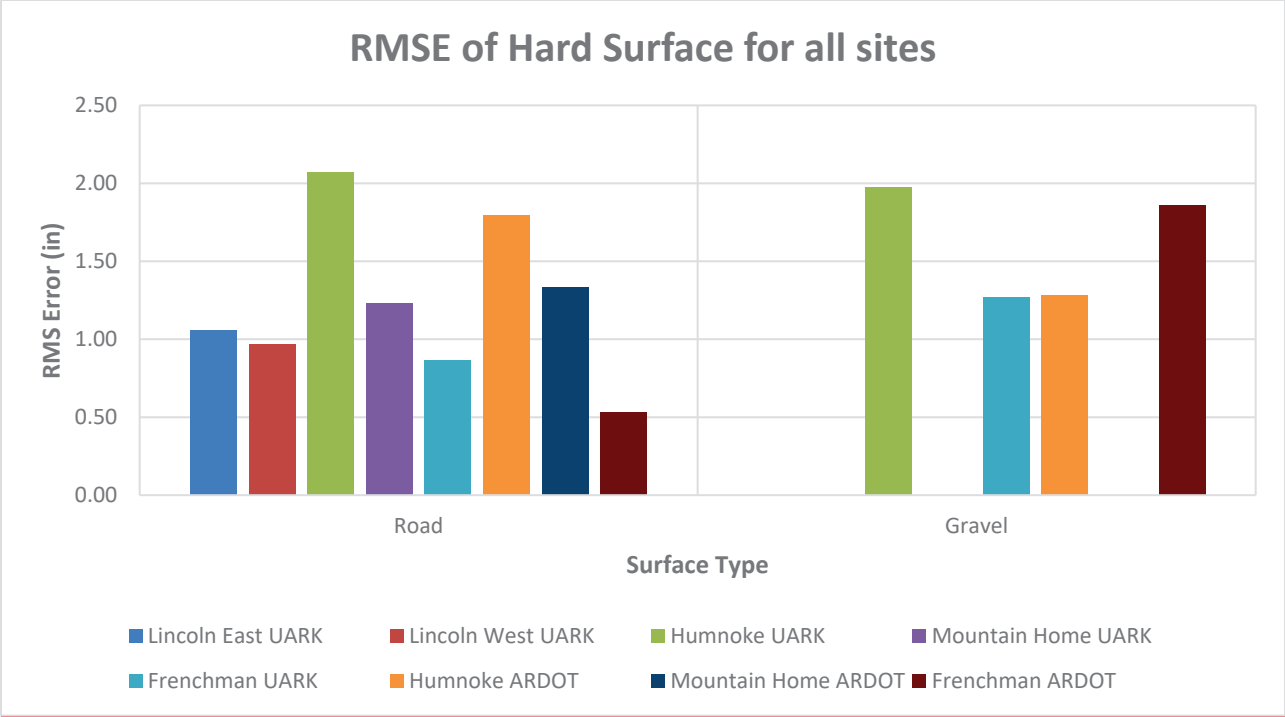
Figure 72. RMSE for All Hard Surface Checkpoints at All Sites in the Study

For each hard surface type at each bridge site (Lincoln 1, Lincoln 2, Humnoke, Frenchman's Bayou, and Mountain Home) and LiDAR dataset (ARDOT and UARK), the RMSE was calculated and is tabulated in Table 8 and visualized in Figure 73. The soft surface types were again categorized as grass (0 inches to 3.0 inches), tall grass (>3 inches to 3 ft), and tree.

The LiDAR elevation of grass surface area for the GNSS and total station measurements had an RMSE of 1.0 to 2.0 inches for all sites, with some sites having an RSME of up to 4.0 inches. This is higher than the error observed for the hard surface checkpoints. The RMSE for the tall grass checkpoints was higher than that for the short grass checkpoints at 2 to 3 inches, with the Frenchman's Bayou and Humnoke sites having values of 3 to 5 inches. Obviously, larger errors can be expected in taller grass than shorter grass. For areas with trees, the largest RMSE was observed, with values between 3 and 7 inches being typical.

Table 8. RMSE for Soft Surface Checkpoints at All Sites in the Study

Site Names	Grass Checkpoints RMS Error (in)	Tall Grass Checkpoints RMS Error (in)	Trees Checkpoints RMS Error (in)
Lincoln East UARK	1.67		2.29
Lincoln West UARK	2.38		3.73
Humnoke UARK	3.36	5.11	3.82
Humnoke ARDOT	2.15	3.75	4.55
Mountain Home UARK	1.80		3.36
Mountain Home ARDOT	3.43		4.44
Frenchman UARK	1.12	2.28	4.12
Frenchman ARDOT	1.72	3.33	6.95T
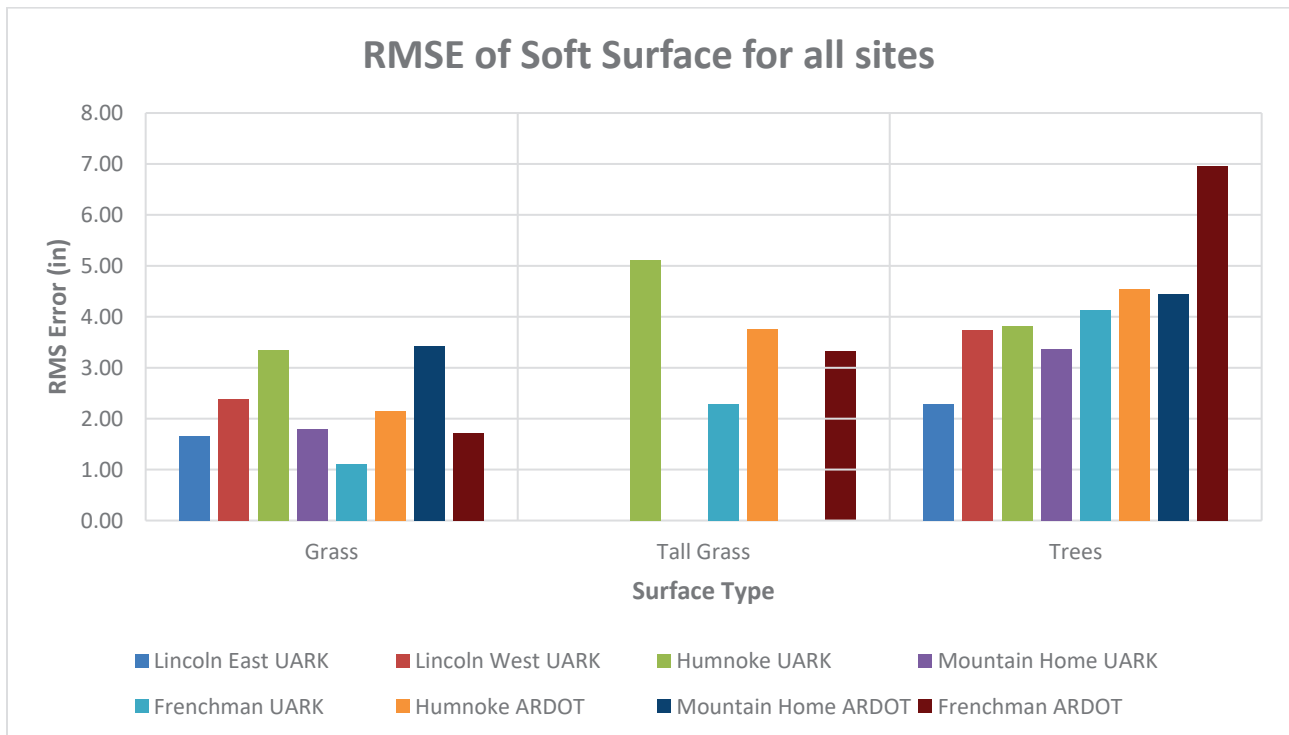
Figure 73. RMSE for All Soft Surface Checkpoints at All Sites in the Study

CHAPTER 6. COST SAVINGS ANALYSIS

The cost-saving analysis for the project was conducted using project surveying cost information provided by ArDOT (Hall 2023).

COMPARISON OF HELICOPTER AND UAS LIDAR COSTS

The cost of helicopter LiDAR per ArDOT project is provided in Table 9. These data (all projects in the table) were collected under a single task order, with the mobilization distributed into each job. It is expected that if a single project site was flown by the contractor, the cost per bridge would be higher than the numbers provided in the table. Overall, there are seven separate jobs and 20 bridges included in the dataset. It should be noted that for Job 090559, the project was a 3-mile passing lane project, so the cost is per mile of lane but still demonstrates a similar project cost. This dataset does not include any costs for feature extraction or field surveys and only includes the cost of conducting LiDAR surveys and providing the resulting point clouds. From the dataset, the average cost per bridge for helicopter LiDAR is $5,794.52 with a maximum amount of $7,514.17 and a minimum amount of $4,823.88 per bridge.

Table 9. Helicopter LiDAR Survey Costs for ARDOT Small Bridge Projects

Job	Year Acquired	Fee	Bridges in Job	Cost/Bridge
100955	2020	$27,520.69	5	$5,504.14
101012	2020	$11,938.83	2	$5,969.42
101017	2020	$14,471.65	3	$4,823.88
110568	2020	$15,029.54	2	$7,514.77
110707	2020	$5,054.48	1	$5,054.48
110713	2020	$20,139.81	4	$5,034.95
090559	2020	$19,980.00	3	$6,660.00
			Avg. Cost	$5,794.52

The cost of UAS LiDAR per ArDOT project is provided in Table 10. For these projects, the surveys were for a single bridge, so the maximum mobilization cost was included in the project's costs. Overall, only two jobs and bridges were included in the dataset. This dataset included the cost for feature extraction, but not for field surveys. The cost of feature extraction was estimated at $6,000 for each project and removed from the cost to provide a more direct comparison with the Helicopter LiDAR data in Table 9. From the dataset, the average cost of UAS LiDAR per bridge is $4,597.11, with a maximum amount of $5,595.90 and a minimum amount of $3,598.32 per bridge.

Table 10. UAS LiDAR Survey Costs for ARDOT Small-Bridge Projects

Job	Year Acquired	Fee	Bridges in Job	Cost/Bridge	Cost/Bridge W/O Feature Extraction
020736	2023	$9,598.32	1	$9,598.32	$3,598.32
020737	2023	$11,595.90	1	$11,595.90	$5,595.90
			Avg. Cost	$10,597.11	$4,597.11

Compared to the helicopter LiDAR, the UAS LiDAR was, on average, $1,195.41 less expensive, resulting in a 20 percent reduction in the cost of collecting UAS LiDAR data for small-area bridge projects. Therefore, UAS LiDAR clearly provides a cost benefit over helicopter LiDAR for these types of projects.

COMPARISON OF UAS PROJECT SURVEYING COSTS AND CONVENTIONAL PROJECT SURVEYING COSTS

A breakdown of the complete surveying cost for projects using UAS LiDAR is shown in Table 11. These project costs included the acquisition of UAS LiDAR, feature extraction from the LiDAR, and additional field surveys for utility and drainage information. These projects were completed using a single-task order, and therefore, reduced mobilization costs are included in these numbers. Overall, seven jobs and bridges were included in the dataset. From the dataset, the average cost per bridge using UAS LiDAR surveying is $32,269.78, with a maximum amount of $36,684.22 and a minimum amount of $27,729.12 per bridge.

Table 11. UAS LiDAR Survey Costs for ARDOT Small-Area Bridge Projects, Including Acquisition, Feature Extraction, and Field Survey Costs

Job	Year Acquired	Fee	Bridges in Job	Cost/Bridge
110748	2023	$29,856.05	1	$29,856.05
110749	2023	$29,997.62	1	$29,997.62
110751	2023	$32,453.00	1	$32,453.00
110752	2023	$36,746.72	1	$36,746.72
101125	2023	$32,421.75	1	$32,421.75
101138	2023	$36,684.22	1	$36,684.22
101139	2023	$27,729.12	1	$27,729.12
			Avg. Cost	$32,269.78

A breakdown of the complete surveying cost for projects that used conventional surveying is shown in Table 12. These project costs include conventional field surveys for all aspects of the project. Job CB1701 did originally include a control survey with an approximate value of $10,000, which is not included in the amount shown in Table 12. Overall, seven jobs and 10 bridges were included in the dataset. From the dataset, the average cost per bridge for conventional style surveying is $42,808.96, with a maximum amount of $50,083.93 and a minimum amount of $22,253.43 per bridge.

Table 12. Conventional Bridge Survey Costs for ARDOT Small-Area Bridge Projects

Job	Year Acquired	Fee	Bridges in Job	Cost/Bridge
BR2606	2022	$44,641.90	1	$44,641.90
C18016	2022	$39,854.45	1	$39,854.45
CB1701	2023	$49,017.25	1	$49,017.25
110703	2020	$47,419.53	1	$47,419.53
070508	2020	$89,013.73	4	$22,253.43
101003	2020	$50,083.93	1	$50,083.93
101002	2019	$46,392.23	1	$46,392.23
			Avg. Cost	$42,808.96

Comparing the costs of UAS LiDAR style survey and conventional surveying, the UAS LiDAR is, on average, $10,539.18 less expensive per bridge, resulting in a 25 percent reduction in the cost of collecting surveys for small-area bridge projects. Therefore, UAS LiDAR clearly provides a cost benefit over conventional surveying for these types of projects.

CHAPTER 7. CONCLUSIONS, RECOMMENDATIONS, AND FUTURE WORK

As part of the TRC2106 project, UAS LiDAR data were collected at five ArDOT bridge project sites in the state of Arkansas, including Lincoln West, Lincoln East, Humnoke, Frenchman's Bayou, and Mountain Home. For each site, the UAS LiDAR data were collected over the bridge and along the approach and departure for the bridge by the University of Arkansas (referred to as UARK LiDAR). In addition, conventional surveying checkpoints were collected at each site using GNSS and total station equipment. The checkpoints were collected for various surface conditions including hard (asphalt, concrete, gravel) and soft (grass, tall grass, and trees) surfaces. The checkpoints were used to evaluate the accuracy of the UAS LiDAR for each site by comparing the elevations of each point to the UAS LiDAR-derived elevations. These checkpoints were not used in LiDAR data processing, so they were complete independent evaluations. In addition, at three of the sites, ArDOT collected UAS LiDAR data or a contractor collected helicopter LiDAR data and compared them to the same checkpoints (referred to as ArDOT LiDAR).

Comparing the UARK and ArDOT LiDAR to the GNSS/total station checkpoints for hard surfaces showed that the accuracy was generally within the -1.0 inch to +1.0 inch range, with the Lincoln West and East sites generally underpredicting slightly and Humnoke and Mountain Home overpredicting slightly. Frenchman's Bayou showed almost zero bias for hard surfaces. For soft surfaces, the LiDAR generally overestimated the elevation for grass surfaces between 0.0 to +2.0 inches for most sites. However, the Humnoke site generally overpredicted by close to +3.0 inches, which was likely caused by the taller grass in the area. UARK LiDAR slightly underpredicted grass elevation at the Mountain Home site while the ArDOT LiDAR overpredicted it. This is believed to be caused by the variations in grass height during the conventional survey, UARK LiDAR, and ArDOT LiDAR acquisitions. The Frenchman's Bayou site generally had the lowest error for grass, with a slight overprediction of approximately +1.0 inch. For tall grass, the UAS LiDAR generally overpredicted by larger margins than standard grass checkpoints, with errors of between 0.0 inches and +4.0 inches and some errors of over +6.0 inches. Frenchman's Bayou was an exception as it had generally lower errors than the other sites. The tree checkpoints generally had the highest variability errors of +2.0 inches to +6.0 inches, with some errors higher than +6.0 inches.

Comparing the RMSE for all the sites, errors of 0.5 inches to 1.5 inches for hard surfaces (asphalt) were the most common. Humnoke had a higher error of around 2.0 inches, while Frenchman's Bayou had the lowest error at around 0.5 inches. The gravel checkpoints have a slightly higher RMSE of between 1.0 inch and 2.0 inches. For grass points, an RMSE of 1.0 inch to 3.0 inches was observed, depending on the height of the grass. Tall grass had a higher RMSE of 2.0 inches to 5.0 inches as expected. Tree checkpoints had the most error, with an RMSE of 2.0 inches to 7.0 inches observed.

Overall, an error of approximately 1.0 inch can be expected for asphalt surfaces, considering both over- and under-predictions. An error of 1.0 inch to 2.0 inches can be expected for gravel surfaces. For soft surfaces (grass), an overprediction error of 1.0 inch to 3.5 inches can be expected, depending on the height of the grass. For tall grass, larger overprediction errors of 2.0 inches to 5.0 inches are expected. For areas with trees, larger errors between 2.0 inches and 7.0 inches can be expected, with larger errors possible.

To determine the potential costs saved by conducting UAS LiDAR, two comparisons were made, 1) one between UAS LiDAR cost and helicopter LiDAR cost for several ARDOT projects and 2) another between UAS LiDAR project costs and conventional surveying methods. For the first comparison, it was determined from the data that compared to helicopter LiDAR, UAS LiDAR is $1,195.41 less expensive per project, resulting in a 20 percent reduction in the cost of collecting data for small-area bridge projects. Therefore, UAS LiDAR clearly provides a cost benefit over helicopter LiDAR for small-area projects. For the second comparison, it was determined that compared to conventional surveys, UAS LiDAR is $10,539.18 less expensive per bridge than conventional surveying, resulting in a 25 percent reduction in the cost of collecting data for small-area bridge projects. Therefore, UAS LiDAR clearly provides a cost benefit over conventional surveying for small-area bridge projects.

Overall, UAS LiDAR can clearly provide elevation data with good accuracy for hard surfaces and, as expected, less accuracy for soft surfaces; moreover, it provides a cost benefit compared to alternative surveying methods. For future work, 1) the accuracy of using multiple flights at the same site can be compared, as surveys on different dates resulted in different accuracy levels; 2) different LiDAR processing techniques can be compared to understand the accuracy differences between the methods; and 3) different flight patterns can be compared to understand the impact of flight line choices.

REFERENCES

Amon, P. Riegl, U., Pieger, P., and M. Pfennigbauer. 2015. "UAV-Based Laser Scanning to Meet Special Challenges in Lidar Surveying." *In* Geomatrics Indaba Proceedings.

ASPRS Map Accuracy Standards Working Group. 2014. *ASPRS Positional Accuracy Standards for Digital Geospatial Data.* 1st ed.

Brooks, C., Dobson, D., Banach, D., Dean, D., Oommen, T., Wolf, R., Havens, T., Ahlborn, T., and B. Hart. 2014. *Evaluating the Use of Unmanned Aerial Vehicles for Transportation Purposes*. Final Report Michigan DOT.

Cliffen, S., and Weeden, G. 2010. "Best Practices for assessing NEXTMAP Europe Data Quality and Accuracy." Paper presented at *ASPRS/MAPPS 2009 Conference, San Antonio, TX, Nov. 16-19, 2010*.

Fitzpatrick, B. 2016. "Unmanned Aerial Systems for Surveying And Mapping: Cost Comparison of UAS Versus Traditional Methods of Data Acquisition." MS Thesis, University of Southern California.

Falco, N., Wainwright, H., Ulrich, C., Dafflon, B., Hubbard, S., Williamson, M., Cothren, D., Ham, R., McEntire, J. and McEntire, M. 2018. "Remote Sensing to UAV-Based Digital Farmland." In *IGARSS 2018-2018 IEEE International Geoscience and Remote Sensing Symposium*, 5936–5939. IEEE.

G. I. S. G. 2022. "What is An Aspect Map?" GIS Geography, June 29, 2022. https://gisgeography.com/aspect-map/

Jozkow, G., Wieczorek, P., Karpina, M., Walicka, A., and A. Borkowski, "Performance Evaluation of sUAS Equipped with Velodyne HDL-32E LiDAR Sensor". *The International Archives of the Photogrammetry, Remote Sensing and Spatial Information Sciences* 42 (2017): 171–177.

Jozkow, G., Toth, C., and D. Grejner-Brzezinska, "UAS Topographic Mapping with Velodyne LiDAR Sensor". *ISPRS Annals of the Photogrammetry, Remote Sensing and Spatial Information Sciences* III-1 (2016): 201–208.

Platt, b. Suarez, C., Boss, S., Williamson, M., Cothren, J., and J. Kvamme, "LiDAR-Based Characterization and Conservation of the First Theropod Dinosaur Trackways from Arkansas, USA". *PloS ONE* 13, no. 1 (2018): e0190527.

Van Sickle, J., and J. Dutton. "GEOG862: GPS and GNSS for Geospatial Professionals." *Department of Geography, Pennsylvania State University, University Park, Pennsylvania (www. e-education. psu. edu/geog862/home. html)* (2014).